INVESTIGATION OF THE EFFECT OF PLASTICITY ON THE PREDICTION OF GENETIC INTERACTIONS AND PHENOTYPES IN *SACCHAROMYCES CEREVISIAE*

by

Duygu Dikicioğlu

B.S, Chemical Engineering, Boğaziçi University, 2003

M.S, Chemical Engineering, Boğaziçi University, 2005

Submitted to the Institute for Graduate Studies in
Science and Engineering in partial fulfillment of
the requirements for the degree of
Doctor of Philosophy

Graduate Program in Chemical Engineering

Boğaziçi University

2011

ACKNOWLEDGEMENTS

"The hardest thing of all is to find a black cat in a dark room, especially if there is no cat."

Confucius

I have learned in these past six years that it might even be challenging to find the cat in a lighted room and sometimes you wish that you did not find any cat at all. Still I have also learned to survive with what I had at the end of the day. Along the way, some great support came from much loved people and this had really made it easy to bear the days the cat was not in sight and wonderful to share the days the cat was on my lap peacefully purring. Among the many to mention, the following are very dear…

Mom, dad;
No words are needed to explain or justify your place in my life; I hope you enjoy what you have ended up with.

Prof. Kırdar, Prof. Oliver, Prof. Onsan;
You have not only guided me along (and pushed me when I needed) on academic terms but also provided me with wonderful role models to look up to. I'm forever indebted to you.

Corporate gals, corporate guy and the one who tried so hard to be corporate before pursuing a PhD degree;
I guess you are family now. You don't thank family for anything, it just comes with the package…

The gals (you definitely know who you are) and the Cam gal;
Just because I have isolated you out from the previous crowd, it's not that we're not family but it's just that we are the yeasties. Let's just make sure that our paths cross in the future, too…

Last but certainly not the least, I think I should also note that the financial support from various associations through the following projects is greatly acknowledged;

Bogazici University Research Fund: Projects 631, 736, 863, 5574.
TUBITAK BDP Program
TUBITAK MAG: Project 106M444
DPT: Project 09K120520
EU: Projects YSBN (018942), SYSINBIO (212766), UNICELLSYS (201142)
BBSRC

ABSTRACT

INVESTIGATION OF THE EFFECT OF PLASTICITY ON THE PREDICTION OF GENETIC INTERACTIONS AND PHENOTYPES IN *SACCHAROMYCES CEREVISIAE*

Prediction of phenotype from genome-scale high-throughput network and component information still remains a challenge for systems based approaches in biological research. The enhancement of our power of prediction of phenotype information would help unravel the complete quantitative genetic interaction network, which in turn would provide the link between genotype and phenotype, enabling to reach deductions about phenotype just with the knowledge of genotypic information on functional relationships and in return, this might set a milestone for the construction of quantitative genetic interaction networks of higher organisms including *Homo sapiens* as well as providing clues as to the open reading frames encoding human genetic disorders through the use of their homologues in a model organism. The aim of this thesis was to identify the effect of plasticity on the prediction of novel genetic interactions leading to a decrease in fitness and causing synthetic sickness or lethality within the network of yeast in a quantitative manner. In this study, systems-based information on various components and interaction levels was used for the prediction and identification of novel interactions leading to phenotypes. For this purpose, the yeast model organism was investigated under carefully controlled environments. The applicability of flux balance analysis for the prediction of epistasis was investigated in conjunction with the effect of biomass composition and environmental perturbations on metabolism in order to enhance the predictive power of metabolic flux analysis. Flux balance analysis was concluded to be suitable for the prediction of phenotypic information and genetic interactions through implementation of regulatory information and plasticity information provided from the response of organisms to environmental perturbations.

ÖZET

SACCHAROMYCES CEREVISIAE'DA GENETİK ETKİLEŞİMLERİN VE FENOTİPİN BELİRLENMESİNDE PLASTİSİTE ETKİSİNİN İNCELENMESİ

Genom-boyutlu çoklu platform ağyapıları ve hücresel birim bilgisinden fenotip belirlenmesi, biyolojik araştırmalarda sistem bazlı yaklaşımlar için bir sorun oluşturmaktadır. Fenotip bilgisini tahmin gücünün geliştirilmesi tamamlanmış kantitatif genetik etkileşim ağyapısının belirlenmesine ve buna bağlı olarak genotip ve fenotip arasındaki bağlantıyı sağlayarak işlevsel bağıntılar üzerinden sadece genetik bilgi ile fenotip hakkında çıkarımlar yapılmasına olanak sağlayacaktır. Böylelikle *Homo sapiens*'in de içinde bulunduğu evrimin yüksek aşamasında bulunan organizmalarda kantitatif genetik etkileşim ağyapılarının belirlenmesinde bir kilometre taşı olacak ve model organizmalardaki homolog genler üzerinden insandaki genetik hastalıkları kodlayan açık okuma çerçeveleri hakkında ipuçları sağlayacaktır. Bu tezin amacı, maya ağyapısı içerisinde sentetik hastalık/ölümcüllük fenotipine yol açan yeni genetik etkileşimlerin belirlenmesinde plastisite etkisinin sayısal olarak tahmin edilebilmesini sağlamaktır. Bu çalışmada, çeşitli hücresel birimler ve etkileşim seviyeleri hakkında sistem bazlı bilgiler, farklı fenotiplere yol açan yeni etkileşimlerin tahmin edilmesi ve belirlenmesinde kullanılmıştır. Bu amaçla maya model organizması kontrollü ortamlarda incelenmiştir. Epistatik etkileşimlerin belirlenmesinde akı denge analizinin uygulanabilirliği, metabolik akı analizinin tahmin gücünü iyileştirebilme amacı ile biyokütle bileşenlerinde ve çevresel faktörlerdeki değişikliklerin metabolizma üzerindeki etkisi ile birlikte incelenmiştir. Akı denge analizi, metabolizma düzenleyicilere ait bilgilerin ve organizmaların çevresel değişkliklere verdiği tepkileri içeren plastisite bilgisinin birlikte kullanımı ile fenotip bilgisi ve genetik etkileşimlerin belirlenmesi için uygun bir araç olarak belirlenmiştir.

TABLE OF CONTENTS

Acknowledgement ……. iii
ABSTRACT ……. v
ÖZET ……... vi
LIST OF FIGURES ……. xii
LIST OF TABLES ……. xv
LIST OF SYMBOLS/ABBREVIATIONS ……. xvii
1. INTRODUCTION …….. 1
2. STUDIES ON METABOLIC NETWORKS FOR IMPROVING THE PERFORMANCE OF METABOLIC FLUX ANALYSIS FOR THE PREDICTION OF EPISTATIC INTERACTIONS ……..…… 3
2.1. Quasi-steady state flux balance analysis applications for *in silico* determination of query genes for the prediction of synthetic lethality…..…… 3
2.1.1. Background……...…..…..…….……... 3
2.1.2. Methods…… 5
2.1.2.1. Medium and Growth Conditions…… 5
2.1.2.2. Sampling, Quantification of Biomass, Glucose, and Extracellular Metabolites ……..... 5
2.1.2.3. Determination of Growth Parameters..... 5
2.1.2.4. Flux Balance Analysis (FBA)……. 5
2.1.3. Results and Discussion..…….…..…….…….. 6
2.1.3.1. Properties of the Model Fermentations……..……... 6
2.1.3.2. Prediction of Flux Distributions using Quasi-steady State Flux Balance Analysis……. 8
2.1.4. Study Conclusions…… 13
2.2. Prediction of lethality as phenotype in the amino acid production and utilization pathways using flux balance analysis …….……..…….. 14
2.2.1. Background……...…..…..…….……... 14
2.2.2. Methods…… 18
2.2.2.1. Flux Balance Analysis (FBA)……....……... 18
2.2.2.2. Determination of Epistasis..... 18

2.2.3. Results and Discussion……..…….…….. 18
2.3. Investigation of the effect of plasticity and biomass composition at different metabolic states on metabolic flux distribution…….……..……. 20
2.3.1. Background……...…..…..…….…..……... 20
2.3.2. Methods…… 22
2.3.2.1. Determination of Metabolic Constraints...…… 22
2.3.2.2. Flux Balance Analysis (FBA)..... 22
2.3.2.3. Variations in the Biomass Composition……. 22
2.3.3. Results and Discussion…….…..…….…..……... 22
2.3.4. Conclusions and Future Prospects…… 26
3. INVESTIGATION OF TRANSIENT CHANGES IN YEAST METABOLISM IN RESPONSE TO AN ENVIRONMENTAL PERTURBATION…….. 28
3.1. A comparison of how yeast re-programs its transcriptional profile in response to different nutrient impulses……. 28
3.1.1. Background ….....…….…..…….…..……... 28
3.1.2. Methods…..……... ……..... 30
3.1.2.1. Strain and Growth Conditions...……....…..…..... 30
3.1.2.2. Pulse Injections and Sampling..……....…..……..... 31
3.1.2.3. Sampling for Transcriptome Analysis, RNA Isolation and Transcriptome Analysis……..…….…..... 31
3.1.2.4. Microarray Data Acquisition and Analysis……...…..…….. 32
3.1.2.5. Dynamic Regulatory Events Miner Analysis…… 33
3.1.3. Results and Discussion…….…… 33
3.1.3.1. Correlation Analyses of Genome-wide Expression Profiles. 33
3.1.3.2. Temporal Organization of the Global Transcriptional Response…….. 34
3.1.3.3. Genes Showing a Significant Change in Expression Level in Response to the Nutrient Impulses…….. 35
3.1.3.4. Dynamic Transcriptional Reprogramming of the Cell During Transition Created by a Nutrient Impulse……... 43
3.1.4. Study Conclusions……. 47
3.2. Long-term dynamic response to changing nutritional environment and time dependent re-organization of yeast cells……. 48

3.2.1. Background……...……..…….…….……... 48
3.2.2. Methods…… 51
3.2.2.1. Data Acquisition……...…….…….. 51
3.2.2.2. Sampling and Extraction of the Endometabolome, Analytical Methods for Fingerprinting …….……..... 51
3.2.2.3. Identification of Gene Expression in Co-clustered Time Spans and Mapping of the Transcriptome and the Metabolome on Metabolic Pathways ……..……...…..…….…..... 51
3.2.3. Results and Discussion..……..……..…….. 52
3.2.3.1. Changes in the Central Carbon Metabolism …….…… 55
3.2.3.2. Re-organization of the Nucleotide Pools in Response to Catabolite Repression ……..……...…..……. 60
3.2.3.3. Changes in the Purine and Pyrimidine Biosynthetic Pathways and their Salvage Pathways ……..……..……...… 61
3.2.3.4. Folate Metabolism…….…… 66
3.2.3.5. Superpathway of Serine and Glycine Biosynthesis .....…… 68
3.2.3.6. Sulphur Assimilation and Methionine Metabolic Pathways. 68
3.2.3.7. Aspartate Biosynthetic Pathway and the Superpathway of Glutamate Biosynthesis……... 69
3.2.4. Study Conclusions…… 71
3.3. A novel tool for the prediction of hidden genetic interactions embedded in dynamic gene expression data enriched with an a priori knowledge on network information ……. 74
3.3.1. Background……...……..…….…….……... 74
3.3.2. Methodology……. 75
3.3.2.1. Construction of the Linear Model …… 76
3.3.2.2. Segregation of the Interaction Matrix…… 76
3.3.2.3. Model Network…..……...…..……..... 77
3.3.2.4. Test Model……. 78
3.3.2.5. Implementation of Metabolic Pathway Information……. 79
3.3.2.6. Implementation of Regulatory Information…… 79
3.2.3. Evaluation of the Applicability of the Test Model……... 80
3.2.4. Future Prospects……...……..…….…….……... 84

4. INVESTIGATION OF HOW GENETICALLY ALTERED YEAST STRAINS RESPOND TO DIFFERENT NUTRITIONAL ENVIRONMENTS ……..…… 85
4.1. Drug resistance in yeast: Is that all there is to it?...……. 85
4.1.1. Background……...…..…..…….…..……... 85
4.1.2. Methods…… 88
4.1.2.1. Strain, Growth Conditions and Sampling ……. 88
4.1.2.2. Endo-metabolome and Exo-metabolome Sampling, Endo-metabolome Extraction, Analytical Methods for Footprinting and Fingerprinting…….…….... 88
4.1.2.3. Transcriptome Sampling RNA Isolation and Transcriptome Analysis ……..……....…..…….... 89
4.1.2.4. Microarray Data Acquisition……. 89
4.1.2.5. Data Analysis……. 89
4.1.3. Results and Discussion..…..…..…….…..…….. 90
4.1.3.1. Nutritional Conditions Determine the Transcriptional and Metabolic Response of the Deletion Mutants …….…..…….. 90
4.1.3.2. Deletion and Nutrition Specific Gene Expression Profiles Reveal How Yeast Re-adjusts Itself to its Current Condition.…… 91
4.1.3.3. The Expression Levels of Transcription Factors were Re-arranged to Compensate for the Loss of the Drug Resistance Genes.. 99
4.1.3.4. Alterations in Glycerol Metabolism to Cope with the Loss of Drug Resistance Genes.…..…….…… 104
4.1.4. Study Conclusions…… 108
4.2. Prediction of genetic interactions from phenotype via chemical genomics and synthetic genetic arrays……..… 110
4.2.1. Background……...…..…..…….…..……... 110
4.2.2. Methods…… 113
4.2.2.1. Selection of Drug Resistance Mutants...……... 113
4.2.2.2. Determination of Drug Dosages..... 113
4.2.2.3. Randomization of Strains on Pinning Plates and Wells, Pinning and Replication……...…..…..... 113
4.2.2.4. Colony Visualizations, Size Determination and Calculation of Significance and Epistasis……..……. 114

4.2.3. Study Results…….…..…….…..…….. 114
4.2.3.1. Growth Defects……..……..……..…….... 114
4.2.3.2. Determination of Epistasis……..…..……. 114
4.2.4. Future Prospects……... 116
5. CONCLUSION ……... 118
APPENDIX……... CD
A. Flux Distributions……. ……..... CD
B. Flux Distributions in Response to Variations in Biomass Composition…….... CD
C. Dynamic Metabolome Data File…….…….. CD
D. Metabolic Pathway Figures……..……. CD
E. Metabolome, Flux Distribution, Transcripotome Data File, Drug…… CD
F. Drug Treatment Colony Details……..…….. CD
REFERENCES ……. 121

LIST OF FIGURES

Figure 2.1.	Variations in cell optical density in exponential phase..……..	6
Figure 2.2.	Remaining glucose and ammonium concentrations, produced ethanol and glycerol concentrations at exponential phase.....	8
Figure 2.3.	Determination of the maximum specific growth rate and the saturation constant……..…….....	9
Figure 2.4.	Metabolic flux disribution in amino acid production and utilization pathways at M5…….……...	13
Figure 2.5.	Mechanisms of synthetic lethal interactions…….	17
Figure 3.1.	Correlation analysis of genome-wide transcriptional response with each data point corresponding to samples collected at 20, 40 and 60 sec, 8, 16, 24 and 32 min, 1, 2, 3, 4, 5 and 7 hr and the 2nd steady state in comparison to the 1st steady state……..	34
Figure 3.2.	Hierarchical clustering of the dynamics of liberation from glucose ((a) and (b)) and from ammonium limitation ((c) and (d)) with Pearson correlation coefficient as the distance metric and the time spans indicated as periods annotated from P1 to P5…….....	36
Figure 3.3.	Dilution of pulse..……..……	37
Figure 3.4.	Clustering of significantly expressed transcripts in glucose (a) or ammonium (b) perturbations with the number of genes in each cluster shown in top centre and enclosing lines indicating the confidence interval around the centroids……..	42

Figure 3.5. Identification of bifurcation points under carbon (a) or nitrogen catabolite repression (b) with the average expression of a set of transcripts represented as a single branch and the size of the circles indicating the variance in expression levels for that time…..…… 45

Figure 3.6. Hierarchical organization of the response to the impulse like addition of glucose (a) or ammonium (b) and the dynamic change in the concentration of the catabolite in its respective culture..…… 53

Figure 3.7. A schematic overview of the data overlying process..…...…….. 55

Figure 3.8. General trends displaying the changes in the $\log_2$ expression values of the genes in energy metabolism…….…… 57

Figure 3.9. Re-arrangement of metabolism upon an impulse-like nutritional perturbation…….…….. 61

Figure 3.10. Schematic overview of alternative routes for ATP production during inactivation of the TCA cycle and the down-regulation of *YNK1* upon addition of glucose into the fermentation medium…… 63

Figure 3.11. Hypothetical network ……... 78

Figure 3.12. Electrical wiring diagram of the hypothetical metabolic network… 79

Figure 3.13. The finalized metabolic pathway with the observable variables x, and M0 and the hidden variables M…….. 80

Figure 3.14. Deterministic logical evaluation of the direction of flow for the metabolic information……... 81

Figure 3.15. The interaction matrix……... 82

Figure 3.16. Randomly assigned gene expression level and metabolite concentration profiles…… 83

Figure 3.17. Similar expression profiles for x_4 and z_2 deliberately embedded into the data……... 84

Figure 4.1. Hierarchical organization of transcriptome (a), and metabolome (b) with QDR3-QDR3: Δ*qdr3/*Δ*qdr3*, PDR3-PDR3: Δ*pdr3/*Δ*pdr3*, HO-HO: Δ*ho/*Δ*ho*…….. 92

Figure 4.2. Distribution of the differentially up-regulated (a) and down-regulated (b) transcripts with Nlim: ammonium limitation, Clim: glucose limitation, pdr3: Δ*pdr3/*Δ*pdr* and qdr3: Δ*qdr3/*Δ*qdr* and the numbers indicating the number of genes in that set..…….. 96

Figure 4.3. Differences in glycerol production mechanism for Δ*qdr3/*Δ*qdr3* and Δ*pdr3/*Δ*pdr3* under glucose or ammonium limitation…..…….. 105

Figure 4.4. Chemical-genetic and synthetic lethal interactions…….. 112

Figure 4.5. Drug screens for the replicates (in red or in blue) in quinidine untreated (a) and quinidine treated (b) strains with Δ*qdr3* indicated by blue arrow, Δ*ho* indicated by red arrow, Δ*ngg1*indicated by red circles and Δ*pdr5* indicated by blue circles……..…..... 115

LIST OF TABLES

Table 2.1. Biomass (BM) concentrations at time from inoculation during exponential phase ……..…… 7

Table 2.2. Growth parameters of replicate batch fermentations (B1, B2 and B3)..…….. 7

Table 2.3. Metabolite fluxes in mmol/g biomass · hr for the samples in exponential phase…….. 10

Table 2.4. Evaluation of the predictive power of the model using flux balance analysis…….. 12

Table 2.5. Viability prediction success through the use of flux balance analysis…. 20

Table 2.6. Major nutritional constituents of foot printing medium (FPM) in the simulated fermentations…… 23

Table 2.7. Flux constraints in mmol / g biomass hour for the studied physiological cases…….. 23

Table 2.8. Categorization of biomass constituents…… 24

Table 3.1. Gene Ontology (GO) annotations to differentially expressed genes…… 38

Table 3.2. Gene Ontology enrichment of transcripts following bifurcation that was controlled by transcription factors…….…... 44

Table 4.1. Biological process GO terms significantly associated (p value < E-02) with differentially expressed transcripts under glucose limitation with U-R: up regulation, D-R: down regulation and non-significant associations denoted with *……. 93

Table 4.2. Biological process GO terms significantly associated (p value < E-02) with differentially expressed transcripts under ammonium limitation as well as at all times with U-R: up regulation, D-R: down regulation and non-significant associations denoted with *……. 94

Table 4.3. The expression levels of the physically interacting proteins for *QDR1*, *QDR2*, *QDR3*, and *PDR1*, *PDR3*, *PDR5* with the interactions within the DHA12 drug resistance family and the pleiotropic drug resistance family of the ABC transporters…… 98

Table 4.4. Differentially expressed genes encoding transcription factors (TFs)….. 100

Table 4.5. Determination of epistasis between *QDR3 – NGG1* and *QDR3 – PDR5* gene pairs……. 116

LIST OF SYMBOLS / ABBREVIATIONS

h	Hour
m	Exponential growth rate
x, y, z, w	Enzyme nomenclature
C	Carbon
D	Dilution rate
M	Metabolite
N	Nitrogen
P	Phosphorous
S	Sulphur
W	Fitness
μ	Specific growth rate (hr^{-1})
μ_{max}	Maximum specific growth rate (hr^{-1})
min	Minutes
mmol	Milli-mole
red-ox	Reduction-oxidation
rpm	Revolutions per minute
sec	Seconds
v/v	Volume per volume
vvm	Volume per volume per minute
cDNA	Complementary deoxyribonucleic acid
dO_2	Dissolved oxygen
mRNA	Messenger ribonucleic acid
rRNA	Ribosomal ribonucleic acid
tRNA	Transfer ribonucleic acid
GC-ToF-MS	Gas chromatography-time of flight-mass spectrometry
K_s	Saturation constant (kg m^{-3})
No.	Number
RNAi	Ribonucleic acid interference

ABC	ATP binding cassette
ADP	Adenosine diphosphate
AMP	Adenosine monophosphate
ATP	Adenosine triphosphate
AXP	Adenosine X phosphate
BM	Biomass
ALD	Alcohol dehydrogenase
BLASTP	Basic Local Alignment Search Tool Protein
BPS	Brominated polystyrene
CDP	Cytidine diphosphate
CLIM	Glucose limitation
CTP	Cytidine triphosphate
CXP	Cytidine X phosphate
DHA12	The Drug:H+ Antiporter-1 (12-Spanner)
DREM	Dynamic Regulatory Event Miner
END	Endometabolome
ER	Endoplasmic reticulum
EX	Exometabolome
FBA	Flux balance analysis
FPM	Foot printing medium
GDP	Guanosine diphosphate
GMP	Guanosine monophosphate
GO	Gene ontology
GPD	Glyceraldehyde-3-phosphate dehydrogenase
GTP	Guanosine triphosphate
GXP	Guanosine X phosphate
HCE	Hierarchical Clustering Explorer
IMP	Inosine monophosphate
KEGG	Kyoto Encyclopaedia of Genes and Genomes
MAT	Mating
MDR	Multidrug resistance
MFS	Major facilitator superfamily
MIAME	Minimum information about microarray experiments

MIPS	Munich Information Centre for Protein Sequences
NLIM	Ammonium limitation
NXP	Nucleotide X phosphate
OD	Optical density
ORF	Open reading frames
P(1, 2, 3, 4, 5)	Phase (1, 2, 3, 4, 5)
PDR	Pleiotropic drug resistance
PI	Inorganic phosphate
PLS	Partial least squares
QDR	Quinidine drug resistance
RNA	Ribonucleic acid
SGA	Synthetic genetic array
SGD	Saccharomyces Genome Database
SSU	Small subunit
TCA	Tricarboxylic acid
TF	Transcription factor
THF	Tetrahydrofolate
TOR	Target of rapamycin
UDP	Uracil diphosphate
UMP	Uracil monophosphate
UTP	Uracil triphosphate
UXP	Uracil X phosphate
XMP	X monophosphate
XDP	X diphosphate
XTP	X triphosphate
YPD	Yeast extract – peptone - dextrose

1. INTRODUCTION

The emergence of novel technology platforms in biological research has enabled vast amounts of data to be made available to the scientific community. Making sense of piles of accumulated data, extracting information, and finding connections and links between bundles of newly acquired information has been the most challenging legacy of these technological developments. The need for handling and managing the available information has required the development of novel techniques or the novel application of already known techniques in order to integrate several data sets of similar or disparate types. The study of biological entities using a systems-based approach aims to obtain a comprehensive level of understanding of the whole entity, not just of its parts. An understanding of the synergetic functioning of the parts may only be obtained through an integrative and quantitative study of the whole system. Only then will applications such as novel drug design and personalized medicine, as well as advanced therapies for treating complex human disorders, be developed and the design of advanced cell factories for the production of fuels, chemicals, food ingredients and pharmaceuticals be achieved [1]. In addition to its role in the food and beverage industries, yeast has also been extensively used as a relatively simple but still relevant model in systems-based studies. The yeast genome is well studied with whole-genome sequence data being available for many natural and industrial strains [2-4]. Most high throughput genomic techniques have first been developed for yeast and then applied to other organisms. The ease of genetic manipulations and the ability of yeast to be grown under carefully controlled conditions make yeast an ideal toolbox for eukaryotic cells. Additionally, many fundamental processes are conserved among eukaryotes, making yeast a suitable organism for the study of many human disorders [1].

High-throughput information on all types of cell components can be provided through omics data sets; genomics, transcriptomics, proteomics, metabolomics, interactomics, fluxomics and phenomics. These data provide priceless information on biological systems but also impose challenges that are characteristic to information-rich environments. Phenomics and fluxomics are both categorized as functional states data since they provide an integrated readout of all omics data types by revealing the overall

cellular phenotype. High-throughput determination of cellular fitness in response to environmental or genetic perturbations is termed phenomics. Phenotype arrays, chemogenomics and RNAi technologies enable the investigation of cellular phenotype. Integration of the various types of omics data to yield predictions for cellular fitness is yet another challenge for systems-based studies to be overcome [5].

In this study, systems-based information on various components and interaction levels was used for the prediction and identification of novel interactions leading to phenotypes. For this purpose, the yeast model organism was investigated under carefully controlled environments.

In the first part of the study, the application of flux balance analysis for the prediction of epistasis was investigated. The effect of biomass composition and environmental perturbations on metabolism were analysed in order to enhance the predictive power of metabolic flux analysis for the identification of metabolic epistasis.

In the second part of the study, yeast cells were subjected to perturbations leading to changes in nutrient availability and the dynamic transcriptional and metabolomic responses of yeast cells were investigated. The transient data on transcript and metabolite levels were then integrated with metabolic pathway information, protein-protein interaction data, and protein-gene interaction data to build a model for the prediction of novel epistatic interactions.

In the last part of the study, genetically manipulated yeast strains, namely drug resistance mutants, were grown under nutrient limitation and the steady state transcriptional and metabolomic responses were investigated. A chemogenomics approach was used to predict lethal drug-gene interactions as a measure of fitness using drug treatment as bait to replace the QDR family genes and the deletion mutants of two drug resistance families; QDR and PDR, were screened against these drugs. Novel fitness defects were identified among drug-mutant pairs.

2. STUDIES ON METABOLIC NETWORKS FOR IMPROVING THE PERFORMANCE OF METABOLIC FLUX ANALYSIS FOR THE PREDICTION OF EPISTATIC INTERACTIONS

This chapter of the study investigates the use of flux balance analysis in predicting epistatic interactions among metabolic genes. In the first section of the chapter, the quasi steady state approximation to predict the flux distributions at the mid-exponential phase of batch fermentations of wild type yeast cells is presented. Although the quasi-steady state approach for predicting flux distributions were not within a sufficiently acceptable range of the experimentally observed values, the individual predictions using metabolic snapshots along the exponential phase were. The distribution of fluxes indicated an increased flux activity on amino acid production and utilization pathways. The metabolic genes in amino acid production and utilization pathways were selected as the query genes for the *in silico* prediction of metabolic epistasis. In the second section of this chapter, the fitness evaluation of synthetic mutants in terms of lethality is presented. The *in vivo* fitness of the single deletion mutants in terms of lethality were incorrectly predicted by the *in silico* predictions in 11% of the viable mutants and 20% of the lethally sick mutants, which would have led to as much as 40% error in the predictions for double mutants. In order to enhance the predictive capability of flux balance analysis, the effect of composition of the biomass constituents; mainly the amino acid constituents, on flux distributions was investigated under different nutritional conditions in the last section of this chapter.

2.1. Quasi-steady state flux balance analysis applications for *in silico* determination of query genes for the prediction of synthetic lethality

2.1.1. Background

The quantitative description of biological systems for accurate predictions of genotype-phenotype relationships is a major goal of post-genomic biology. While the completion of genome sequences for many species has triggered a phase of systematic analysis of gene function [6-9], the Human Genome Project and sequencing of model organisms resulted in the annotation of many genes. Although genome-scale models of the

metabolic networks of model organisms such as *E. coli* [10] or *S. cerevisiae* [11, 12] have been shown to have remarkable predictive power [13], new methods are still required to reduce the dimensionality of the large parametric space encompassed. Metabolomics is the level of functional genomic analysis that is closest to function and, therefore, a practical approach to overcome system complexity and the use of metabolic "snapshots" may be used to provide clues as to the relationships between the activities of gene products and their resultant phenotypes [14].

Flux balance analysis (FBA) is a mathematical method for computing whole cell metabolic fluxes and growth rates based on steady state and optimality assumptions. Two fundamental steps in FBA are the use of linear constraints to define a space of feasible reaction fluxes for the network and an optimization step, aimed at finding the set of fluxes in this space that maximize a given linear objective function, using linear programming. The major set of constraints stem from mass conservation and reaction stoichiometry. Exchange reactions, maintenance and growth reactions are included in the stoichiometric information. Organism specific biomass compositions as well as simulated environmental settings are also included to set a more realistic ground for the simulations [15].

Flux balance analysis (FBA) was used to predict metabolic phenotypes under different conditions, such as substrate and oxygen availability, by simply constraining the appropriate fluxes [16, 17]. FBA could be applied to genome-scale constraint-based models of the metabolic network to predict a particular flux distribution using linear optimization [17, 18]. The predicted growth or by-product secretion rates were found to be consistent with the experimental data in cases where *E. coli* was grown on acetate or yeast was grown on glucose [13, 19]. However, in other cases, FBA predictions may be inconsistent with experimental data, even after the adaptation to a particular environment, as in the case of some *E. coli* strains bearing deletions in metabolic genes [20]. Identification of a physiologically relevant objective function is important and methods have been developed for constraint-based models to identify such objective functions [21, 22].

In this study, quasi-steady state flux balance analysis was used as a computational tool initially for the confirmation of the method for the prediction of metabolic flux

distributions within the cell. The genes, which were associated with a specific pathway, catalysing the reactions, through which the fluxes were distinctively high or low, were selected for further analyses. These genes would make the refined set of query genes to be used in the prediction of genetic interactions based on computationally determined fitness effects.

2.1.2. Methods

2.1.2.1. Medium and growth conditions. Wild type BY4743 (*MAT**a**/MATα his3Δ/his3Δ leu2Δ/leu2Δ LYS2/lys2Δ MET15/met15Δ ura3Δ/ura3Δ*; [23]) was cultivated in 2L fermenters (Sartorius Stedim Biotech) with 1L working volume under aerobic conditions in F1 media [24] operated in batch mode. Temperature and pH were controlled to 30^{o}C and pH 4.5, respectively. Fermenters were stirred at 800 rpm which, together with constant air flow at a rate of 0.1 vvm, provided dissolved oxygen at ≥ 80% dO_2 saturation at all times during cultivation. Fermentations were carried out in triplicates.

2.1.2.2. Sampling, quantification of biomass, glucose, and extracellular metabolites. Samples taken from the fermenter at regular intervals during exponential phase during the period of steady growth were centrifuged at 8 000 rpm for 6 minutes (Eppendorf 5415C, Germany) to determine substrate utilization and extracellular product formation and metabolite concentrations. The dry weight was determined gravimetrically using triplicate samples collected during the exponential phase of growth. Extracellular glucose, ammonium, ethanol and glycerol concentrations during exponential phase of growth were determined enzymatically using Boehringer – Mannheim kits.

2.1.2.3. Determination of growth parameters. Maximum growth rate (μ_{max}) and saturation constant (K_s) were calculated from the biomass concentration and the glucose concentration based on Monod kinetics.

2.1.2.4. Flux Balance Analysis (FBA). The comprehensive genome-scale model (GSM) iFF708 [12] was employed using the maximization of biomass production as the objective function. Glucose and ammonium consumption, glycerol and ethanol production fluxes were introduced to the system as constraints. The simulations were carried out via

TOMLAB run under MATLAB 7.0. Alternate optima were eliminated using the method of Mahadevan and Schilling [25]. Among the remaining possibilities of flux distributions, the set leading to the highest amount of biomass production was selected for analysis since synthetic sickness or lethality was the key parameter in this analysis.

2.1.3. Results and discussion

2.1.3.1. Properties of the model fermentations. Wild type yeast cells were grown in defined medium under carefully controlled batch fermentations. The biomass and metabolite concentrations were determined from the samples, which were collected throughout the exponential phase, during which steady growth was assumed. The sampling frequency was adjusted such that the difference between samples would be close enough to assume a quasi-steady state condition.

Variation in the optical densities throughout the exponential phase, where intracellular steady state was assumed, is provided in Figure 2.1.

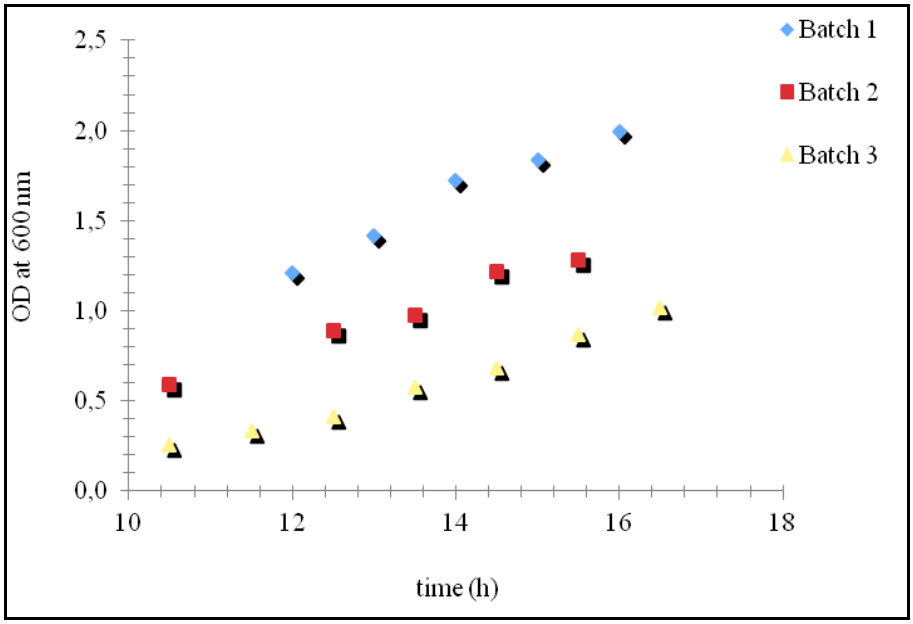

Figure 2.1. Variations in cell optical density in exponential phase

The biomass values that were gravimetrically determined from the samples collected at the exponential phase, which was determined based on optical densities, are provided in Table 2.1 for the replicate fermentations (B1, B2 and B3).

Table 2.1. Biomass (BM) concentrations at time from inoculation during exponential phase

Time (h)	**BM B1 (g/L)**	**Time (h)**	**BM B2 (g/L)**	**Time (h)**	**BM B3 (g/L)**
10.0	0.6	10.5	0.5	9.5	0.4
11.0	0.9	12.5	1	10.5	0.5
12.0	1.0	13.5	1.1	11.5	0.6
13.0	1.1	14.5	1.2	12.5	0.7
14.0	1.8	15.5	1.3	13.5	0.8
15.0	2.5	16.5	1.4	14.5	0.9
16.0	2.9	17.5	1.5	15.5	1.1
17.0	3.0	18.5	2.3	16.5	1.3
				17.5	1.5

The remaining glucose and ammonium that were not utilized by the cells as well as the excreted ethanol and glycerol concentrations that were enzymatically determined are presented in Figure 2.2. The growth parameters of the wild type were determined from the concentrations of biomass produced and glucose consumed (Figure 2.3). These parameters are provided in Table 2.2 for all three replicates (B1, B2 and B3).

Table 2.2. Growth parameters of replicate batch fermentations (B1, B2 and B3)

	μ_{max} (h^{-1})	**K_s (g/L)**
B1	0.2344	2.697
B2	0.1529	2.007
B3	0.1603	2.376
Mean	0.1825	2.360
Standard Deviation	0.0451	0.345

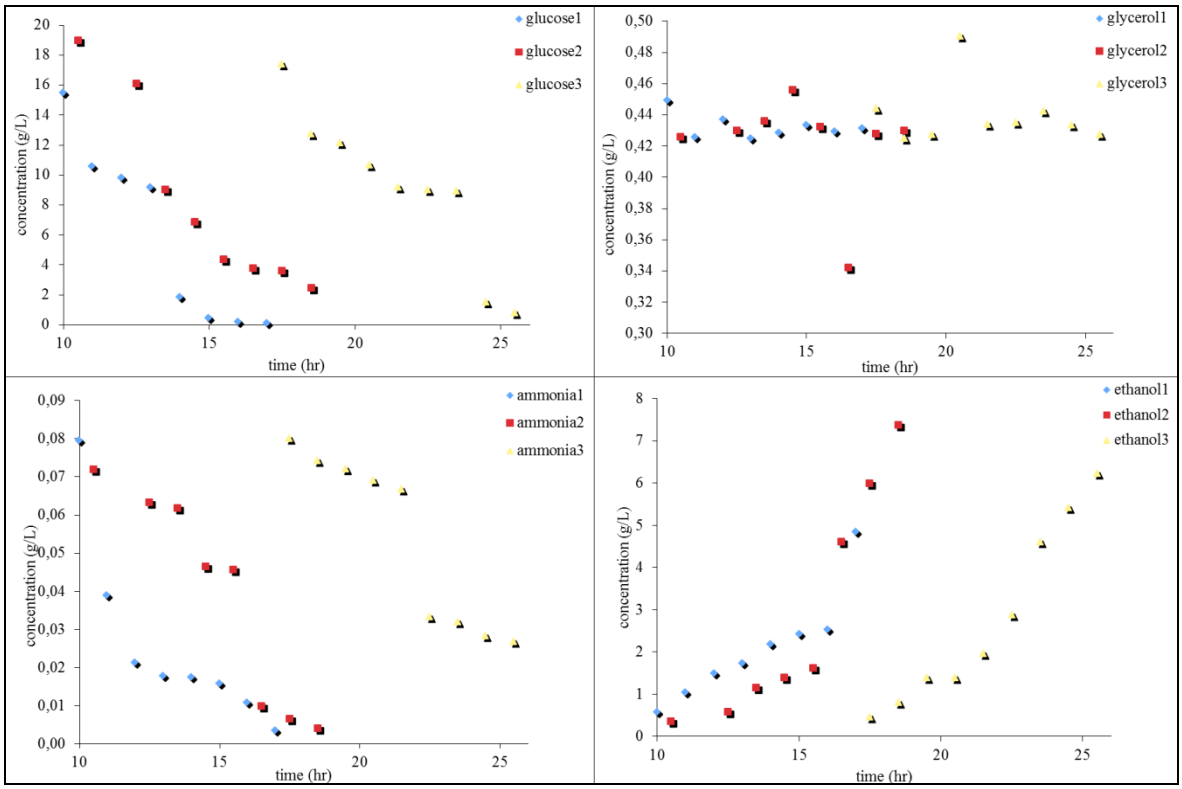

Figure 2.2. Remaining glucose and ammonium concentrations, produced ethanol and glycerol concentrations at exponential phase

2.1.3.2. Prediction of flux distributions using quasi-steady state flux balance analysis. The range of the exponential phase was determined during the determination of the Monod kinetic parameters. The flux distributions at each point in the exponential phase were determined using a quasi-steady state assumption. The experimentally determined metabolite concentrations at the initial point of exponential phase were used as constraints only at the first time point. The predictions obtained from the flux distributions at this time point were used as the constraints in calculating the flux distributions at the following time point. For the next time point, the simulation results from the previous time point would be used until the last sampling point within the mid-exponential phase. However, using this methodology, the predictions could not be improved to achieve less than 50% difference with the experimentally determined biomass values (data not shown). Therefore, the quasi-steady state assumption was discarded and individually determined concentrations were used as constraints in the predictions.

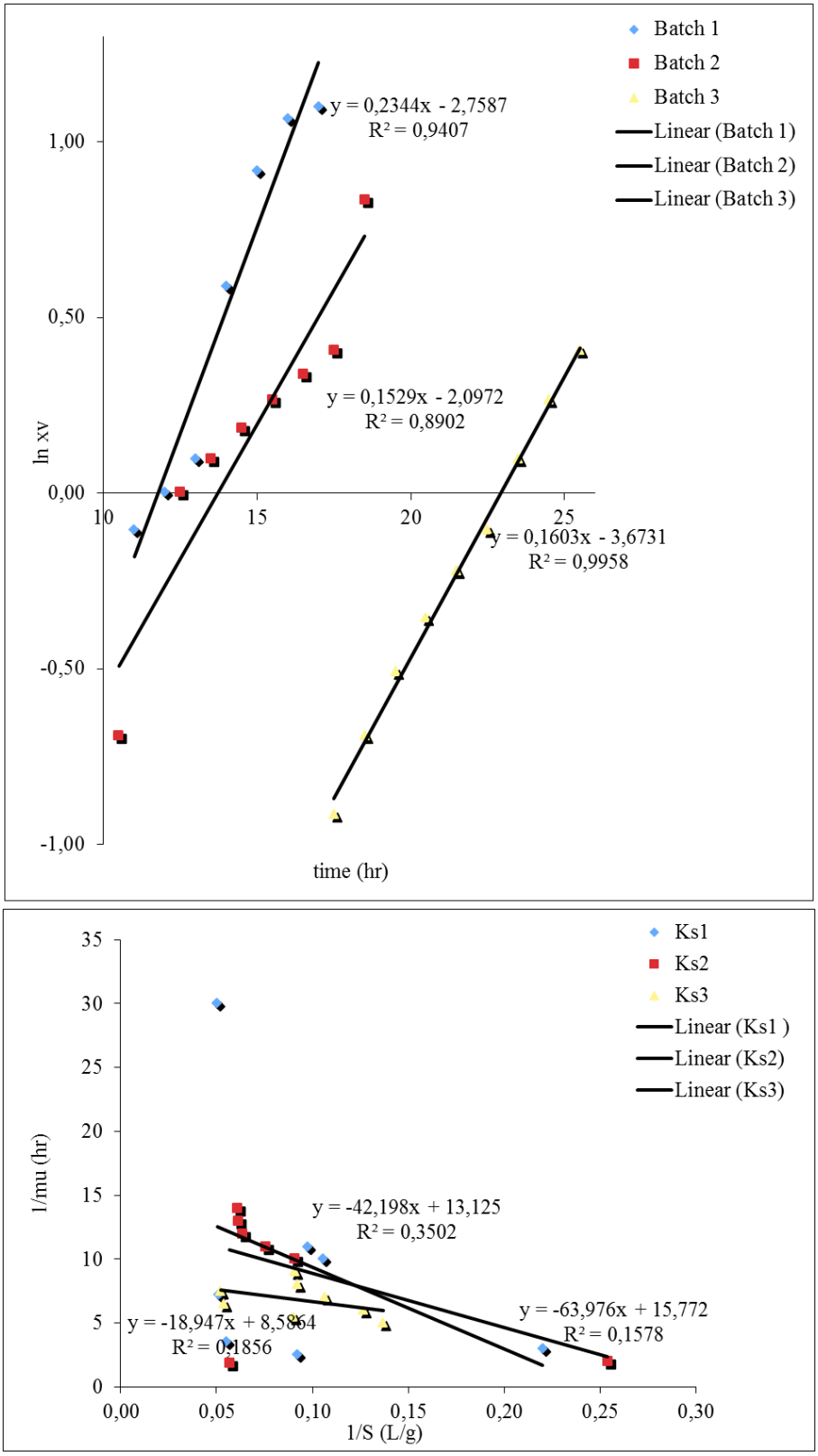

Figure 2.3. Determination of the maximum specific growth rate and the saturation constant

Since flux balance analysis assumed that a dynamic equilibrium existed within the biological system at a particular snap-shot, each time point along the exponential phase of

the batch fermentation could be assumed to be at equilibrium, theoretically at individual steady states. The exponential phase metabolite concentrations (M2-M9) from the triplicate batch fermentations (B1-B3) were thus used in flux balance analysis. The metabolite concentrations were used to represent fluxes through the utilization of specific growth rates (μ) and all fluxes were calculated in terms of mmol / g biomass · h (Table 2.3).

Table 2.3. Metabolite fluxes in mmol/g biomass · h for the samples in exponential phase

Sample	Ethanol flux	Glucose flux	Ammonium flux	Glycerol flux	Biomass flux
B1 M2	8.3460	19.4721	67.3416	1.7131	12.6263
B1 M3	3.2549	5.6893	18.2869	0.4745	3.7879
B1 M4	3.1039	4.9795	15.1302	0.3815	3.4435
B1 M5	10.2779	21.8286	39.5575	1.0055	14.7306
B1 M6	5.8889	12.1758	20.5174	0.5272	10.6061
B1 M7	2.6199	5.2391	8.7269	0.2218	5.2247
B1 M8	1.0622	1.1175	1.8577	0.0474	1.2626
B2 M2	6.2595	10.9336	90.1980	2.3343	18.9394
B2 M3	2.2762	5.5647	16.4079	0.4305	3.7879
B2 M4	2.2762	5.5459	13.7413	0.3751	3.4435
B2 M5	2.2470	5.5847	11.6303	0.3008	3.1566
B2 M6	5.9261	5.3538	10.8602	0.2197	2.9138
B2 M7	7.1537	5.0241	10.0955	0.2552	2.7056
B2 M8	65.7407	40.0724	75.4409	1.9153	20.2020
B3 M2	7.0106	16.2319	71.9010	1.8463	7.5758
B3 M3	8.3460	12.2051	49.9660	1.2888	6.3131
B3 M4	6.1317	10.6316	36.7450	1.0869	5.4113
B3 M5	6.6507	9.4143	28.1546	0.7362	4.7348
B3 M6	7.7278	7.5569	22.4893	0.5835	4.2088
B3 M7	16.554	10.1969	30.1223	0.7939	6.8871
B3 M8	13.9264	12.184	21.5924	0.5570	5.8275
B3 M9	12.0182	9.4927	16.2260	0.4124	5.0505

The fluxes for glucose and ammonium consumption and for ethanol and glycerol production at each time point along the exponential phase, which were obtained from the enzymatic determination of the metabolite concentrations, were used as constraints in the dimension reduction of the convex space in flux balance analysis (FBA). The objective function was selected as the optimization of biomass production since fitness effects would be investigated in further analyses, which would use the results from this study. The gravimetrically determined biomass concentrations were used for the comparison of the experimental results with the results from *in silico* flux predictions.

Flux balance analysis was carried out at each time point using these flux values with objective function being the maximization of biomass production [12]. The flux distributions at each point at exponential phase were thus determined. The biomass fluxes that were determined as predictions were compared with the experimentally determined values in order to evaluate the predictive power of the model (Table 2.4).

Investigation of the mean values of the repetitions indicated that the model had a prediction success of more than 90% for the mid-exponential phase except for the early- and late-exponential phase.

The investigation of the flux distributions indicated that non-zero fluxes were mainly concentrated around amino acid production and utilization pathways (Appendix A). The distribution of fluxes regarding amino acid production and utilization at a particular snapshot of M5 is provided in Figure 2.4. It has been previously suggested that as a parameter for evolutionary selection of an organism in terms of fast growth, the overall intracellular flux distribution could be minimized since organisms prefer to maximize enzymatic efficiency through the course of evolution [26]. The non-zero fluxes in amino acid and utilization pathways could indicate that the enzymes taking role in these pathways would be more sensitive to the alterations leading to phenotypes that could be attributed to reduced fitness. Therefore, these active pathways were selected for providing candidate query genes in metabolic flux analysis applications for the prediction of epistatic interactions.

Table 2.4. Evaluation of the predictive power of the model using flux balance analysis

Sample	Experimental BM Flux (g / g biomass · h)	Predicted BM Flux (g / g biomass · h)	Prediction Error Per cent (%)
B1 M2	0.33	0.45	-
B1 M3	0.10	0.14	-
B1 M4	0.09	0.10	-
B1 M5	0.39	0.42	-
B1 M6	0.28	0.34	-
B1 M7	0.14	0.14	-
B1 M8	0.03	0.01	-
B2 M2	0.50	0.24	-
B2 M3	0.10	0.08	-
B2 M4	0.09	0.04	-
B2 M5	0.08	0.09	-
B2 M6	0.08	0.05	-
B2 M7	0.07	0.04	-
B2 M8	0.53	0.17	-
B3 M2	0.20	0.47	-
B3 M3	0.17	0.18	-
B3 M4	0.14	0.17	-
B3 M5	0.12	0.12	-
B3 M6	0.11	0.11	-
B3 M7	0.18	0.18	-
B3 M8	0.15	0.13	-
M2 Avg.	0.34	0.38	12
M3 Avg.	0.12	0.13	8
M4 Avg.	0.11	0.10	6
M5 Avg.	0.20	0.21	5
M6 Avg.	0.16	0.17	7
M7 Avg.	0.13	0.12	6
M8 Avg.	0.24	0.11	56

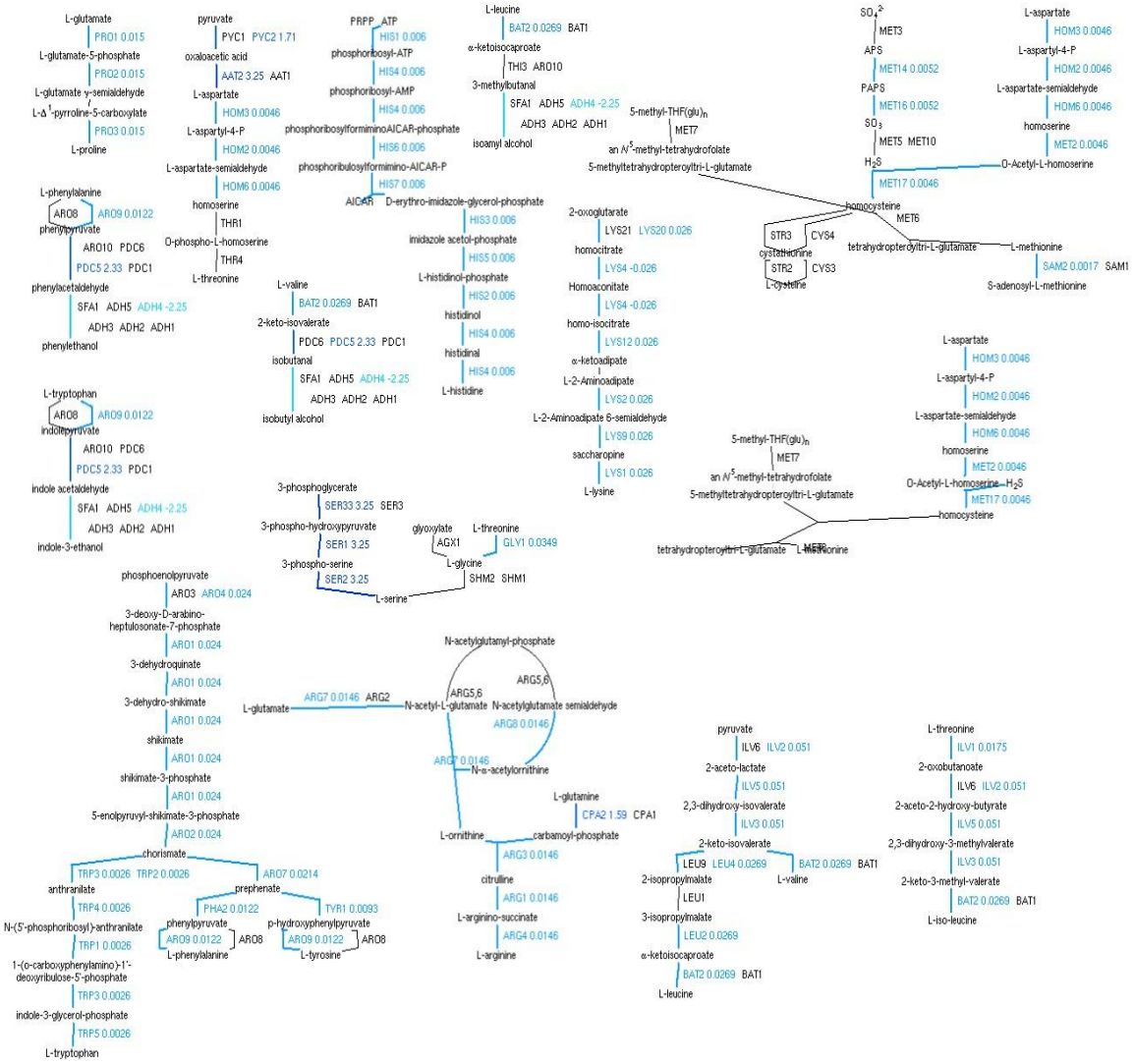

Figure 2.4. Metabolic flux distributions in amino acid production and utilization pathways at M5

2.1.4. Study conclusions

Both the experimentally determined and the computationally predicted values of biomass fluxes indicated that the growth properties and physiological structure of the three batch fermentations were within acceptable limits of being replicates during the mid-exponential phase, during which steady state conditions were assumed. The outliers of either the experimental or the predicted data were no longer outliers once the replicate values were averaged out and the mean values would be accepted as data points, indicating the necessity for parallel replicate runs during experimentation. The prediction of metabolic flux distributions from the analysis were consistent with the experimentally

obtained values with less than only 10% discrepancy, only for the mid-exponential phase, during which a quasi-steady state would be assumed, but not for the early or the late exponential phase. The distribution of fluxes during this period of fermentation indicated that amino acid production and utilization pathways would be a suitable choice for monitoring fitness through manipulations in metabolic fluxes since most of the non-zero fluxes were through the enzymes belonging to these pathways. The non-zero fluxes; possible cases of inefficient enzyme utilization during biomass production were selected as possible candidates for further investigation of fitness defects.

2.2. Prediction of lethality as phenotype in the amino acid production and utilization pathways using flux balance analysis

2.2.1. Background

As genome sequencing is being accomplished for many organisms, one of the major challenges has become the extraction of biologically meaningful information from the available data [27]. *Saccharomyces cerevisiae* genome was the first eukaryotic genome to be sequenced [2]. Yeast genome is compact and simple in comparison to other eukaryotic genomes and it has short non-coding regions and only less than 7% of its genes contain introns [28]. Nature of this genome makes it less complex than other eukaryotic genomes and this feature helps simplify functional analyses [27].

Together with the advent of whole genome sequencing, emergence of high throughput experimental technologies provided large-scale data sets that need to be interpreted to derive fundamental and applied biological information about whole systems [5]. With the knowledge of interactions affecting one another as well as co- and counter-acting behaviour of these biological entities provide clues to the functioning of the metabolism but still, obtaining a deep insight into the regulation mechanisms of the organism as a whole and how entities function as parts of a complete network are yet challenges to be overcome.

Genetic interactions are used to describe interactions occurring between genes themselves, not their products. In contrast to designation of physical interactions by the

method with which the interaction is detected, genetic interactions are named according to the strength and method of the effect they impose on the organism. The resulting interaction causes a phenotype, which can be observed and measured in several different ways. Several types of genetic interactions are categorized as phenotypic enhancement, phenotypic suppression, dosage rescue, synthetic rescue, dosage growth defect, synthetic growth defect, dosage lethality and synthetic lethality. In genetic interactions, bait/query is the starting strain or the construct and the gene participating in the interaction is called the hit [29].

Random mutations that are not neutral to the phenotype are more likely to impair biological functions rather than improving them. This is considered as a simple consequence of a long era of natural evolution. It is generally accepted that natural evolution has already fixed practically most of the beneficial mutations [30]. Mutations, especially null mutations also tend to be recessive. This recessivity results from the dynamics of the metabolic pathways. Metabolic pathways have a safety margin allowing them to function despite small changes in the component enzymes. According to the metabolic control theory, most enzymes have little influence on the flux through a pathway unless their activity level decreases to become limiting. Therefore, although the absence of an enzyme might be problematic, halving the enzyme activity is likely to have little effect on the overall metabolic flux. Consequently, mutations will generally have a much more severe effect when homozygous than when heterozygous. Dominance relationships are also affected from natural selection to some extent. Metabolic pathways themselves have evolved through natural selection in order to be more stable and robust against perturbations, including mutations [31-34].

The fact that most mutations are recessive and deleterious raises another question of whether interactions among these mutations reinforce or weaken their individual effects. Quantification of the degree of dominance, direction and synergy of genetic interactions is critical in understanding the working principles of natural selection against mutational loads [35]. Genetic variation is observed in every population, even in such populations that are well adapted to their environment. Because of this reason, they have been evoked to explain the evolution of several biological phenomena including diploidity, reproduction, recombination, dominance and epistasis [36].

The interaction data obtained from various types of analyses are used to construct a genetic interaction network for the complete organism. Analysis of a subset of the yeast genetic network provides information on the complete network. Using a set of SGA screens, nearly 4000 interactions were obtained from nearly 1000 genes [37]. For each non-essential gene, the average number of interactions was found to be 34 while it was 5 fold higher for the essential genes. Extrapolating from this subset, the global network is thought to contain nearly 200 000 synthetic lethal interactions. In a different perspective, there are 200 times more combinations of ways to generate a lethality phenotype than it is possible to do with the essential genes. This provides clues to present why the single gene effects of many phenotypes are limited to explain cellular functionality [38].

Large-scale genetic analyses reveal evidence that mutations in most eukaryotic genes have apparent effect. Supporting this view, the systematic gene deletion studies conducted in the yeast *S. cerevisiae* present the fact that only nearly 20% of all the genes are essential for viability determined from the studies on the mutant haploids growing in standard laboratory conditions [39-40]. Even though recent systematic analyses showed a measurable growth phenotype under at least one condition for every yeast gene [41], the ability of most deletion mutants to grow under optimal conditions provides support for the robustness of biological circuits and cellular buffering against genetic variations. This emphasizes an important property of networks, which is resistance to attack at a single node [42]. Synthetic enhancement genetics is the term used for examining how mutations in two genes interact to modulate a phenotype, which is an application of Fisher's definition of epistasis. Synthetic enhancement combinations are rare possibilities when all combinatory pairs of interactions are considered, therefore sensitive and selective screening methods and computational tools are developed to serve this purpose [38].

Synthetic lethality, a subset of synthetic enhancement phenotypes, is observed when the absence of two or more genes simultaneously results in a non-multiplicative phenotype, being inviability whereas the absence of individual genes in single mutants does not present itself with such a phenotype. Due to the incomplete knowledge of cellular functions, it is not clear most of the time why a particular double mutant shows a synthetic lethal phenotype, however, several possible mechanisms have been proposed depending on the characteristics of the interacting alleles [38]. If both mutations occur in non-essential

genes and are null alleles, it is generally considered that the genes function in parallel pathways working on a shared essential function. This is called the 'between pathways' model and is typically associated with bidirectional genetic redundancy meaning that each pathway compensates for defects in the other [43-45]. Another case of genetic interactions, which is of interest involve duplicated genes or paralogs. Recent studies show that patterns of genetic interactions between duplicates are divergent indicating that paralogous genes maintain functional specificity [46]. Conversely, distant paralogs encoding metabolic genes are also shown to interact indicating that the product of the duplicated gene might retain sufficient activity to mask the loss of the conserved copy [15]. Conditional or hypomorphic alleles of essential genes can be used to evaluate synthetic phenotypes. In such cases, the interactions may occur 'within pathways' as well as 'between pathways'. In 'within pathway' models, synthetic lethality is an indication of genes functioning in the same essential pathway, the function being diminished by each mutation [41] (Figure 2.5).

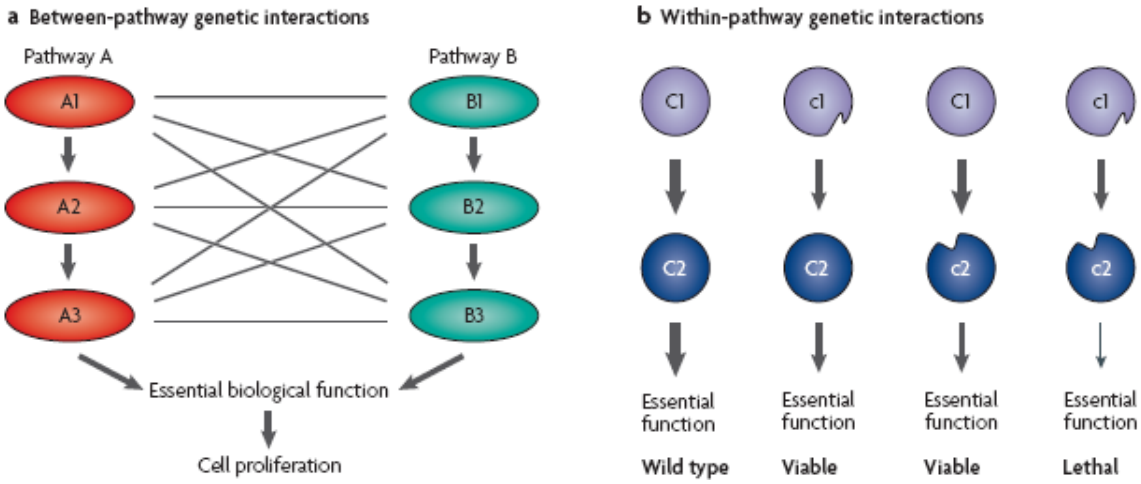

Figure 2.5 Mechanisms of synthetic lethal interactions [38]

In this study, the *in silico* fitness of metabolic gene deletion mutants of the amino acid production and utilization pathways was investigated using flux balance analysis. The query genes, which were selected in the previous section, were used for *in silico* prediction of the genetic interactions amongst themselves using maximization of the flux through biomass as the objective function in the metabolic flux analysis so that the fitness effect of the wild type as well as strains where one or more genes were absent could be determined. Epistatic interactions would thus be quantified from the predicted specific growth rates for wild type, single and double deletion mutants.

2.2.2. Methods

2.2.2.1. Flux Balance Analysis (FBA). Flux balance analysis has been carried out as described in Section 2.1.2.4. The fitness of the mutants was assessed by constraining the reactions, which were catalysed by the query genes, to zero.

2.2.2.2. Determination of epistasis. Epistatic interactions were determined using the product rule where fitness (W) is defined by the exponential (specific) growth rate (m) of a strain relative to that of the wild type or control (m_{wt}) [37, 47-49] – proposing relative growth rate measure for genes y and x:

- $W_x = m_x / m_{wt}$ $W_y = m_y/m_{wt}$ and $W_{xy} = m_{xy} /m_{wt}$

with the neutrality function: $W_{xy} = W_x W_y$; any inequality meaning presence of an interaction.

2.2.3. Results and discussion

In accordance with the findings stated in Section 2.1.3, the set of query genes were determined from the reactions associated with amino acid metabolism and amino acid transport reactions stated in iFF708. These genes, which were taking role in amino sugars metabolism (glucosamine), arabinose, xylose and mannitol metabolisms, alanine and aspartate metabolism, asparagine metabolism, glycine, serine and threonine metabolism, methionine metabolism, cysteine metabolism, branched chain amino acid metabolism, lysine biosynthesis and degradation, arginine metabolism, histidine metabolism, aromatic amino acids metabolism, proline biosynthesis, β-alanine metabolism, selenoamino acid metabolism, proteins, peptides and amino acids metabolism, glutathione biosynthesis and membrane transport of amino acids, were selected.

Eliminating the reactions that were facilitated by yet unknown enzymes, 154 enzymes were identified as taking role in the amino acid metabolism and 32 enzymes were taking place in amino acid transport (Table 2.5).

The metabolic flux constraints for glucose and ammonium uptake as well as ethanol production were determined at a plausible hypothetical point in the mid-exponential phase of batch fermentations. The specific growth rate was selected as 0.15 h^{-1}. The consumed glucose was set at 10 g/L and the consumed ammonium was set at 1.67 g/L. Ethanol production was taken as 2.5 g/L. The robustness of the observed phenotype; lethality or fitness was confirmed by varying the concentration of the consumed and produced metabolites by 25% and by varying the specific growth rate by 25%. The results indicated that although the distribution of fluxes varied in magnitude, these variations were not sufficient to alter the observed phenotype, changing the viability outcome.

The *in silico* gene deletions were made by constraining the fluxes through the reactions catalysed by the gene products to zero. The deletion of 114 annotated genes involved in amino acid metabolism did not cause a change in viability whereas the deletion of 40 known genes were predicted to yield lethal phenotypes. This fitness data were then verified by the Saccharomyces Genome Database. However, out of the 114 viable predictions, 13 genes were reported as being inviable in the database and out of the 40 inviable predictions, 8 genes were reported as viable. This corresponded to 11% discrepancy in the viability predictions and 20% discrepancy in the inviability predictions. Only two incorrect viability predictions were determined for the genes involved in amino acid transport although the evaluation could not represent the transport genes adequately since 50% of them were not annotated (Table 2.5).

The discrepancy rate was observed to increase as much as up to 35% for the prediction of lethality in double deletions. This high rate would result in incorrect predictions of epistasis, genetic interactions and redundancy in the amino acid pathways. Therefore, the need for the investigation of parameters affecting the predictive capability of flux balance analysis emerged. For this purpose, one of the most important parameters affecting the flux distributions in a metabolic model, the biomass composition, and the effects of its variation on flux distributions were investigated in the next section in order to be able to better manipulate the model for obtaining more successful predictions.

Table 2.5. Viability prediction success through the use of flux balance analysis

Gene functions in	**amino acid production and utilization**	**amino acid production and utilization**	**amino acid transport**
No. of genes	138	44	65
No. of un-annotated genes	24	4	33
No. of annotated genes	114	40	32
Predicted phenotype	viable	inviable	viable
Incorrect predictions	13 (*GFA1*, *GNA1*, *PCM1*, *QRI1*, *CHS2*, *DED81*, *KRS1*, YDR341c, *DYS1*, *HTS1*, *DIM1*, *SPB1*, *NMT1*)	8 (*HOM3*, YGR012w, *LYS1*, *ARG5*, *HIS1*, *HIS6*, *ARO9*, *TRP1*)	2 (*HIP1*, *FCY21*)
% error in single deletions	11%	20%	6%
% error projection for double deletions	78%	64%	88%

2.3. Investigation of the effect of plasticity and biomass composition at different metabolic states on metabolic flux distributions

2.3.1. Background

Plasticity refers to how cellular response is adapted to different environmental conditions and it is an important aspect of handling epistasis. Many of the genes do not affect growth under normal conditions and therefore may seem dispensable. This implies that organisms compensate for null mutations via redundant pathways and redundant gene duplicates. This phenomenon is termed as mutational robustness. However, many of the duplicates and alternate pathways are found to contribute to fitness only under certain

conditions. This is called environmental adaptation. This connection between mutational robustness and environmental adaptation is yet unclear and requires further investigation. If environmental variability (plasticity) affects the robustness of an organism against mutations and combinations of mutations, then these two phenomena should be investigated within the same context [15].

The mechanisms of metabolic change and adaptation to an environmental stimulus are still not well understood. Approximately 3% of yeast metabolic reactions were reported to be always active under different simulated growth conditions. However, the rest of the metabolic pathways were reported only to respond to certain environmental changes being conditionally active under certain conditions. This is defined as flux-based plasticity. The metabolic core, which was constituted from a sub-network of constantly active reactions, was reported to display a higher fraction of essential enzymes [50]. This would indicate that the remaining part of the network, which was affected from variations in environmental conditions, would be more susceptible to phenotypic variations resulting from epistatic effects displayed under specific conditions.

It has been previously reported that living systems might switch their biological objective when a physiological change was imposed on them. Understanding of such changes as seen during diauxic shift in yeast would still remain a challenge to be overcome. Since the knowledge on changing objectives would be limited, this would also limit the capability of FBA to correctly describe the system. The metabolic flux objectives under different metabolic states would be inferred from the available data. Such available data would be on biomass compositions and the comparative analysis of this data between wild type and mutants as well as throughout physiological transitions or under different metabolic conditions would be used to infer suitable cellular objectives to enhance the predictive capability of metabolic flux analysis [51]. Within this perspective, an analysis of how variations in the biomass composition through alterations in the stoichiometric ratios of its individual constituents would affect flux distribution was carried out in the last section of this chapter.

2.3.2. Methods

2.3.2.1. Determination of metabolic constraints. The growth environment was selected to imitate synthetic defined minimal medium [52] with no limitation and with carbon, nitrogen, sulphur or phosphorous limitations, in which the concentration of the compound(s) imposing the limitation on the element balance was reduced to 10% of its value. The approximate chemical composition of yeast nitrogen base without amino acids and without ammonium sulphate was obtained from the manufacturer (Difco Microbiology). Steady state condition with a specific growth rate of $0.1h^{-1}$ was assumed. Total carbon from all sources was expressed in terms of glucose, total nitrogen from all sources was expressed in terms of ammonium, total sulphur from all sources was expressed in terms of sulphate and total phosphorous from all sources was expressed in terms of inorganic phosphate.

2.3.2.2. Flux balance analysis (FBA). Flux balance analysis has been carried out as described in Section 2.1.2.4.

2.3.2.3. Variations in the biomass composition. Flux distributions were determined individually by varying the coefficient of every biomass constituent in the biomass composition equation by a factor of two. The coefficients were doubled or halved and the new flux distributions were obtained (Appendix B). For each environmental condition, the differences in flux distributions between the unaltered biomass composition and the altered biomass compositions were determined and for the purpose of visualization, the flux distributions were overlaid on metabolic pathways [53].

2.3.3. Results and Discussion

In order to identify the effect of variations in the composition of the biomass constituents on flux distributions, the coefficients of amino acid constituents and the other constituents were doubled or halved under different physiological conditions. These effects were evaluated within the context of inferring suitable cellular objectives to enhance the predictive capability of metabolic flux analysis.

Approximate metabolite concentrations were determined for the amount of remaining glucose and ammonium as well as the produced biomass based on the values obtained from previously conducted fermentation (Table 2.6).

Table 2.6. Major nutritional constituents of foot printing medium (FPM) in the simulated fermentations

Medium	Consumed ammonium (g/L)	Consumed glucose (g/L)	Produced biomass (g/L)	Consumed inorganic phosphate (g/L)	Consumed sulphate (g/L)
FPM	1.6930	20.0000	2.5000	0.2400	4.1460
C-lim FPM	1.6930	2.0000	2.5000	0.2400	4.1460
N-lim FPM	0.1693	20.0000	2.5000	0.2400	4.1460
S-lim FPM	1.6930	20.0000	2.5000	0.2400	0.4146
P-lim FPM	1.6930	20.0000	2.5000	0.0240	4.1460

The fluxes of four major compounds were determined for 5 physiological cases at a specific growth rate of 0.1 h^{-1} (Table 2.7) and were used as constraints in the flux balance analysis.

Table 2.7. Flux constraints in mmol / g biomass hour for the studied physiological cases

Medium	Consumed ammonium	Consumed glucose	Biomass	Consumed inorganic phosphate	Consumed sulphate
FPM	3.9835	4.8489	3.7879	0.3000	1.7275
C-lim FPM	3.9835	0.9600	3.7879	0.3000	1.7275
N-lim FPM	0.3984	4.8489	3.7879	0.3000	1.7275
S-lim FPM	3.9835	4.8489	3.7879	0.3000	0.1728
P-lim FPM	3.9835	4.8489	3.7879	0.0300	1.7275

The changes in the distribution of fluxes when the biomass composition was varied were first investigated for the case when the medium constituents were not limited for C, N, S or P. Then the differences when an environmental limitation was imposed on the

system were analysed comparatively. The 44 biomass constituents could be grouped under functional categories (Table 2.8).

Table 2.8. Categorization of biomass constituents

Functional group	Constituents
Amino acids	L-alanine, L-arginine, L-asparagine, L-aspartate, L-cysteine, L-glutamine, L-glutamate, glycine, L-histidine, L-isoleucine, L-leucine, L-lysine, L-methionine, L-phenylalanine, L-proline, L-serine, L-threonine, L-tryptophan, L-tyrosine, L-valine
Lipid/steroid constituents	Phosphatidate, phosphatidylcholine, phosphatidylethanolamine, 1-phosphatidyl-D-myo-inositol, phosphatidylserine, triacylglycerol, ergosterol, zymosterol
Nucleosides and deoxynucleosides	ATP, ADP, AMP, CMP, GMP, UMP, dTMP, dCMP, dGMP, dAMP
Storage and wall carbohydrates	Mannan, glycogen, alpha-alpha-trehalose, 1,3-β-glucan
Inorganic substances	Sulphate, orthophosphate

Alterations in the amount of either constituent induced changes in the fluxes in the TCA cycle and the redox metabolism, however, these changes were not coupled to the glycolytic and gluconeogenic fluxes at all times and they were never coupled with the glycerol production or utilization.

Variations in the amounts of amino acid constituents induced changes in redox metabolism, the TCA cycle, folate metabolism, glycolysis, gluconeogenesis and serine-glycine-threonine metabolism. Variations in proline, phenylalanine and threonine content induced changes in the glutamate metabolism, whereas variations in glycine, serine, glutamate and proline content induced changes in the pentose phosphate shunt.

The changes in the lipid and steroid content of biomass induced changes in similar pathways to those that were responsive to variations in amino acid content. Additionally, fatty acid metabolism was also affected.

The redox metabolism and the tricarboxylic acid cycle were affected from changes in the nucleotide and deoxynucleotide content of the biomass. Only dTMP, dAMP and AMP induced changes in glycolysis and gluconeogenesis. Phosphoenolpyruvate pathway was affected only from changes in the GMP content and the folate metabolism was only affected by the dAMP and dTMP content.

The redox metabolism, the TCA cycle, folate metabolism, glycolysis, gluconeogenesis and serine-glycine-threonine metabolism were affected from changes in storage and wall carbohydrate content as well as the pathways converting pyruvate to alcoholic compounds.

Orthophosphate content only induced changes in the redox metabolism and the tricarboxylic acid cycle whereas sulphate also induced additional changes in the pentose phosphate shunt and the pathways converting pyruvate to isoamylalcohol and butyl alcohol.

Forcing the metabolism to optimize the distribution of its fluxes under carbon limitation caused an overall decrease in the non-zero fluxes in the biological system on which forced biomass changes were not imposed. Only when the AMP content of the biomass was doubled, the overall distribution of non-zero fluxes was larger than that observed when the environment was not carbon limited. This unexpected increase in intracellular fluxes would be an indicator of very inefficient use of metabolic enzymes, thus might indicate an unrealistic combination of nutritional limitation and biomass constituent variation. Non-zero fluxes were smaller when the orthophosphate content was varied, AMP and dGMP content was increased or glutamate, methionine or ADP content of biomass was decreased indicating a more efficient utilization of metabolic activity.

The magnitude of fluxes was lower under N-limitation, similar to the observations for C-limitation. However, unlike the case observed for carbon limitation, nitrogen limitation did not cause a decrease in the magnitude of fluxes in wild type yeast cell. On the other hand, manipulation of the biomass content only caused increase in the magnitude of fluxes except for the decrease in AMP content of the biomass. Specifically decreasing the glycine, serine, leucine, proline, valine or mannan content of biomass or increasing

ATP or sulphate content caused an increase in the magnitude of metabolic fluxes. The flux distribution was induced by any change in dGMP content.

The magnitude of flux distributions were lower in yeast cells grown under sulphate limitation in all cases regardless of the manipulation of the biomass components. Specifically, changes in the lipid and steroid content of the cell as well as its amino acid content caused many non-zero fluxes to diminish. This finding would be an indicator of how metabolic cellular response rearranges itself to optimize its survival under strict nutritional limitations.

Alterations in the ATP content, increasing the leucine, glycogen or mannan content, decreasing the ADP, PI or asparagine content of the cell would induce the metabolic fluxes under phosphorous limitation.

2.3.4. Conclusions and future prospects

This study highlighted the significance of plasticity and biomass contents in predicting flux distributions. In broad terms, carbon or nitrogen limitations were observed to cause an overall decrease in the metabolic distribution of enzymatic fluxes. This change was thought to occur as an attempt of the organism to more efficiently utilize its already decreased resources. The observed decrease might directly be attributed to decreased influx of nutritional supplements in addition to the metabolic efforts to enable the optimization of available resources on a stricter balance sheet.

An interesting outcome of constraining the uptake of sulphur into the organism was identified as only the lowering of overall fluxes whenever a change in the biomass content induced a change in flux distributions. The availability of extracellular sulphur was strictly related to the lipid and steroid content of the cell and this finding would require further investigation of the mentioned association. The relationship between the increase in the storage carbohydrate content of the cell and the limited availability of phosphate also requires further investigation.

In conclusion, the effect of changing the biomass composition caused different parts of the metabolic pathway to become active or inactive in the *in silico* predictions in which yeast model was subjected to different metabolic constraints representing growth in different nutrient concentrations causing limitation in most of the cases. Therefore, it is important to understand how the environment affects metabolism and its regulation (plasticity) in order to increase the predictive power of FBA. For this purpose, further studies were conducted in order to investigate how yeast cells dynamically respond to environmental perturbations and how genetically altered yeast cells respond to nutrient limitation.

3. INVESTIGATION OF TRANSIENT CHANGES IN YEAST METABOLISM IN RESPONSE TO AN ENVIRONMENTAL PERTURBATION

Transient changes in yeast metabolism were investigated as a response to two different nutritional perturbations involving glucose or ammonium, which are (respectively) among the most highly abundant carbon and nitrogen sources for yeast. The re-arrangement in the organism both at the transcriptome and the metabolome levels were considered of interest. In the first part of this chapter, the transcriptional response of yeast cells to variations in the availability of nutrients in an otherwise carefully controlled environment is presented. In the second part of the chapter, the additional information provided by the endometabolome were discussed in conjunction with the transcriptome and the two sets of data were overlaid on metabolic pathways to get a more comprehensive view of how yeast seeks for alternative paths to cater for its energy and other requirements. The last section of this chapter introduces a still on-going study on the application of transient high throughput data providing information at various levels (metabolite and gene expression levels, in this particular case) for the prediction of novel interactions among genes through the integration of protein-protein interaction, epistatic interaction and transcription factor-gene interaction networks as well as the metabolic network.

3.1. A comparison of how yeast re-programs its transcriptional profile in response to different nutrient impulses

3.1.1. Background

The ability of a microorganism to adapt changes in its physicochemical (e.g. temperature [54], pH [55]) or nutritional [56, 57] environment is crucial for its survival. The yeast, *Saccharomyces cerevisiae*, has developed mechanisms to respond to such environmental changes in a rapid and effective manner; such responses may demand a widespread re-programming of gene activity [55, 58]. This is especially true of changes in the nutrient environment and the ability to sense and respond to changes in nutrient availability is essential for cells from both unicellular and multicellular organisms. Glucose is the most abundant monosaccharide on earth and is the preferred carbon source for most

organisms and, accordingly, changes in glucose availability often have profound consequences in many types of cell [59]. The introduction of glucose to a culture of *S. cerevisiae* cells growing by respiration evokes changes at both the level of gene expression and of metabolism, with several proteins being activated or deactivated and gene expression being completely re-programmed to accommodate the switch from respiration to fermentation. Carbon catabolite repression down-regulates the expression of genes that encode enzymes involved in gluconeogenesis, the Krebs cycle, respiration, mitochondrial development, and the utilization of carbon sources other than glucose, fructose or mannose [60]. While the main effect of glucose is exerted at the transcriptional level [61], changes in mRNA and protein stability are also involved in the process [62, 63].

Ammonium assimilation in yeast occurs through its incorporation into glutamate, the source of nearly 80% of all cellular nitrogen [64]. Growth on ammonium causes a decrease in the activities of the enzymes used to assimilate less favourable nitrogen sources. This phenomenon is termed nitrogen catabolite repression, although the effect is not as well characterised as its carbon counterpart, particularly with respect to sudden changes in ammonium availability. Much less is known of the cellular response to sudden changes in the concentration of ammonium available to the cell. It should be noted that, while ammonium is not one of the most preferred nitrogen sources for *S. cerevisiae*, the yeast grows well on ammonium and its presence evokes nitrogen catabolite repression [65]. Ammonium is taken via two high-affinity permeases (Mep1p and Mep2p) as well as by a low-affinity permease (Mep3p). The expression of the GDH1, GLN1, and GAP1 genes is regulated by the concentration of ammonium present in the growth medium [65, 66]. The expression of nitrogen-regulated genes is controlled by both positively (Gln3p and Nil1p) and negatively acting proteins (Nil2p and Dal80p). In addition, it has been shown that the TOR kinases play an essential role in preventing the expression of nitrogen-regulated genes [65], and they probably have an important integrative role.

Several investigations of the transient responses of yeast metabolism to a sudden change in nutritional availability have been carried out. Kresnowati *et al.* [56] have investigated the transient short-term transcriptome and metabolome response of yeast cells to glucose perturbation in chemostats and have indicated that both the transcriptomic and metabolomic changes mediate two kinds of response – one concerned with the transition

from fully respiratory to respiro-fermentative metabolism and the other with the increase in growth rate that is the consequence of an increase in nutrient supply. Ronen and Botstein [57] have investigated the transient transcriptional response to switching carbon sources between galactose and glucose and concluded that experimental designs that involve short-term transient perturbations may be useful in understanding dynamic metabolic regulatory networks. The transient response to nitrogen catabolite repression was investigated by introducing an ammonium pulse into a glutamine-limited culture [66] and showed that the ammonium-induced repression was not due to a generalised stress response but, instead, represented a specific signal for nitrogen catabolite regulation. The effect of sulphate or phosphate limitation in the growth medium, together with uracil and leucine deficiency, was also investigated and it has been deduced that the cells adjust their growth rate to nutrient availability and maintain homeostasis in the same way in both batch and steady-state conditions [67].

In this study, the dynamic re-organization of yeast's cellular activity was analysed by following the short- and long-term transcriptomic response to a sudden relaxation of either carbon and nitrogen limitation by an impulse of glucose or ammonium, respectively. The experimental design was such that the specific perturbation was uniquely introduced into an otherwise carefully controlled environment. Thus a glucose impulse was given to a steady-state glucose-limited culture and an ammonium impulse to a corresponding ammonium-limited steady-state culture. The response of the yeast cells was monitored at the transcriptomic level until the steady state was re-established. Thus the time-scale of this investigation ranged from seconds to hours, allowing the elucidation of both the metabolic and regulatory switches that enable yeast cells to adapt to, and recover from, a transient change in nutrient availability. We believe that this study makes a significant contribution to our understanding of nutritional control in yeast since the response is studied over both short and long time-scales for two different nutrients under well-*controlled physiological conditions.*

3.1.2. Methods

3.1.2.1. Strain and Growth Conditions. Wild type BY4743 (*MAT**a**/MATα his3Δ/his3Δ leu2Δ/leu2Δ LYS2/lys2Δ MET15/met15Δ ura3Δ/ura3Δ*; [23]) was cultivated in 2L

fermenters (Applikon®) with 1L working volume under aerobic conditions in glucose- or ammonium-limited F1 media [24] in chemostat mode at a dilution rate of $0.1h^{-1}$. Temperature and pH were controlled to $30^{o}C$ and pH 4.5, respectively. Fermenters were stirred at 800 rpm which, together with constant air flow at a rate of 0.1 vvm, provided dissolved oxygen at $\geq$ 80% dO_2 saturation at all times during cultivation.

3.1.2.2. Pulse Injections and Sampling. After the 150^{th} hour of continuous fermentation, when the chemostat had spent > 5 residence times at steady state, the limiting nutrient was injected into the fermentation broth aseptically to provide non-limited F1 Medium concentrations for that nutrient. 50 ml of 40% (w/v) glucose or 50 ml of 6.26% (w/v) $(NH_4)_2SO_4$ were sufficient to provide 2% (w/v) glucose and 0.313% (w/v) $(NH_4)_2SO_4$ concentrations in the growth media. The mixing of the pulse injection was complete within milliseconds. Duplicate samples were collected at steady state prior to the impulse and as soon as the nutrient was injected, 3 samples were collected at the 20^{th}, 40^{th} and 60^{th} seconds, 4 more samples were taken with 5-minute intervals within the first 20 minutes. Hourly samples were collected for five hours, and another sample was taken two hours after the last hourly sample. At that point, > 95% of the fermentation broth had been replaced with fresh medium, either by means of sampling or due to the nature of continuous cultivation. After the 210^{th} hour, when the chemostat had spent more than 5 residence times at steady state after the impulse disturbance, duplicate samples were collected at the second steady state. Samples for transcriptome analyses were collected at every time point. Biomass was determined gravimetrically at the two steady states.

3.1.2.3. Sampling for Transcriptome Analysis, RNA Isolation and Transcriptome Analysis. A culture sample (20 ml) was centrifuged at 4000 rpm for 3 min. Most of the supernatant was discarded, allowing re-suspension of cells in a small volume of growth medium. The cell suspension was released into liquid nitrogen and stored at $80^{o}C$ until RNA isolation. Total RNA was isolated as described by [68]. Total RNA was qualitatively assessed on an Agilent 2100 Bioanalyser (Agilent Technologies) and quantified using Nanodrop ultra- low-volume spectrophotometer (Nanodrop Technologies). cDNA was synthesised, and double-stranded cDNA was retrieved from ca.15μg of total RNA as described in the Affymetrix GeneChip® Expression Analysis Technical Manual, using appropriate kits. cDNA was checked for quality using the Agilent 2100 Bioanalyser and

was quantified using Nanodrop. Biotin-labelled cRNA was synthesized and was purified using clean up kits and it was quantified using the Nanodrop spectrophotometer before hybridization. Hybridization and loading onto Affymetrix Yeast2 arrays were carried out as described in the GeneChip® Expression Analysis Technical Manual. The chips were then loaded into a fluidics station for washing and staining using Microarray Suite 5 with EukGe W S2v4 programme. Lastly, the chips were loaded onto the Agilent GeneArray scanner 2500 and another quality check was performed using Microarray Suite 5 [69].

3.1.2.4. Microarray Data Acquisition and Analysis. The raw data files were assessed with dChip software for outliers at the array level as well as at the probe-set level [70]. Different nutritional conditions (glucose and ammonium pulse experiments) were treated as different sets and were assessed for their quality control separately. RMA Express software was then used to normalize the data, again as two separate data sets [71]. The data was $\log_2$ transformed prior to analysis. In compliance with MIAME guidelines [72], the microarray data from this study has been submitted to ArrayExpress at the European Bioinformatics Institute under accession number E-MTAB-643.

In order to identify transcripts whose expression significantly differed from steady-state levels following the nutrient pulse [73, 74], the software package EDGE [75] was used. For dimension reduction in principal components and partial least squares analysis, PLS Toolbox in MATLAB 2007a environment was utilized. Microsoft Excel Built-In commands were used to calculate the Pearson correlation coefficients of the transcriptome at the first steady state and the rest of the sampling times. All p-values were corrected for the false positives introduced by multiple testing using Bonferroni correction and 10^{-3} was selected as the cut-off threshold for p-values. The Benjamini-Hochberg method was used for the calculation of false discovery rates. GeneCluster 2.0 [76] was used for clustering via self-organizing maps and Hierarchical Clustering Explorer (HCE) 3.0 [77] was used for hierarchical clustering purposes. The significantly enriched functional categories and the process ontology terms of the genes falling into the same cluster were determined by Saccharomyces Genome Database GO Term Finder tool [78] or AmiGO Term Finder tool [79]. The threshold p-value was selected as 10^{-3}. Transcription factors (TF) were taken from two sources TRANSFAC Professional Gene Transcription Factor Database [80] and

YEASTRACT [81] and TFs that are common in both databases were considered in further analyses.

3.1.2.5. Dynamic Regulatory Events Miner Analysis. Bifurcation points were determined using hidden-input/hidden-output Markov model based software, DREM - The Dynamic Regulatory Events Miner as described by the authors [82]. Different nutritional perturbations, where glucose and ammonium sulphate were introduced into their corresponding limited cultures, were analysed independently. The chromatin immunoprecipitation experiments (chip-CHIP experiments) from which the TF-gene interactions were acquired were garnered from [83, 84].

3.1.3. Results and Discussion

The immediate, as well as the adaptive (long-term), response to the release from nutritional limitation, followed by the system's slow return to the nutrient-limited steady state was investigated using a systems biology approach. Glucose (as a carbon source) and ammonium (as a nitrogen source) were injected into their respective nutrient-limited cultures in two matched fermenters operated in fully controlled chemostat mode. Samples for transcriptome analysis were taken at different time intervals, ranging from seconds to hours, until the culture had reached a second steady state.

3.1.3.1. Correlation Analyses of Genome-wide Expression Profiles. The change in the transcriptional program of *S. cerevisiae* upon suddenly switching to a surplus of a single, previously limiting, nutrient was first investigated by comparing the array data to the preceding glucose- or ammonium-limited steady state using Pearson correlation coefficients. Introduction of glucose into the limiting medium was observed to have a pronounced and immediate effect, with a continuous decrease in correlation until the 16^{th} minute after the injection, transcript levels determined in later samples were found to be more correlated with those observed at the first steady state (Figure 3.1). In contrast, the transcriptional response of the ammonium-limited cells to an ammonium impulse was more subtle, with the Pearson correlation coefficient between each sample and that from the preceding steady state always >0.95 (Figure 3.1). It had been reported previously that

carbon limitation evoked a more profound transcriptional response from yeast than other limitation for other primary nutrients, i.e. nitrogen, sulphur or phosphorus [85, 86].

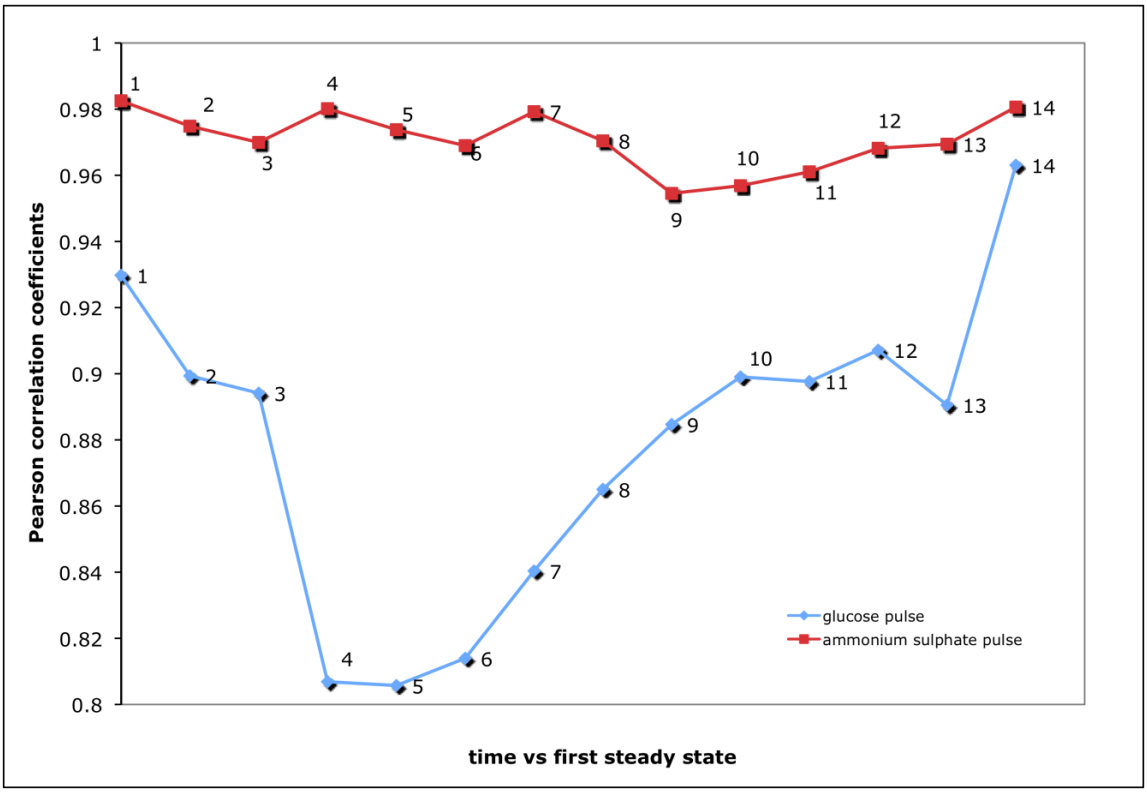

Figure 3.1. Correlation analysis of genome-wide transcriptional response with each data point corresponding to samples collected at 20, 40 and 60 sec, 8, 16, 24 and 32 min, 1, 2, 3, 4, 5 and 7 h and the 2nd steady state in comparison to the 1st steady state

3.1.3.2. Temporal Organization of the Global Transcriptional Response. Correlation analysis of the transcriptome data from cells released from glucose limitation clusters samples taken within the first hour following the glucose impulse and separates them from the samples from the later time points. More detailed analysis allows a further partitioning of these two main temporal clusters. The response observed in the first minute, the first hour, the first three hours, and the rest of the sampling times following the glucose impulse were found to be clustered into distinct groups, the last of which had very similar transcriptome profile to that of the preceding glucose-limited limiting steady state. This clustering analysis revealed that the transcriptional responses obtained in the first minute were quite similar as was the case for the response in the first hour. Following the first

hour, the transcriptional response was observed to be moving towards that of the steady states (Figure 3.2a).

The release from ammonium limitation, by providing an ammonium impulse, revealed a very different transcriptional response to that observed upon release from glucose limitation, in that the re-programming of gene expression started later and took longer both to complete and to return to the steady-state profile. Thus, the transcriptome profile recorded 20 sec. after the ammonium impulse was not significantly different to that of the preceding steady state. The profiles of cells collected 40 and 60 sec post-impulse were clustered with those from the 8 and 16 min samples and were still closely related to the steady state. The main impact of the ammonium impulse on gene transcription is seen in the period between 24 min and 3 h post-impulse, while the period 4-7 h post-impulse represents a slow return to the steady-state profile (Figure 3.2b).

The individual temporal transcriptional profiles were also clustered via self-organizing maps to distinguish the general dynamic trends in transcriptional response of yeast cells, growing in either glucose- or ammonium-limiting chemostats at steady state, to a glucose or ammonium impulse. The transcriptome profiles fall into 81 clusters in the response to glucose perturbation and 49 clusters in that to ammonium perturbation (taking into account confidence intervals about the centroids). The impact of the impulse can be expected to last for 7 h at a dilution rate, $D = 0.1\ h^{-1}$. Changes in the concentration of the limiting nutrient supplemented by an impulse in the chemostat excluding the consumption by cellular growth and maintenance and the biomass concentration within the growth vessel were modelled as shown in Figure 3.3. This figure will be the same for both the glucose and the ammonium impulses and mid-length and longer-term responses were observed at similar times for both perturbations. However the short-term responses to the two impulses differed markedly. The short-term response to the ammonium impulse started later and was more prolonged than that to glucose. Moreover, the ammonium impulse triggered an oscillatory, rather than a sustained response in some of the transcript levels.

3.1.3.3. Genes showing a significant change in expression level in response to the nutrient impulses. Gene ontology (The Gene Ontology Consortium, 2000) biological process terms

associated with genes showing a significant change in their transcript levels in response to a nutrient impulse are shown in Table 3.1.

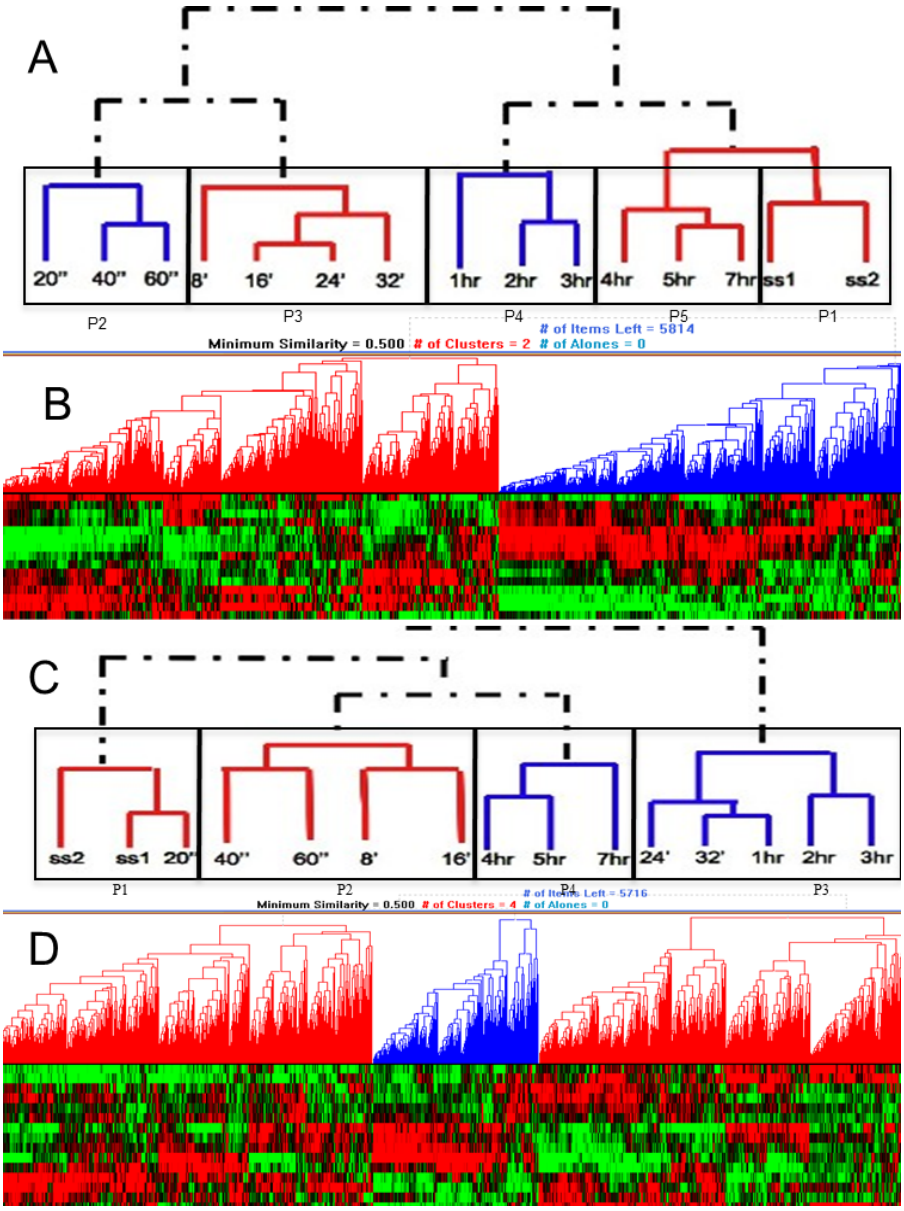

Figure 3.2. Hierarchical clustering of the dynamics of liberation from glucose ((a) and (b)) and from ammonium limitation ((c) and (d)) with Pearson correlation coefficient as the distance metric and the time spans indicated as periods annotated from P1 to P5

A glucose impulse was found to elicit significant changes in the transcript levels of 372 genes which are associated with the following biological process terms: carboxylic acid metabolic processes; aspartate, glutamine, methionine and serine family amino acid metabolic processes; purine metabolic processes; glycolysis; oxidative phosphorylation;

alcohol catabolic processes; energy-coupled proton transport (Table 3.1). Kresnowati *et al.* [56] studied the changes in transcript levels during the first 6 min following a glucose impulse and have also reported significant changes in transcript levels belonging to energy, purine ribonucleotide, amino-acid metabolism, and signal transduction functional categories in the MIPS classification as a short-term response to shifting from glucose limitation to conditions where glucose was in excess.

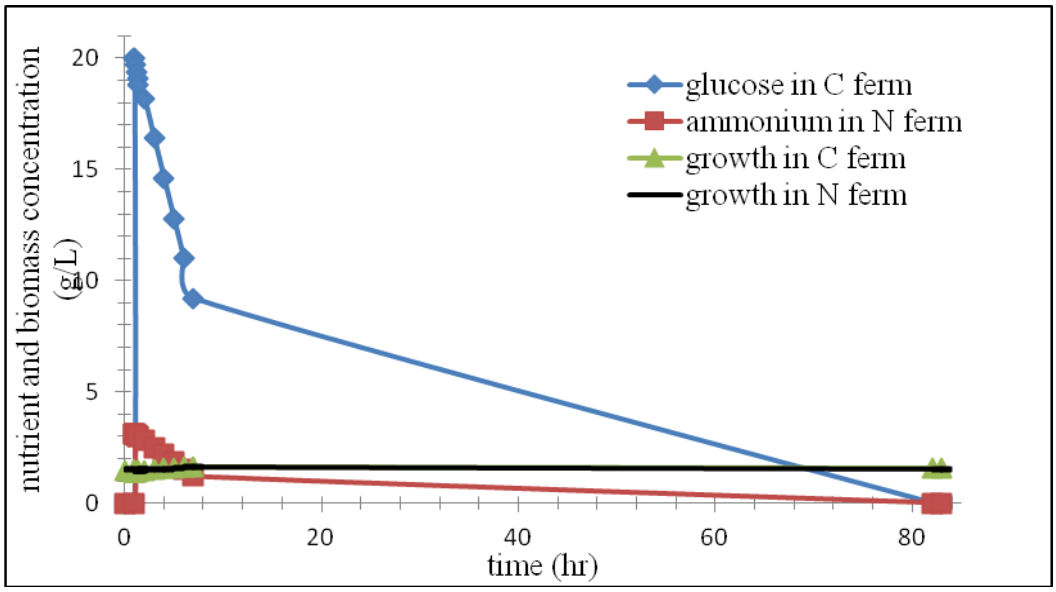

Figure 3.3. Dilution of pulse

Transcripts that showed a significant response to the glucose impulse were placed into 8 co-responding clusters (c0 to c7; Figure 2.4a) using self-organizing maps [87]. Six of these clusters could be associated with a biological process GO term. Glucose stimulated the expression of 138 genes significantly associated with 'translation' term and the maximum response was recorded within the first hour following the impulse (c0 and c4). For 33 genes, the increase in their transcript levels occurred later, reaching its highest level in the last three hours (c2, Figure 2.4a); this cluster was enriched for genes associated with the term 'glycolysis'. A group of transcripts significantly enriched with in carboxylic acid metabolic processes were immediately down-regulated with excess glucose in the fermentation medium, the expression levels slowly recovering to the initial carbon-limited state after the first 10 minutes following the glucose pulse (c3).

Table 3.1. Gene Ontology (GO) annotations to differentially expressed genes

Significantly Associated Process GO Term	**p-value**	**Fraction of the Subset Associated with the Term**	**Fraction of Transcriptome Associated with the Term**
Carbon Catabolite Repression			
Carboxylic metabolic processes	4.07×10^{-21}	74 / 372	344 / 6353
Aspartate family amino acid metabolic processes	1.09×10^{-6}	17 / 372	48 / 6353
Glutamine family amino acid metabolic processes	2.35×10^{-4}	11 / 372	27 / 6353
Methionine family amino acid metabolic processes	1.69×10^{-3}	10 / 372	26 / 6353
Serine family amino acid metabolic processes	9.85×10^{-3}	13 / 372	37 / 6353
Purine metabolic processes	2.37×10^{-9}	17 / 372	35 / 6353
Glycolysis	4.20×10^{-8}	13 / 372	22 / 6353
Oxidative phosphorylation	4.79×10^{-8}	18 / 372	46 / 6353
Alcohol catabolic processes	1.19×10^{-7}	19 / 372	54 / 6353
Energy coupled proton transport	3.81×10^{-7}	11 / 372	17 / 6353
Nitrogen Catabolite Repression			
glycolysis	3.95×10^{-16}	15 / 369	22 / 6353
gluconeogenesis	5.85×10^{-6}	9 / 369	15 / 6353
Proton transport	8.02×10^{-6}	11 / 369	21 / 6353
Oxidative phosphorylation	2.98×10^{-4}	14 / 369	46 / 6353
Aspartate family amino acid metabolic process	5.38×10^{-4}	14 / 369	48 / 6353
Amino acid and derivative metabolic process	4.19×10^{-3}	36 / 369	273 / 6353

The glucose impulse also rendered the expression of genes associated with aerobic respiration low in the first half-hour after pulse. During this period of excess glucose, the expression of oxidative phosphorylation genes, including the ATP synthesis pathway, were found to be down-regulated after the first minute following the perturbation (c7). This result is also in good agreement with the observation that gene clusters exhibiting a significant enrichment in energy and metabolism MIPS functional categories were down-regulated immediately (within 120-210 seconds) after the glucose pulse [54].

Introduction of glucose also immediately stimulated the expression of genes associated with the sulphate assimilation pathway (c5) but, as the glucose levels started to decline again, the genes associated with this pathway were down-regulated gradually after the first hour and later recovered to levels similar to that of the preceding steady state. Expression of genes for transcription factors related to sulphur metabolism were also up-regulated within 5 minutes following the introduction of glucose [56]. This is most likely to be associated with methylation, reflecting the huge demand for the post-transcriptional processing of rRNA to sustain the transiently boosted growth rate.

The transcripts in clusters c1 and c6 (Figure 3.4a) displayed a sustained response of either up- (c1) or down-regulation (c6) throughout the experiment after the introduction of the glucose pulse. However, analysis of the genes in these clusters failed to reveal their significant (p-value < 10^{-4}) enrichment for any GO biological process category. Among the genes in c1 (the cluster displaying sustained up-regulation following the glucose impulse) were a sub-group of transcripts that were related to methylation: *SAM1* and *SAM2*, whose products are S-adenosylmethionine synthetases. It has previously been reported that an increase in growth rate requires Sam1p, and further increases results in yet more demand for methyl donors to sustain rRNA modification, also requiring higher levels of Sam2p, a close homolog of Sam1p [85]. This supports the idea that the initial stimulation of the expression of genes concerned with sulphur metabolism is associated with the increased demand for methyl donors. Five members of the alcohol catabolic process, namely *PFK1*, *PFK2, ENO2, TKL1* and *CTS1* were also members of the up-regulated cluster c1. Cluster 6 contains genes that displayed sustained down-regulation following the glucose impulse and included several amino-acid metabolism genes: *CIT2*, *CPA2*, *IDP2, ARG1* and *CPA1* in the glutamine family amino-acid metabolic process; *LYS20*, *LYS21*, *LYS9* and *HOM3* in the

aspartate family amino acid metabolic process; *HOM3*, *CYS4* and *FPR1* in homoserine metabolic process, as well as four members of the nicotinamide nucleotide metabolic process, *PYC1*, *PYC2*, *ADH2* and *ALD4*.

Interestingly, the transcript levels of genes for glucose transporters did not go through any major change in response to a sudden shift from glucose-limited to glucose-abundant conditions. Expression of the high-affinity glucose transporters would be expected to be fully de-repressed during the preceding glucose-limited steady state. However, of the genes encoding high-affinity glucose-repressible hexose transporters, only *HXT7* displayed a significant down-regulation in the level of its transcript immediately following the pulse. Transcript levels for the other three genes encoding high-affinity glucose transporters *(HXT2, HXT4* and *HXT7*) are up-regulated from 1 h post-impulse as the glucose concentration in the growth medium starts to fall.

Published values [88] for the poly (A) tail lengths of all mRNA molecules were checked in order to identify any possible differences in mRNA degradation since no direct measurement was available. The down-regulated transcripts were not found to be significantly enriched with short poly (A) tails neither for carbon or nitrogen catabolite repression with the distribution of poly (A) tail length among up- and down-regulated transcripts appearing to be random. Since the shortest mRNA half-lives in yeast were in the range of 3 to 6 minutes [89], even the transcripts of the samples taken within the first minute are likely to be the result of an increase in transcription activity rather than mRNA degradation.

Relieving nitrogen limitation in the fermentation with an ammonium impulse resulted in significant changes in the transcription levels of 369 genes. The members of this gene set are significantly enriched for GO bioprocess annotations associated with: central carbon metabolism, including glycolysis; gluconeogenesis; proton transport and oxidative phosphorylation; as well as amino acid production pathways, such as aspartate family amino acid metabolic process and amino acid and derivative metabolic process (Table 3.1).

A similar clustering of genes with a significant change in their transcript levels following the ammonium impulse, using self-organizing maps, produced 9 groups with

bioprocess GO terms that can be significantly associated with each subset (Figure 3.4b). It was observed that the cells respond to the ammonium impulse more slowly than they do to a carbon impulse.

Down-regulation of the transcripts clustered in c0 started after the first minute displaying a sharp decrease in the expression levels after the first hour. This cluster was significantly enriched for glycolytic genes whose expression levels recovered towards the second steady state. Another cluster (c1), which was also significantly enriched with glycolytic genes, exhibited a delayed up-regulated transcriptional profile. This indicated that recovery from nitrogen limitation allowed the yeast cells also to utilize glucose better, thus resulting in down-regulation of glycolytic genes in mid-length response periods and then an up-regulation towards the cessation of the effect of the pulse as the re-establishment of high glucose concentrations resulted in the cells switching back into fermentative metabolism. Clusters significantly enriched with oxidative phosphorylation and trans-membrane ion transport processes were observed to display a down-regulation trend having the most distinct down-regulation between the 3^{rd} and the 5^{th} hours, recovering towards the second steady state (c6 and c3, respectively). This might have been due to the presence of excess glucose repressing respiration-related events during this latter period.

The transient abundance of ammonium led to an up-regulation of genes concerned with the process, and regulation, of translation. This up-regulated expression profile was displayed at the minute and hour timescales in c2, c5, c7, and c8. Clusters that were significantly enriched with 'translation process' terms (c5, c7 and c8) were also significantly enriched for 'cellular biosynthetic process' (p-value $< 10^{-25}$ (c25), and p-value $< 10^{-37}$ (c8)), which indicated an up-regulation of growth-related events following a release from ammonium limitation. The induction of growth also required a higher demand for the methylation of tRNAs and rRNAs. The expression level of *SAM1* in c2 was also observed to be up-regulated as is the case for the glucose impulse.

The expression levels of transcripts that were enriched with cation transport process were sharply turned off around the first hour following the pulse (c4). Among the members of this cluster, an ammonium permease, Mep2p, works in conjunction with Pmp1p, Pmp3p

and Pma1p to facilitate the trans-membrane transport of the slightly acidic ammonium during the uptake of the nitrogen source. This might have been due to the fast consumption of ammonium at that time, altering the intracellular pH, which resulted in the down-regulation of the relevant genes, only to be up-regulated again at later time points.

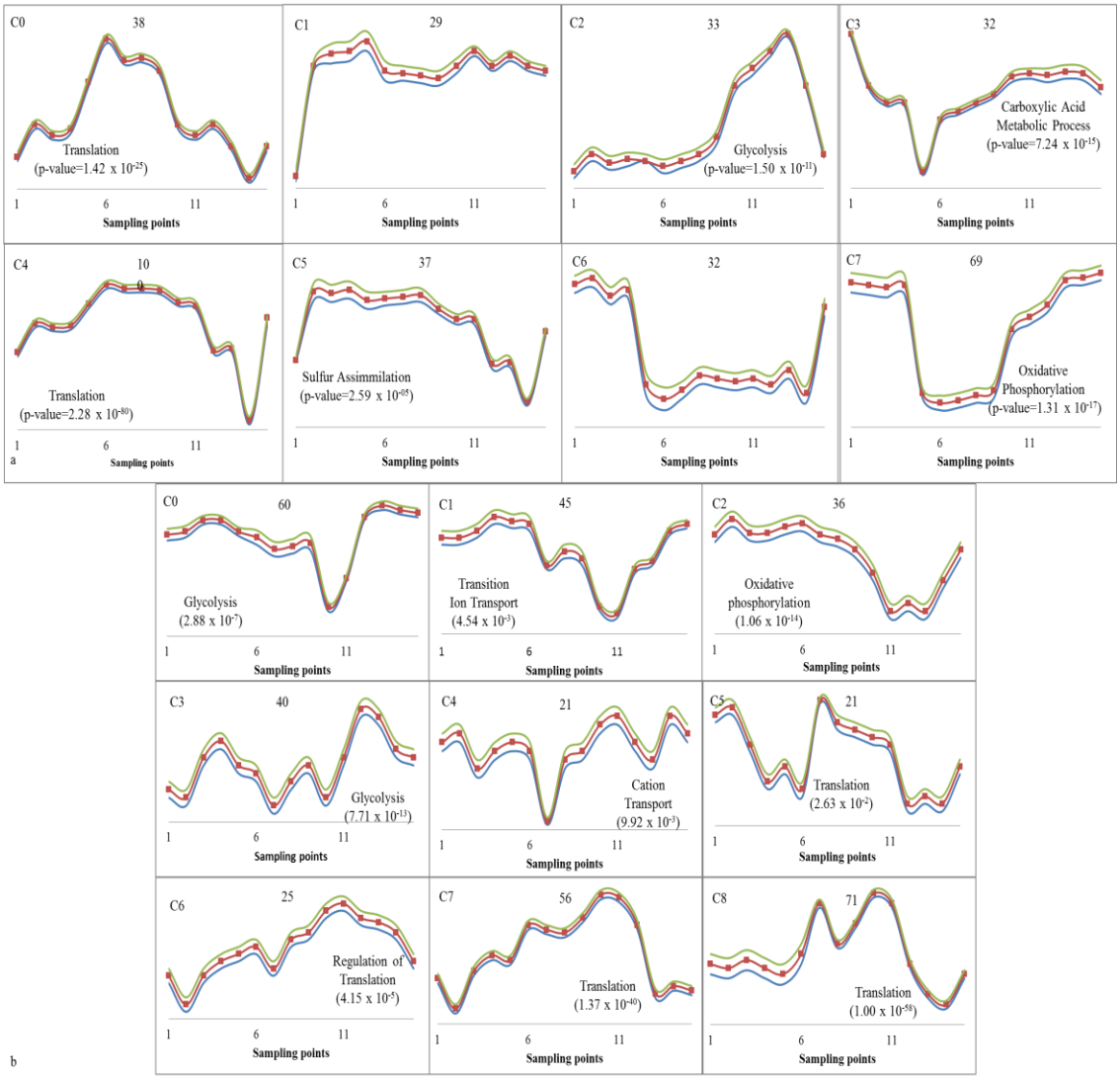

Figure 3.4. Clustering of significantly expressed transcripts in glucose (a) or ammonium (b) perturbations with the number of genes in each cluster shown in top centre and enclosing lines indicating the confidence interval around the centroids

3.1.3.4. Dynamic transcriptional reprogramming of the cell during transition created by a nutrient impulse. Temporal organization of dynamic regulatory events within the transcriptional response of yeast cells to a nutrient impulse was investigated using a systems-based approach, namely Dynamic Regulatory Event Miner (DREM) [82]. A

hidden-input/hidden-output Markov model integration of protein-DNA interactions and dynamic transcriptome data has been used in the Dynamic Regulatory Events Miner. The dynamic programming of the cells in response to nitrogen and carbon catabolite repression was identified using bifurcation points corresponding to times where expression of a subset of genes diverges from the rest under regulation of one or more transcription factors using DREM - Dynamic Regulatory Events Miner software [82]. Regulation of the response to nutritional perturbation for switching to glucose and ammonium surplus was investigated separately.

Perturbing the glucose-limited system with abundant glucose resulted in a complex regulatory behaviour (Figure 3.5a). Immediately after the introduction of glucose, the surplus resulted in a bifurcation into four branches. Up-regulated and down-regulated pairs of branches displayed similar characteristics with the only difference being their levels of expression with respect to the initial steady state. Regulatory events related to glucose-sensing signal transduction (Mth1p), stress conditions (Msn2p and Msn4p), respiration (Hap2p), early meiosis (Swi4p and Ume6p), significantly affected this quadruple split. The transcripts in the upper up-regulated branch were significantly associated with microtubule-associated complex component GO term while the ones in the lower up-regulated branch were associated with the tRNA modification term. It has been reported previously that autophagosomes are attached to microtubules for their delivery to the vacuole and autophagocytosis is significantly stimulated during nutrient deprivation [90]. Release from glucose limitation may have thus caused a re-programming of the genes associated with these processes. This lower branch further split at the 32nd minute with the upper set of transcripts being significantly enriched with the ER membrane component term while the expression of genes constituting the lower part were significantly enriched with proteasome complex process GO term. Autophagosome formation was previously reported also to be associated with the ER membrane [91]. The transcripts in the lower down- regulated branch were enriched for aerobic respiration while those in the upper down-regulated branch were enriched for retrograde transport process GO terms. As the cascade of regulatory events proceeded, a new set of bifurcations was observed at the 32nd minute following the glucose induction. Ino4p; a transcription factor required for de-repression of inositol-choline-regulated genes involved in phospholipid synthesis was responsible for this onset of a late response in the upper down-regulated branch. Following

this split, the transcripts found in the upper division were significantly enriched for G1-specific transcription in the mitotic cell cycle term while the genes in the lower division were enriched for the retrograde transport process GO term (Table 3.2).

Table 3.2. Gene Ontology enrichment of transcripts following bifurcation that was controlled by transcription factors

	Branch of Down-regulated Transcripts			**Branch of Up-regulated Transcripts**		
Case	**TFs**	**Process GO Terms**	**p-value**	**TFs**	**Process GO Terms**	**p-value**
Carbon Catabolite Repression	Mth1p, Msn2p, Msn4p, Hap2p, Swi4p, Ume6p	ion trans-membrane transporter activity	5.3×10^{-5}	Mth1p, Msn2p, Msn4p, Hap2p, Swi4p, Ume6p	endoplasmic reticulum membrane	4.7×10^{-5}
		G1-specific transcription in mitotic cell cycle	5.0×10^{-3}		microtubule associated complex	2.8×10^{-3}
		aerobic respiration	8.4×10^{-5}		tRNA modification	1.0×10^{-3}
		retrograde transport	8.1×10^{-3}		proteasome complex	1.3×10^{-3}
Nitrogen Catabolite Repression	Hms1p, Mga1p, Msn1p, Phd1p, Hap2p	ion trans-membrane transport	5.9×10^{-3}	Gcr2p	ribosome biogenesis and assembly	2.9×10^{-3}

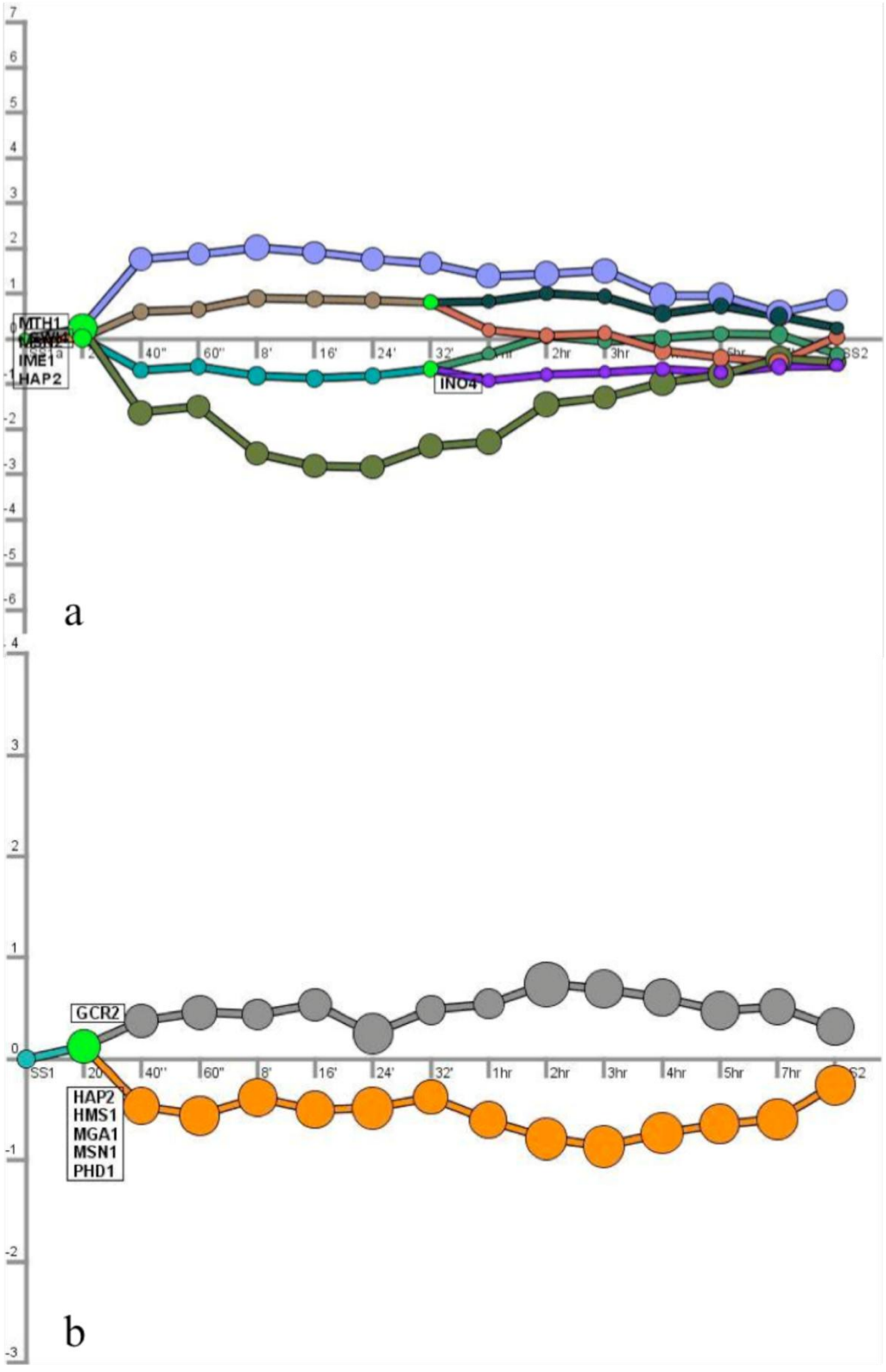

Figure 3.5. Identification of bifurcation points under carbon (a) or nitrogen catabolite repression (b) with the average expression of a set of transcripts represented as a single branch and the size of the circles indicating the variance in expression levels for that time

Pulse injection of ammonium sulphate into fermentation medium after prolonged periods of limitation resulted in a bifurcation of transcripts into up-regulated and down-regulated branches (Figure 3.5b). However, the observed response was delayed for 20 seconds, similar to what has been observed by the hierarchical clustering of sampling time points from the transcriptome data. Similar to the findings here, the first sampling point (20 seconds after the pulse injection) was clustered together with the initial and final steady-state samples. A single transcription factor, Gcr2p; glycolysis regulatory protein, was found to be significantly responsible for the split of the up-regulated branch with transcripts significantly enriched for ribosome biogenesis and assembly. Five transcription factors four of which were related to nitrogen starvation directly (Hms1p, Mga1p, Msn1p and Phd1p); also regulating pseudohyphal growth, suppressing pseudohyphal growth defects of ammonium permease mutants and pseudohyphal differentiation, as well as another transcription factor activating respiratory gene expression (Hap2p) were significantly associated with the down-regulated branch of transcripts which were enriched for ion trans-membrane transport (Table 3.2).

The dynamic re-programming of the cells in response to a perturbation causing a change in nutrient availability exhibits a more complex pattern when carbon limitation is relieved than when ammonium was added to nitrogen-limited culture. Additionally, the change in the expression levels of the sub-set of genes in an individual ‘branch’ identified by the DREM analysis is much more coherent in response to the glucose impulse than in response to the ammonium impulse. The glucose impulse resulted in an almost immediate sub-division of the transcripts into four branches under the control of the Mth1p, Msn2p, Msn4p, Hap2p Swi4p and Ume6p transcription factors and, after a further half an hour, two of the four branches bifurcate, one of the new sub-branches being under the control of Ino4p. The up-regulated transcripts following the initial sub-division were enriched for genes with microtubule-associated complex and tRNA modification GO terms, while down-regulated transcripts were enriched for genes with ER membrane, proteasome complex, aerobic respiration, retrograde transport and G1-specific transcription in the mitotic cell cycle GO terms.

The transcripts responding to the ammonium impulse bifurcate into two branches 20 seconds after the ammonium impulse. Gcr2p was the transcription factor identified as

responsible for the up-regulated branch while Hap2p, Hms1p, Mga1p, Msn1p and Phd1p were those responsible for the down-regulated branch. The expression of genes involved ribosomal activities was up-regulated while that of genes involved in ion transport was down-regulated during this perturbation.

3.1.4. Study conclusions

The dynamic re-organization of gene expression in *S. cerevisiae* cells in response to a sudden relaxation of either carbon or nitrogen limitation has been examined over both short and long time-scales using a system-based integrative approach. The observation of the genome-wide response at both levels, in a wide-ranging time span from seconds to hours, revealed metabolic and regulatory switches of yeast cells to adapt to and recover from an impulse-like perturbation.

Analysis of transcripts that were significantly responsive to the relaxation from nutritional limitations indicated that several metabolic processes were affected at distinct time scales. Following the glucose perturbation, the changes in expression levels of transcripts were more pronounced and sudden when compared to the relaxation from ammonium limitation. Clustering of the transcriptional profiles of the significantly expressed genes revealed the time-dependent up- or down-regulation of specific processes in both cases. In response to additional glucose in the fermentation broth, the cells responded by significantly changing the expression level of transcripts whose gene products take part in translation, sulphur assimilation, glycolysis, carboxylic acid metabolic process and oxidative phosphorylation processes. The yeast cells respond to the availability of additional nitrogen source, by displaying a significant change in the expression level of transcripts enriched with translation, regulation of translation, and transition ion transport process ontology terms.

The dynamic re-programming of the cell in response to carbon catabolite repression displayed a complex behaviour, which was regulated by the glucose-sensing signal transduction, stress, respiration, late G1-specific transcription and early meiosis controlling transcription factors. Dynamic analysis of the transcriptome revealed, for the first time, the up-regulation of genes enriched with the microtubule-associated process term as well as

the down-regulation of genes associated with the retrograde transport term. A further delayed bifurcation occurred under the regulation required for the de-repression of inositol-choline-regulated genes involved in phospholipid synthesis, *INO4*. This delayed re-organization, after 30 minutes, of the genes associated with endoplasmic membrane, proteasome and G1-specific transcription revealed the presence of a more complicated organization of the yeast cells to the return to carbon limitation conditions. The nitrogen catabolite repression resulted in a single bifurcation of transcripts into up-regulated and down-regulated branches with a delayed response in comparison to what has been observed for the carbon catabolite repression. A single transcription factor; *GCR2*, responsible for the regulation of glycolysis, was found to be significantly responsible for the split of the up-regulated branch whereas nitrogen starvation, respiration and pseudohyphal growth regulating transcription factors; *HAP2*, *HMS1*, *MGA1*, *MSN1* and *PHD1*, were significantly associated with the regulation of the down-regulated genes.

The presented study revealed the importance of long-term analysis of the response to the relaxation from nutritional deprivation to understand the molecular basis of the dynamic behaviour of the cells. A further detailed systems-based study that integrates additional levels of functional genomics analyses may provide further information on the dynamic re-organization of yeast cells to changing environmental conditions.

3.2. Long-term dynamic response to changing nutritional environment and time dependent re-organization of yeast cells

3.2.1. Background

The survival of a free-living microorganism depends on its ability to deal with changes in its physicochemical environment, including variations in temperature [54], pH [55] or nutritional availability [56, 57, 92-94]. Appropriate mechanisms to deal with such changes rapidly and effectively have been developed over evolutionary time, and the expression of more than half of yeast's genes has been observed to change in response to environmental perturbations [55, 58]. The mechanism underlying the sensing and the utilization of glucose, which is the most abundant monosaccharide on earth and most preferred carbon source for most organisms, are of particular importance and have been

studied extensively (see [59]).

Glucose has a central role in yeast metabolism, both as both a nutrient and a regulator. The introduction of excess glucose into the growth environment of respiring *Saccharomyces cerevisiae* cells switches metabolism to the fermentative mode, inducing various signal transduction pathways and causing several proteins to be activated or inactivated. Carbon catabolite repression, which is the ability of glucose to repress the expression of several genes that encode enzymes involved in gluconeogenesis, respiration, mitochondrial development, and the utilization of carbon sources other than glucose, fructose or mannose [60]. The regulation and control determined by the availability of glucose may be exerted occurs at different levels; however, its main effect has been reported to take place at the transcriptional level [61]. The increase in growth rate invoked by the introduction of glucose into a carbon-limited culture was observed to cause a distinctive restructuring of yeast's transcriptional profile. The Snf1-Rgt pathway has a specific, but limited, role in this response, while protein kinase A and Sch9p are responsible for triggering more than 90% of all glucose-induced changes, including those to the respiratory and gluconeogenic pathways [95]. Similarly, an increase in medium glucose concentration has been associated with a pronounced drop of adenine nucleotide content and the interconversion of adenine nucleotides and inosine was proposed to provide a rapid and energetically cost-efficient mechanism of adaptation [96].

Ammonium is assimilated in yeast via its conversion into glutamate [64]. Although glutamate, itself, is the most preferred nitrogen source for the organism, laboratory strains of yeast grow very well on ammonium as the principal source of nitrogen [65]. Thus, on ammonium-based media, yeast cells decrease the activities of enzymes involved in the utilization of poor nitrogen sources – a phenomenon termed nitrogen catabolite repression. The cellular response to sudden changes in the amount of available ammonium has been studied much less than an equivalent transition for glucose (see above).

The transient response of the yeast metabolism to rapid changes in nutrient availability was investigated in several studies. The transient short-term transcriptome and metabolome response of yeast cells to glucose perturbation in continuous cultures was investigated by Kresnowati *et al.* (2006) who interpreted the changes at both the

transcriptomic and metabolomic changes to reflect two major responses: one involving the transition from fully respiratory to respiro-fermentative metabolism, and the other involving the preparation for an increase in growth rate [56]. Ronen and Botstein investigated the transient transcriptional response to switching carbon sources between galactose and glucose and their experimental design proved useful in elucidating the dynamic regulatory networks controlling central carbon metabolism [57].

In order to investigate nitrogen catabolite repression ter Shure *et al*. (1998) investigated the transient response to an ammonium impulse by glutamine-limited yeast cultures [66]. Their study revealed that the ammonium-induced repression did not represent a general stress response but, rather, the relief of ammonium limitation was a specific signal for nitrogen catabolite regulation.

The previous chapter on the transcriptomic responses of yeast cells to the sudden and transient relief of nutrient limitation encompassed both glucose and ammonium responses. When a glucose impulse was applied to a glucose-limited chemostat culture, we found significant changes in the levels of transcripts related to translation, glucose transport, oxidation reduction, nucleobase, nucleoside and nucleotide metabolic process, cell death, aerobic respiration ion transport, sulphur assimilation, glycolysis, carboxylic acid metabolism, and oxidative phosphorylation. The transcriptomic response of ammonium-limited yeast cells to an ammonium impulse indicated significant changes in the expression of genes involved in translation and its regulation, ribosome biogenesis, non-coding RNA metabolism process (including rRNA biosynthesis and maturation), as well as transition ion transport. Thus, for both nutrient impulses, there was a response that could be attributed to the increase in growth rate [85], and another that was specific to the nutrient whose limitation was relieved [86].

In the present study, an integrative approach was used to map long-term dynamic transcriptome and metabolome data onto metabolic pathways and used such maps to reveal the important molecular events that occur in particular pathways at distinct temporal phases following the transient relief of nutrient limitation. This is the first study to encompass both the transcriptomic and metabolomic responses of yeast from an initial nutrient-limited steady, through the period of nutrient excess engendered by a glucose or

ammonium impulse, to the re-establishment of the nutrient-limited steady state. Thus the complete cycle of famine, feast, and famine to which yeast is thought to be frequently exposed in nature has been followed.

3.2.2. Methods

3.2.2.1. Data acquisition. The dynamic transcriptome data were obtained from the previously described chemostat experiments in response to a nutritional perturbation (Section 3.1.2.).

3.2.2.2. Sampling and extraction of the endometabolome, analytical methods for fingerprinting. For metabolic fingerprinting, 5ml of sample was rapidly quenched in 60% (v/v) methanol buffered with tricine at -50^{o}C and the endometabolites were extracted in boiling 75% (v/v) ethanol buffered with tricine at 80^{o}C as described by Castrillo *et al.* (2003) [97]. The vacuum-dried samples were stored at -80^{o}C until analysis. For both foot printing and fingerprinting, derivatization and identification of peaks via GC-ToF-MS were performed as described by Pope *et al.* (2007) [98]. The dynamic metabolome data is provided in Appendix C.

3.2.2.3. Identification of gene expression in co-clustered time spans and mapping of the transcriptome and the metabolome on metabolic pathways. The hierarchical clustering of the transcriptome and the metabolome data were carried out using Hierarchical Clustering Explorer (HCE) 3.0 [77] with the distance metric selected as the Pearson correlation. The periods were identified from the determined clusters. The gene expression levels in each period were statistically confirmed to display insignificant differences within a single period using the Student's t-test with a significance threshold of 0.05. The geometric means of the log.-transformed expression levels in each period were then calculated. The differences in log mean values for the periods following a perturbation and the period consisting of the succeeding or preceding steady-state data (expressed as fold changes in either expression and in the amount of the measured metabolite) were mapped onto the metabolic pathways. Consideration of each period separately enabled the dynamic overview of the decision making involved in the pathway preferences.

The complementary nature of transcriptome and endometabolome data was investigated by mapping expression levels and intracellular metabolite concentrations simultaneously onto metabolic pathways (SGD, http://pathway.yeastgenome.org:8555/expression.html). The direction and reversibility of the reactions were assessed using the KEGG database [99] and the Yeast 4.0 metabolic model [11].

3.2.3. Results and Discussion

In order to understand the dynamic re-organization of the cellular metabolism in response to the sudden and relaxation of glucose or ammonium limitation, a systems-based integrative approach, which maps both transcriptome and metabolome data onto metabolic pathways, was used to reveal the important molecular events that occur in specific pathways in distinct time periods following the perturbation. Re-organization of the pathways associated with the central carbon metabolism and energy homeostasis in yeast was given particular attention in this investigation.

Analysis of the time-course data revealed that the transcriptomic response following nutritional perturbations was organized into distinct periods or phases. The dynamic transcriptional and metabolic responses were clustered into five distinct hierarchical phases in case of the glucose impulse and the phases formed by the clusters into which the responses fell, reflected the presence of a time-scale dependent effect that the responses displayed; the steady states phase (P1), the seconds phase (P2), the minutes phase (P3), the early-hours response (the first three hours) (P4) and the late-hours response (the rest of the sampling period) (P5). On the other hand, a delayed response to the perturbation of the ammonium level was observed rather than a time-scale dependent response as it was the case for the glucose perturbation. The phases developed such that the first sample collected within the first minute (the 20^{th} second sample) was clustered together with the steady states (P1), the remaining two samples collected in the first minute (20^{th} and 40^{th} seconds) were clustered together with the first two samples collected within the first hour (8^{th} and 16^{th} minutes) (P2), the remaining two samples collected in the first hour (24^{th} and 32^{nd} minutes) were clustered together with the response obtained in the early hours (the first three hours) (P3). The rest of the sampling period was clustered together separately from

the other phases (P4) (Figure 3.6).

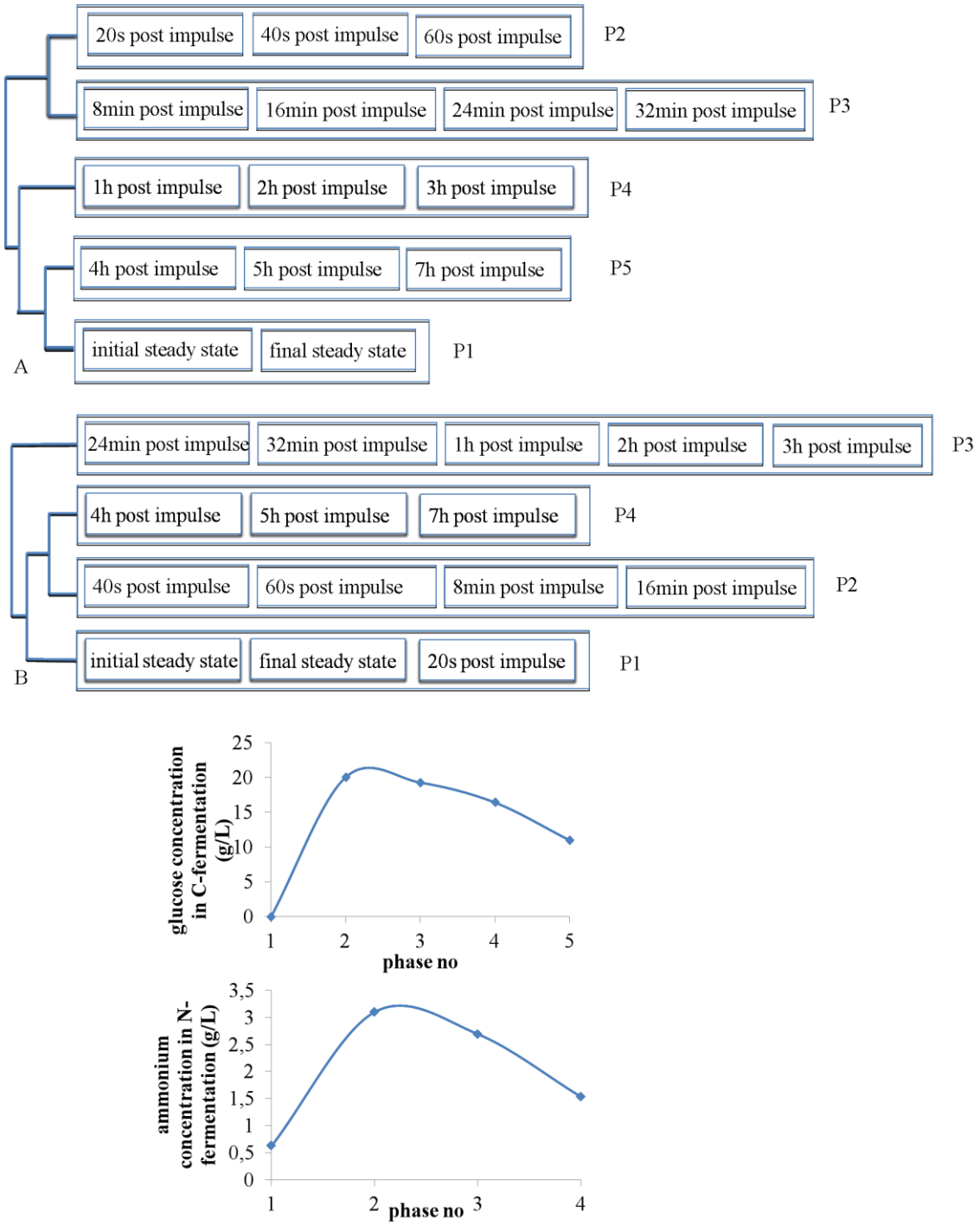

Figure 3.6. Hierarchical organization of the response to the impulse like addition of glucose (a) or ammonium (b) and the dynamic change in the concentration of the catabolite in its respective culture

The investigation of the endometabolomic response to the relaxation from carbon

limiting conditions did not display any time dependent organization. Previous findings also revealed that carbon sufficiency played an important role in the arrangement of endometabolome for different growth rates and glucose sufficient and deficient cases could not be clearly separated by means of principal component analysis [85]. The intracellular concentration of TCA cycle intermediates, sugar derivatives and amino acids were the highest in the later hours following the impulse like addition of glucose. An accumulation of intracellular amino acid derivatives within the cell were observed towards the depletion of additional nutrient introduced into the medium as the cells switched back their metabolism to down regulate the transcripts involved in translation and growth associated events.

As a response to the impulse like addition of ammonium, the endometabolome of the limiting steady state conditions were clustered together and the samples taken at hourly basis could be distinctly identified in a separate cluster from the samples taken within the first minute. On the other hand, the samples taken within the first hour following the impulse ammonium injection were distributed within these two clusters. The dynamic profiles of the intermediary products related to lipid and sphingolipid metabolisms and phosphatidylinositol signalling pathway indicated a decrease in concentration until P3, and then recovering towards the second steady state. The intracellular concentration of amino acids and intermediates decreased sharply with extracellular supplementing of ammonium and recovered gradually as the extracellular ammonium concentration gradually became limited.

The difference in log mean average of each period and the steady-state period corresponding to fold changes in the expression and metabolite levels were calculated for the phases P2 -P5 in the case of glucose pulse experiment, and for P2 - P4 in the case of ammonium pulse experiment. These differences were mapped onto the selected metabolic pathways (Figure 3.7). Consideration of each phase separately enabled a dynamic overview of the cellular decision-making involved in the pathway selection to be obtained (Figure 3.8).

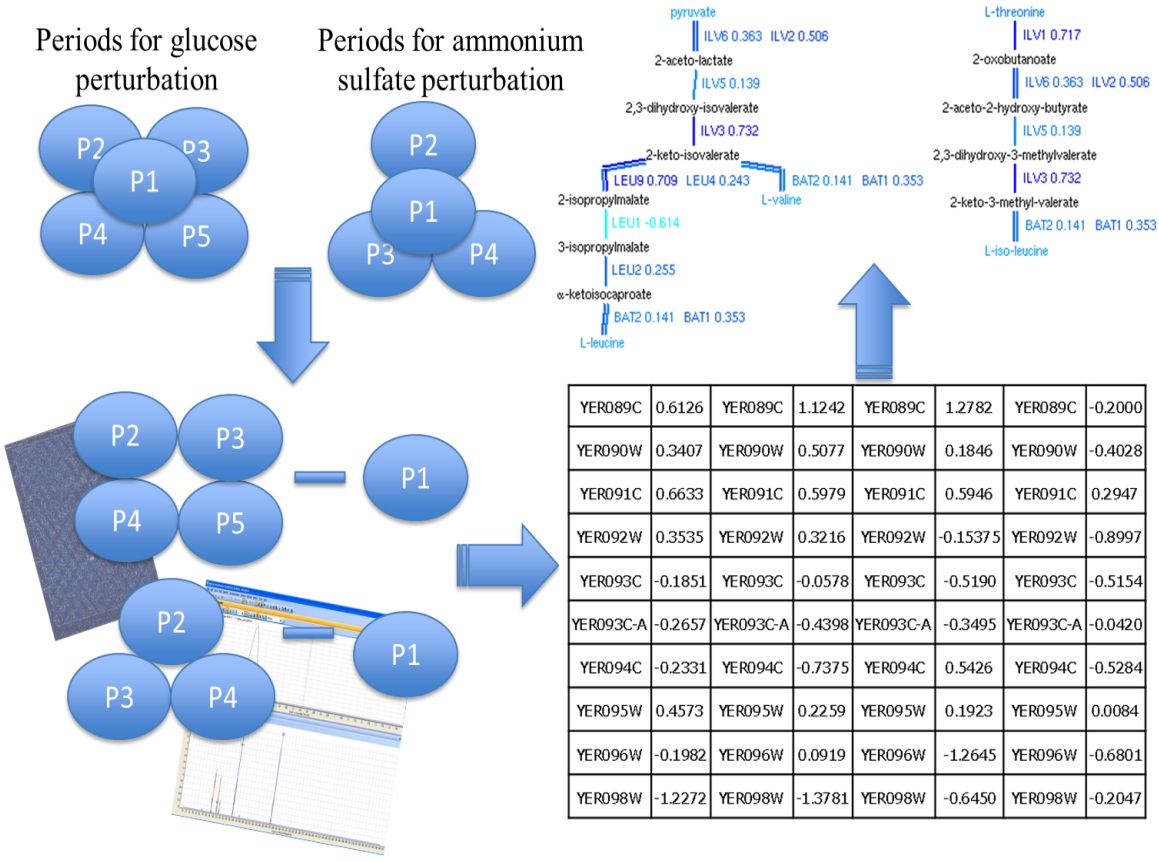

YER089C	0.6126	YER089C	1.1242	YER089C	1.2782	YER089C	-0.2000
YER090W	0.3407	YER090W	0.5077	YER090W	0.1846	YER090W	-0.4028
YER091C	0.6633	YER091C	0.5979	YER091C	0.5946	YER091C	0.2947
YER092W	0.3535	YER092W	0.3216	YER092W	-0.15375	YER092W	-0.8997
YER093C	-0.1851	YER093C	-0.0578	YER093C	-0.5190	YER093C	-0.5154
YER093C-A	-0.2657	YER093C-A	-0.4398	YER093C-A	-0.3495	YER093C-A	-0.0420
YER094C	-0.2331	YER094C	-0.7375	YER094C	0.5426	YER094C	-0.5284
YER095W	0.4573	YER095W	0.2259	YER095W	0.1923	YER095W	0.0084
YER096W	-0.1982	YER096W	0.0919	YER096W	-1.2645	YER096W	-0.6801
YER098W	-1.2272	YER098W	-1.3781	YER098W	-0.6450	YER098W	-0.2047

Figure 3.7. A schematic overview of the data overlying process

3.2.3.1. Changes in the Central Carbon Metabolism. Introduction of glucose into a carbon-limited steady-state culture induced changes in the levels of both transcripts and metabolites involved in the TCA cycle, glycolysis, gluconeogenesis, and glucose fermentation pathways. The down-regulation of the TCA cycle and up-regulation of the glycolytic pathways leading towards ethanol production was observed in response to a perturbation in the amount of glucose. Several other studies also describe switch towards a respiro-fermentative metabolism within 5 minutes upon addition of glucose into a continuous culture [56, 96]. A strong and immediate down-regulation of the expression *HXK1*, *HXK2* and *GLK1* was observed (i.e. in phases P2 and P3, 20-60 sec and 8-32 min post-impulse). This immediate response remains unchanged for nearly an hour post-impulse, although these genes are up-regulated in the later phases of the experiment. Most of the genes that encode enzymes in the lower part of the glycolytic pathway were up-regulated during all phases compared to their expression levels at limiting glucose conditions. Walther *et al.* (2010) have also reported an increase in the phosphorylated sugars of the glycolytic pathway following a relief from glucose limitation, which is

congruent with the present findings [96]. Pyruvate may be considered as a critical branch point, where the flux may be directed towards either the TCA cycle or the fermentation pathway. *PDC1*, *PDC5* and *PDC6* were up-regulated in response to the glucose perturbation, shifting energy metabolism towards fermentation; this up-regulation was particularly marked in the case of *PDC5* in P2 and P3, but decreased in P4 and P5. Kresnowati M. T. A. P. *et al*. (2006) have also reported an up-regulation of *PDC1* and *PDC6* within 5 minutes of the addition of glucose into the medium of a carbon-limited culture growing on glucose [56]. Complementing this flux, *ADH4* was selectively up-regulated starting in P3 and reached even higher expression levels in P4 and P5. On the other hand, *ADH2*, *ADH3* and *ADH5* were down-regulated throughout the experiment. Kresnowati M. T. A. P. *et al*., (2006) have also reported a down-regulation of *ADH5* as a fast response to a glucose pulse in their system [56]. *ADH1*, in contrast, followed a similar pattern to *PDC5*, being initially up-regulated in P2 and P3 and then down-regulated in P4 and P5. The *ALD* family of genes are involved in directing the flux from acetaldehyde towards the production of acetic acid were down-regulated specifically in P3 and P4 (Figure Appendix D1 a1).

The impulse-like addition of ammonium to a steady-state nitrogen-limited culture also provoked changes in central carbon metabolism. The genes involved glycolysis were slightly up-regulated in P2 and P4 whereas they were down-regulated in P3. Consequently, the fluxes were selectively distributed towards both ethanol and acetate in P2 and P4 following the pyruvate branch point. On the other hand, in P3, similar to the observations for carbon catabolite repression, a strong down-regulation of *HXK1*, *HXK2* and *GLK1* was observed as well as of *ALD4* and *ALD6*, thus limiting the direction of flux towards acetate. Genes for enzymes in the ethanol production pathway were slightly up-regulated in response to the addition of ammonium except for *ADH2*, which was down-regulated during P2, P3 and P4 (Figure Appendix D1 b1).

The genes encoding enzymes of the TCA cycle were down-regulated except for *PYC2*, *LSC1* and *LSC2*, which were slightly up-regulated in P2, and *ACO2*, which was up-regulated during P2 and P3, *MDH1* and *IDH2*, which were slightly up-regulated in P5. *DAL7* was strongly up-regulated during P2, P3 and P4. *DAL7* was also reported to take part in allantoin degradation in purine catabolic processes [100]. The induction of this gene

might have allowed the redirection of flux towards purine catabolism.

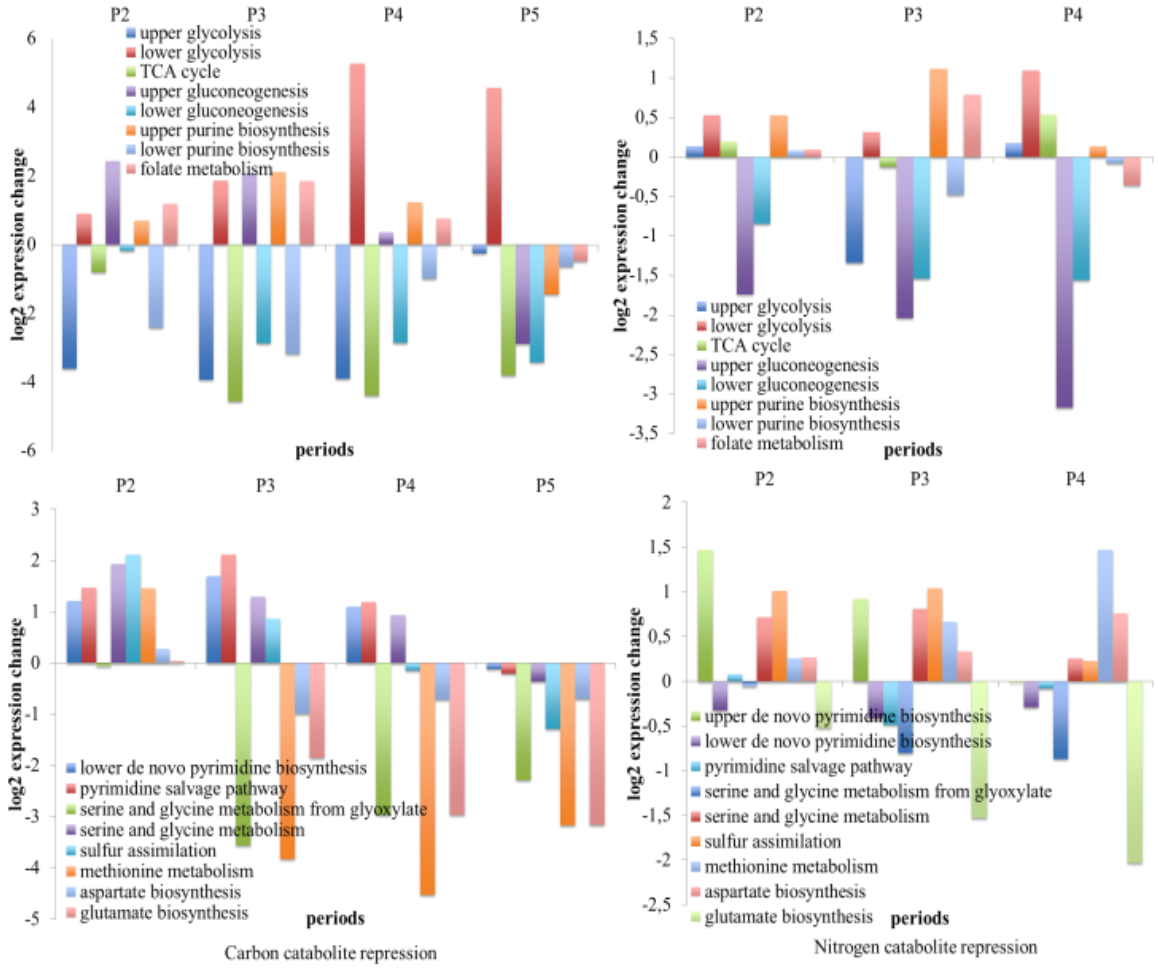

Figure 3.8. General trends displaying the changes in the $\log_2$ expression values of the genes in energy metabolism

The most pronounced down-regulation of the TCA cycle genes was observed during P3. The expression levels of genes encoding subunits of the succinate dehydrogenase complex (*SDH1*, *SDH2*, *SDH3* and *SDH4*) were all down-regulated throughout the effect of the pulse. *SDH1* and *SDH3* were previously reported to be down-regulated during carbon catabolite repression [56]. All of the identified and the measured metabolites; pyruvate, 2-oxoglutarate, succinate, fumarate and malate, showed a slight accumulation in the cells in all periods except for the steady states. This might be the result of the down-regulation of genes that specify enzymes which use these metabolites as intracellular intermediates (Figure Appendix D1 a2).

The genes encoding enzymes involved in the upper gluconeogenic pathway was induced upon the addition of glucose. *MAE1,* catalysing the production of pyruvate from malate, was up-regulated during P2, P3 and P4, gradually decreasing in time and it was down-regulated upon depletion of glucose in P5. The product of the reaction catalysed by this enzyme, pyruvate, is also a precursor for the synthesis of several amino acids including leucine, isoleucine, valine and alanine in addition to being a key intermediate in sugar metabolism [101]. Since *PYC1,* whose enzyme product takes part in the conversion of pyruvate to oxaloacetate, and *MDH2* were down-regulated throughout the effect of the impulse like addition of glucose and *PYC2* was down-regulated during P3-P5, it could be deduced that pyruvate was used as in the amino-acid production pathways upon relief from the glucose limitation as well as in ethanol production. Down-regulation in *PCK1* and *FBP1* is more pronounced after P2. The down-regulation of *MDH2* and *FBP1* upon addition of glucose following a long period of glucose limitation is in accordance with previous findings suggesting the degradation of the enzymes encoded by these genes through a vacuolar degradation pathway [102]. *FBA1* and *PGI1* were slightly down-regulated in P2 and P3 while it was slightly up-regulated in P4 and P5 (Figure Appendix D1 a3).

The expression levels of the TCA cycle genes were not constitutively up- or down-regulated relative to their levels at steady state but they displayed phase-dependent expression upon relaxation of ammonium limitation. *PYC1* was responsive to the addition of ammonium starting with P3 when its expression decreased, and the lowest expression value of this gene was detected in P4. On the other hand, *PYC2* (its paralog), was down-regulated immediately at P2 and it was up-regulated in P3, settling to its steady-state expression level in P4. The citrate synthase, *CIT3* and the malate dehydrogenases, *MDH1* and *MDH2* were down-regulated throughout the experiment; whereas the other citrate synthases *CIT1* and *CIT2* were only down-regulated in P3 and P4, taking more time for their expression levels to decrease. A gene encoding a putative mitochondrial aconitase, *ACO2,* was slightly up-regulated and that for isocitrate lyase, *ICL1,* was down-regulated during P2-P4. On the other hand, *ACO1* was up-regulated in P2 and down-regulated during P3-P4. *IDH1*, *IDH2*, *LSC1* and *LSC2* were up-regulated in P2 and P4 whereas they were down-regulated in P3. *KGD1*, *FUM1* and *MDH3* were down-regulated in P3 while *KGD2* and the succinate dehydrogenases *SDH1*, *SDH2*, *SDH3* and *SDH4* were initially up-

regulated in P2 and down-regulated in P3 and P4. *MLS1*, enabling the glyoxylate shunt, was down-regulated during the periods P2-P4 when the effect of the ammonium impulse could be identified.

MLS1 was previously reported as being repressed on glucose [103]. The constant supply of sufficient glucose, probably perceived as being in excess by the cell, during the ammonium perturbation would explain the repression of *MLS1* in the cell. *DAL7* was only down-regulated in P2 and it was up-regulated in P3 and P4. It has been previously reported that *DAL7* is repressed under standard growth conditions [104]. The introduction of ammonium might have created a temporary situation in which the environment was relieved from all stresses that were created by the limitation of ammonium as well as being supplemented with sufficient but not excess amount of glucose (a balanced diet) causing the down-regulation of the expression of that gene in P2. Ammonium was used up during the course of the fermentation as the growth rate increased and as some of it was removed away from the chemostat due to the nature of continuous fermentation and the medium gradually shifted back towards the limitation of the nitrogen source,. In contrast, to the case of the carbon catabolite repression, the amount of the intermediate metabolite malate was lower in P2, P3 and P4 than it was during ammonium limitation (P1). This might be due to the low flux from fumarate and glyoxylate as a result of the down-regulation of *MLS1* and *DAL7* in P2, *MLS1* and *FUM1* in P3 and *MLS1* in P4. This might indicate that *MLS1* might be one of the most important factors determining malate accumulation (Figure Appendix D1 b2).

The expression of the gluconeogenic gene *PCK1*, whose enzyme product plays role in the conversion of oxaloacetate into phosphoenolpyruvate, decreased upon the addition of ammonium and this down-regulation was stronger in P4 than in P2 and P3. The accumulation of oxaloacetate was prevented by directing the fluxes towards citrate production in P2 and the expression levels of the genes encoding the enzymes catalysing this reaction; *CIT1* and *CIT2* increased. In P3 and P4, however, oxaloacetate accumulation would only be prevented through the activation of the aspartate biosynthetic pathway and the up-regulation of *AAT1* supports this observation. Interestingly, a similar response to relief upon glucose limitation was observed for *MDH2* and *FBP1*, which were both down regulated during P2-P4 although this down-regulation was more pronounced in P3 and P4.

This might indicate that the cells perceived nutrient limitation followed by its abundance through the same mechanisms regardless of the type of the nutrient being glucose or ammonium and this phenomenon requires further investigation (Figure Appendix D1 b3).

2.2.3.2. Re-organization of the Nucleotide Pools in Response to Catabolite Repression. The apparent loss of adenine nucleotides associated with the energy homeostasis, which follows the relaxation from nutrient-limiting conditions in yeast presents an important problem in the understanding of the mechanisms governing the respiro-fermentative transition. Kresnowati M. T. A. P. *et al*., (2006) reported that the immediate decrease in adenine nucleotide (AXP) pools following the relief from glucose limitation was not accompanied by any of the other three nucleotides (NXPs), but rather by the up-regulation of purine biosynthesis, C1 and sulphur metabolism [56]. In response to a glucose pulse, the set of genes with a significant change in their expression levels were previously reported to be involved in purine metabolism and methionine family amino acid metabolic processes. The previous results indicate that clusters of genes that were significantly up-regulated in response to a glucose impulse were found to be enriched with sulphur assimilation process gene ontology terms (Section 3.1.3). Transient accumulation of the purine salvage pathway intermediates IMP and inosine were also reported to account for the pronounced drop in the AXP pool by Walther T. *et al*. (2010) in a series of shake-flask cultivations using trehalose mimicking the growth of yeast on glucose-limited medium and they have reported that the interconversion of adenine nucleotides and inosine facilitates the rapid and energy-efficient adaptation of the AXP pool size to changing environmental conversions [96]. The accumulation and recycling of inosine could be considered as a response to energy homeostatic perturbations under fermentative conditions. AXP concentrations were reported to recover quickly to about 80% of their initial levels within 5-10 minutes whereas the GXP nucleotide concentration was reported to reach a novel steady state that was significantly higher than that prior to the addition of glucose [96].

Consistent with these studies, significant changes in the expression levels of the genes involved in glycolysis, oxidative phosphorylation, translation and aspartate family amino-acid metabolic process as a response to the relaxation from both carbon and ammonium limitation were observed (Section 3.1.3). In this study, in order to shed light on the mechanisms that counterbalance the reduction in AXP pools upon perturbation of

energy homeostasis through a pulse injection of a major nutrient, the yeast cells were analysed by using a systems biology approach. The transcriptomic and the metabolomic data were mapped onto the metabolic pathways that had been implicated to be involved in these processes in previous studies (Figure 3.9).

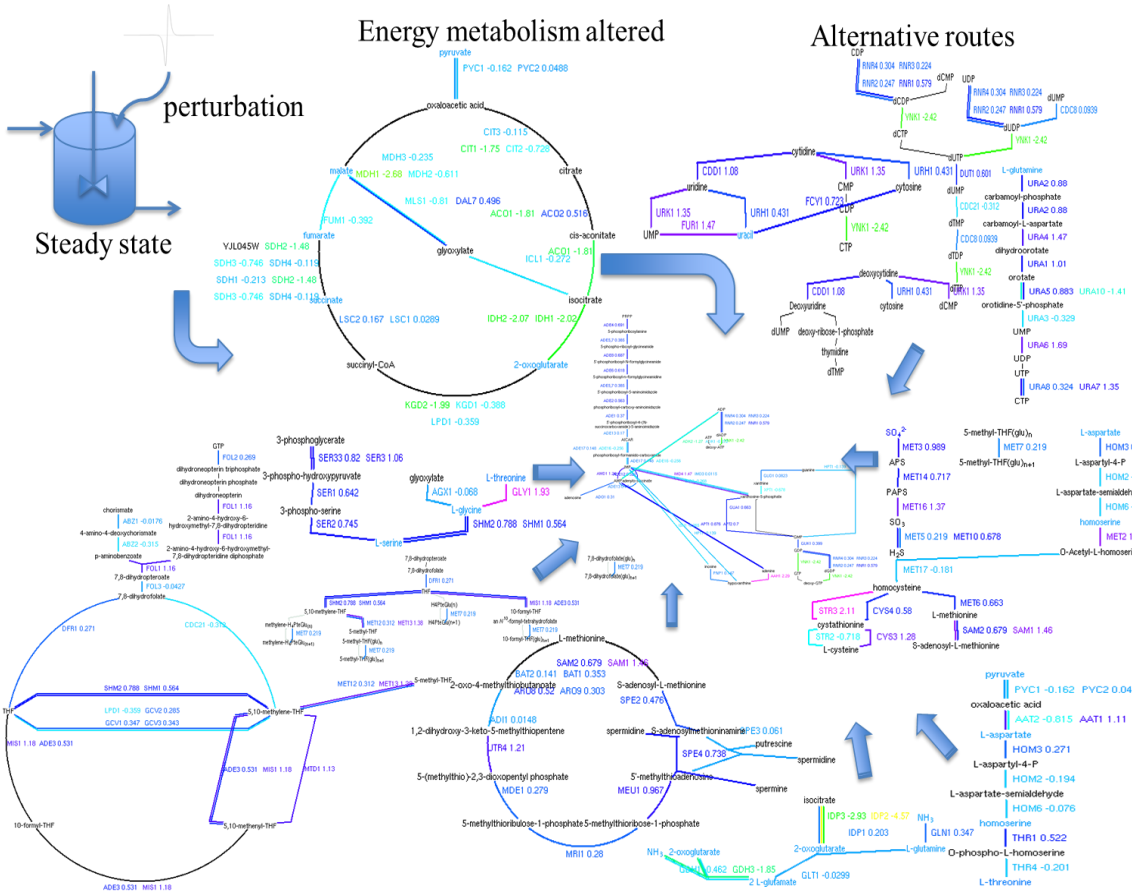

Figure 3.9. Re-arrangement of metabolism upon an impulse-like nutritional perturbation

3.2.3.3. Changes in the Purine and Pyrimidine Biosynthetic Pathways and their Salvage Pathways. Since the tricarboxylic acid cycle becomes inactivated upon addition of glucose, the cells require the activation of alternate routes to provide for the need for the purine nucleotides, ATP and GTP, to sustain energy metabolism. The initial steps of *de novo* synthesis of purine nucleotides were immediately activated as soon as glucose was introduced. The immediate up-regulation of the upper purine biosynthetic pathway upon glucose addition may be responsible for the accumulation of IMP, which was observed by Walther T. *et al*. (2010) [96]. This up-regulation was most pronounced during P3. The observation of the up-regulation in *ADE12*, *ADE13* and *AMD1* during P2-P4 indicated that the cyclic conversion of IMP to adenylosuccinate and AMP was possible. On the other

hand, the up-regulation of *SAH1* (whose product catalyses the release of adenine during methyl transfer from S-adenosyl-L-methionine to S-adenosyl-L-homocysteine) and the up-regulation of *ADO1* (encoding the enzyme that converts adenosine to AMP) may provide an alternative route for the production of AMP. However, the production of ADP from AMP was blocked by the down-regulation of *ADK1* and *ADK2* in P2. The UMP kinase encoded by *URA6*, up-regulated in this perturbation throughout P2-P4, has been reported to compensate for the lack of function in *ADK1* [105]. This might have been used as an alternative route for ADP production. *ADK1* and *ADK2* were observed to become progressively up-regulated through P3-P5 enabling ADP synthesis from AMP.

The accumulated IMP seems to be converted first to XMP and finally GMP by the catalytic action of the enzymes encoded by the up-regulated *IMD3-IMD4* and *GUA1*, respectively. GMP can then be converted to GDP by the product of *GUK1*, which was observed to be up-regulated throughout the experiment.

YNK1, encoding the nucleoside diphosphate kinase, catalysing the phosphorylation of ADP and GDP to ATP and GTP, respectively, was found to be down-regulated throughout the experiment. These results indicated that there might be some indirect routes for the production of ATP and GTP when the tricarboxylic acid cycle becomes inactivated upon addition of glucose. One possibility might be an equilibrium shift towards ATP production in the presence of abundant AMP and ADP, through *ADO1*, or the up-regulation of *GUK1* (encoding guanylate kinase) may catalyse the reaction between ADP and GDP to produce ATP. The produced GMP could then be recycled back to xanthosine-5-phosphate through *GUA1*, and then to IMP through *IMD3* and *IMD4* (Figure 3.10). Conversions between ADP and dADP, as well as between GDP and dGDP were identified to be active through the up-regulated transcripts; *RNR1*, *RNR2*, *RNR3* and *RNR4*.

TAD3 encoding the enzyme that converts adenosine to inosine was found to be up-regulated during P2-P5. Additionally, the up-regulation of *APT1*, *APT2* and *AAH1* may also account for the conversion of AMP to IMP, then to adenylosuccinate, then to adenine and then to hypoxanthine. *PNP1*, which is encoding the purine nucleoside phosphorylase, was also found to be up-regulated. This enzyme catalyses the reversible reactions between inosine and hypoxanthine as well as between adenine and adenosine. Therefore the

accumulation of inosine within 5 minutes upon glucose induction and a delayed accumulation of hypoxanthine within 10 minutes observed by Walther T. *et al*. (2010) [96] can be explained in the light of these observations.

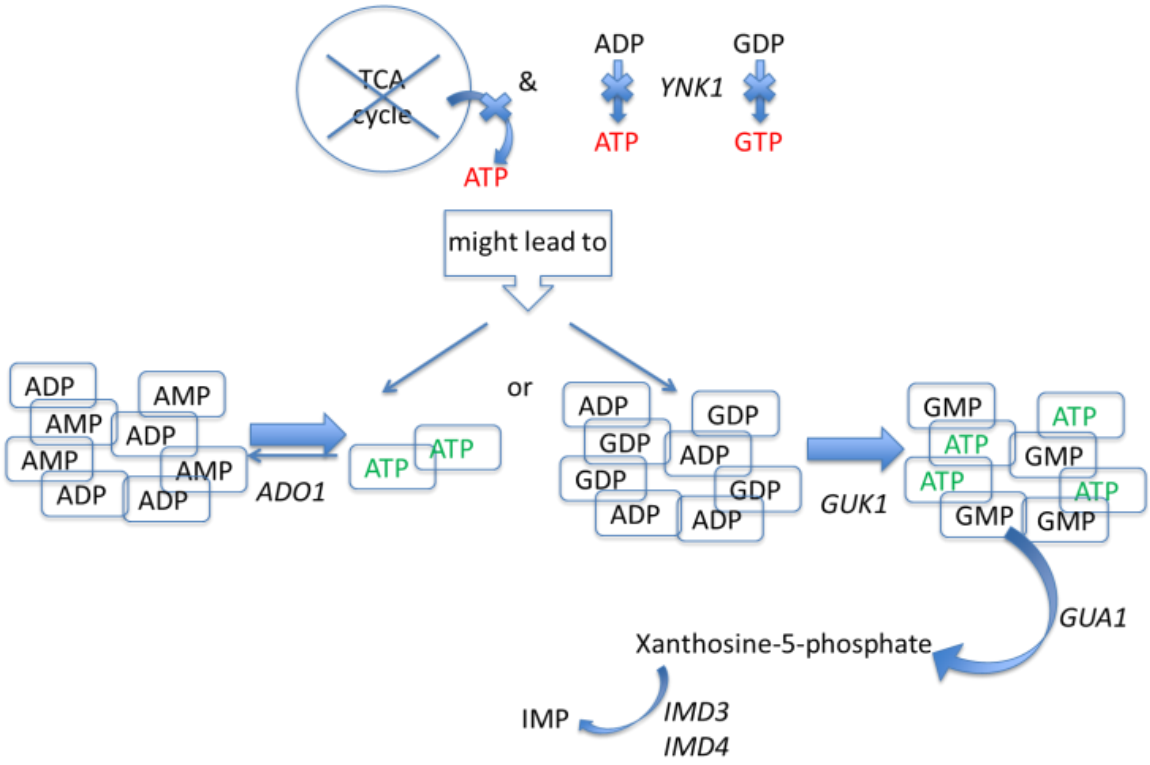

Figure 3.10. Schematic overview of alternative routes for ATP production during inactivation of the TCA cycle and the down-regulation of *YNK1* upon addition of glucose into the fermentation medium

Since *HPT1*, encoding an enzyme that catalyses the conversion of hypoxanthine to IMP was down-regulated throughout the experiment. There are two possible ways to relieve the hypoxanthine accumulation. Both of them require the conversion of hypoxanthine to xanthine in the first step and their conversion into uric acid. Although such an enzyme was identified in other fungi including *Aspergillus niger* and *Yarrowia lipolytica*, the presence of a similar enzyme could not be demonstrated in *S. cerevisiae*. BLASTP search in *S. cerevisiae* genome using the amino-acid sequences of An03g01530, An04g05440 and 1.17.1.4 enzymes did not result to indicate the presence of similar sequences in *S. cerevisiae*. However, it should be noted that the reactions of the purine salvage pathway were not entirely identified according to what the KEGG database reported [106]. Walther T. *et al*. (2010) [96] have also included this potentially relevant

reaction in their purine salvage pathway in *S. cerevisiae* based on the experiments that they have carried out using several *psp* mutants. Since the conversion of xanthine to XMP was not possible due to the down-regulation of *XPT1*, fluxes should be oriented from xanthine towards 5-ureido-4-imidazole carboxylate and later to glycine to be used in the superpathway of serine, threonine and glycine biosynthesis although the detailed mechanism and the enzymes catalysing these reactions are, as yet, unknown. Another alternative route utilizing xanthine and hypoxanthine is purine catabolism, enabling the degradation of the purine compounds into uric acid, allantoin, urea and later into ammonia through the utilization of the gene products of *DAL1*, *DAL2*, *DAL3* together with *DUR1,2* [107]. *DAL1* and *DUR1,2* were up-regulated throughout the experiment. *DAL2* was on the other hand down-regulated throughout the experiment and *DAL3* was up-regulated in P2, P4 and P5 whereas it was down-regulated in P3. The reaction through *DAL3* caused the accumulation of glyoxylate during the production of ammonia. As previously stated, a member of the glyoxylate shunt, *DAL7* may also take role in purine catabolic processes [100, 108] and it was observed to be up-regulated during carbon catabolite repression. The upper-purine biosynthetic pathway was observed to partially become down-regulated upon depletion of glucose. The strong up-regulation observed for *APT1* and *AAH1* as well as the strong down-regulation observed for *YNK1* and *ADK2* appeared to be less pronounced as the amount of available carbon decreased and the steady state conditions were beginning to be restored. In P5, almost all of the pathway components were down-regulated and since the TCA cycle became active again, the ATP production necessary for respiration and maintenance would be supplied through that channel (Figure Appendix D2 a1).

In response to the introduction of ammonium into a nitrogen-limited culture, the genes taking role in the *de novo* synthesis of purine nucleotides as well as the salvage pathways of purines and their nucleosides were up-regulated immediately in P2 except for *ADE16*, *XPT1* and *RNR3*. However, *ADE17* (the paralog of *ADE16*) and *RNR1* (which encodes the major isoform of the large subunit of ribonucleotide-diphosphate reductase with the minor isoform being *RNR3*), were found to be selectively up-regulated. The upper-purine biosynthetic pathway remained up-regulated through periods P2-P4, similar to what has been observed during carbon catabolite repression, being most pronounced in P3, corresponding to a later time than that in glucose repression. *ADE12*, *ADE13*, *AMD1* and *ADK2* were found to be up-regulated providing the synthesis of ADP during P2-P4.

The observation of up-regulation of *IMD4*, *GUA1* and *GUK1* indicated that GDP may also be synthesized during P2-P4. One of the most pronounced changes in P3 was observed in the down-regulation of *YNK1* taking a role in the production of XTPs from XDPs and dXDPs in a similar but delayed response to the carbon catabolite repression of metabolism. As the effect of the impulse of ammonium began to cease in P4, the up-regulation of the genes in upper-purine biosynthetic pathway became less pronounced (Figure Appendix D2 b1).

The *de novo* biosynthesis of pyrimidine ribonucleotides UTP and CTP from L-glutamine was rendered low owing to the down-regulation observed in *URA3* with the introduction of glucose into its limiting culture. This effect was persistent throughout the duration of the pulse effect. It has previously been reported that UXP and CXP profiles also displayed a similar decrease in concentration to what has been observed in AXP and GXP pools, which was in correspondence with this finding [56]. *URA1*, *URA2*, *URA4* and *URA5* mediating the conversion of L-glutamine into orotidine-5'-phosphate in the preceding reactions were all up-regulated throughout P2-P4 and they were down-regulated in P5. *URA10*, the minor isozyme of *URA5*, was down-regulated for the duration of P3-P5. However, this pathway seems to be blocked by the down-regulation of *URA3* throughout the phases during which the effect of the impulse like addition of glucose was observed. This result may indicate that the *de novo* synthesis of UMP was not possible under these conditions. The up-regulation of *URA6*, mediating the conversion of UMP to UDP, also the up-regulation of *FUR1*, mediating the conversion of uracil to UMP may suggest the activation of the salvage pathway of pyrimidine nucleotides for the utilization of uracil, which is supplemented in the fermentation medium. *FUR4*, encoding uracil permease that mediates the uptake of uracil, was observed to be up-regulated in P2 and P3 and became down-regulated in P4 and P5. The presence of uracil was reported to result in the activation of uracil phosphoribosyltransferase (UPRTase) encoded by *FUR1* and the repression of genes involved in the pyrimidine biosynthesis [109]. The genes including *URA6*, *FUR1*, *URK1*, *CDD1* and *FCY1*, which are associated with this salvage pathway, were found to be up-regulated through P2-P4, with expression peaking in P3. The conversion of UDP and CDP to UTP and CTP was also blocked by the down-regulation of *YNK1* in P2-P4. However, *URA7* and *URA8*, whose gene products catalyse the conversion of UTP to CTP, were found to be activated during P2-P5. Additionally, *DUT1*, encoding the enzyme which

catalyses the conversion of dUTP to dUMP, was up-regulated (Figure Appendix D2 a2, a3). Thus alternative routes for the production of UTP and CTP are required. One of two possibilities to overcome this obstacle may be the presence of as yet undefined gene products compensating for the role of *YNK1*. The other alternative may be the equilibrium shift among XDPs and XTPs to favour XTP generation in times of cellular need. UDP first may have been used for the generation of ATP, and ATP may further be used for the conversion of UDP to UTP and further to CTP.

The effect of the addition of ammonium into a nitrogen-limited culture was observed to cause similar but less pronounced changes in the *de novo* synthesis of pyrimidine ribonucleotides pathway than the response to the addition of glucose into its respective limited culture. The most-pronounced down regulation in the *de novo* synthesis of pyrimidine ribonucleotide pathway was observed in the expression level of *URA3* and similar to the observation for the response to glucose impulse, *URA3* acted as a bottleneck, limiting the production of UMP, a significant precursor for the production of UTP and CTP. *URA7* and *URA8* whose products catalyse the conversion between UTP and CTP were both up-regulated in P2 and P4 whereas only *URA8* was down-regulated in P3. The salvage pathway of pyrimidine deoxyribonucleotides were also not as strongly affected in response to the perturbation as in the case of the introduction of glucose. A similar, but slightly delayed, up- or down-regulation pattern was also observed in this case except for *CDD1*, which remained down-regulated during P2-P4 (Figure Appendix D2 b2, b3).

3.2.3.4. Folate Metabolism. The role of folates in metabolism is to donate 1C units to various biosynthetic pathways through the production of tetrahydrofolate (THF), which is an active form of folic acid [110]. Carbons C2 and C8 of purine rings are obtained from the folate metabolism that takes place in the mitochondria [111]. *FOL1* and *FOL2*, taking part in the upper folate biosynthetic pathway starting from GTP, were up-regulated in P2-P4. Although *FOL3* was down-regulated, the putative dihydrofolate synthetase, *RMA1*, was observed to be up-regulated during P2-P5 and this might have replaced the loss of function in *FOL3* [112]. Down-regulation of *ABZ2* throughout P2-P5 demands that 7,8-dihydropteorate be formed from GTP, rather than chorismate. The formation of 1C units was enabled through the interconversions between THF, 5,10-methylene-THF and 5,10-methenyl-THF. The expression levels of the genes encoding the enzymes facilitating these

interconversions were up-regulated in P2 and P3 and these paths gradually became inactive through P4 and P5. The conversion of glycine and THF into 5,10-methylene-THF, NH_3 and CO_2 was facilitated by the active glycine cleavage complex (Lpd1p, Gcv1p, Gcv2p and Gcv3p). All members except for *LPD1* were observed to be up-regulated in P2-P4. *LPD1* was previously reported to be down-regulated in response to catabolite repression and its release from repression requires the activity of the HAP2/3/4/5 complex [113]. Additionally, *SHM1* and *SHM2*; encoding enzymes in the superpathway of serine and glycine biosynthesis facilitated the conversion of serine and THF into glycine and 5,10-methylene-THF [112]. Glycine was reported to lend purine rings their nitrogen at the N7 position and their carbon atoms at the C4 and C5 positions [111]. The folate metabolism switched back to the steady-state configuration as the amount of glucose became progressively limited in P5 (Figure Appendix D3 a).

In response to the addition of ammonium into an N-limited culture, the genes involved in the folate biosynthetic pathways and the folate interconversions were up-regulated in P2. A very similar pattern of regulation to that observed for carbon catabolite repression was encountered in P3. The expression levels of the genes of the pathway were up-regulated except for *LPD1*, *ABZ2* and *CDC21*, which were down-regulated. The interconversions among folate products were active throughout P2-P3 enabling the generation of 1C species to be utilized in purine biosynthetic processes. More genes were down-regulated in P4 including *GCV1*, *GCV2*, *SHM2* and *MTD1*. *CDC21* and *ABZ2* were up-regulated and *LPD1* was only very slightly down-regulated (Figure Appendix D3 b).

3.2.3.5. Superpathway of Serine and Glycine Biosynthesis. The superpathway of serine and glycine biosynthesis was up-regulated, as soon as glucose was introduced into the carbon-limited culture, through the up-regulation of *SER3*, *SER33*, *SER2* and *SER1*. *GLY1*, which mediates the interconversion between L-threonine and L-glycine, became strongly up-regulated in P2 upon relaxation of nutrient limitation. The up-regulation in *GLY1* gradually decreased through P3-P4 and finally it became down-regulated during P5. *SHM2* and *SHM1*, both encoding the enzyme that catalysed the interconversion between L-glycine and L-serine, were found to be up-regulated throughout P2-P4, and down-regulated in P5. A slightly increased accumulation L-serine and L-threonine was also observed through P3-P5. One route leading to the synthesis of L-glycine from glyoxylate was

rendered low through the down-regulation of *AGX1* throughout the experiment. This down-regulation was most pronounced in P3 and P4 (Figure Appendix D4 a1).

Upon relaxation of ammonium limitation, only *AGX1* (of the genes involved in the superpathway of serine and glycine biosynthesis) was slightly down-regulated in P2. This down-regulation was more pronounced in P3. *SER2* and *SHM2* were also down-regulated in P4, reducing the production of L-glycine from glyoxylate and the production of L-serine from 3-phosphoglycerate (Figure Appendix D4 b1).

3.2.3.6. Sulphur Assimilation and Methionine Metabolic Pathways. In response to carbon catabolite repression, methionine biosynthesis was up-regulated in P2 and P3 via the route utilizing sulphate rather than L-aspartate. The only exception was *MET17*, which was down-regulated, creating a bottleneck for the formation of L-methionine. A close homolog, *CYS3* (BLASTP e-value: 5.7e-35), might have replaced its function, allowing information flow in the pathway. L-cysteine was also converted to homocysteine and then to L-methionine through the up-regulation of *CYS3* and *STR3*. *SAM1*, *SAM2* and *MET6* (on the route towards L-methionine and S-adenosyl-L-methionine) were up-regulated once homocysteine was produced. *MET6*, enabling L-methionine production from L-homocysteine also facilitated the interconversion between 5-methyl-THF and THF. Direction of fluxes from S-adenosyl-L-homocysteine towards L-homocysteine was facilitated by *SAH1*, which was up-regulated, releasing additional adenosine for the production of AMP in purine biosynthesis. The fluxes towards cystathionine through *STR2* and *CYS4* were also up-regulated and *CYS3* (whose product converts L-cysteine to L-cystathionine) was also up-regulated. A strong up-regulation of *STR3* may have directed the fluxes towards L-methionine production. A similar response in the methionine biosynthetic pathway was observed in P3. The genes taking role in the upper biosynthetic pathway were gradually down-regulated in P4 and P5. Genes in the salvage pathway of methionine were observed to be up-regulated immediately. Although *BAT1* and *ARO8* remained up-regulated *ADI1*, *BAT2* and *ARO9* became progressively down regulated through P3 to P5. The down-regulation in the salvage pathway was more pronounced in P5 with more transcripts including *MRI1*, *MEU1*, *SPE4* and *SPE2* being down-regulated. *MEU1* was previously reported to regulate the expression of *ADH2*, for which the strongest down-regulation of expression was also observed in P5 [114] (Figure Appendix D4 a2, a3).

Both upper branches of the methionine biosynthetic pathway, utilizing either sulphate or L-aspartate were up-regulated in response to an ammonium perturbation. The down-regulation of *MET17* during P3 might have been compensated by *CYS3* as in the case of glucose perturbations. The low expression levels that were observed for MET2 and STR3 indicated that the production of L-methionine from L-aspartate or from L-cysteine, respectively, was rendered low. A similar up- and down regulation pattern was observed in the salvage pathway of methionine as a response to relaxation from ammonium limitation, except for the fact that this pathway remains functioning in P4 just before reaching the initial (steady-state) condition again (Figure Appendix D4 b2, b3).

3.2.3.7. Aspartate Biosynthetic Pathway and the Superpathway of Glutamate Biosynthesis.

Aspartate biosynthesis donates the nitrogen in the N1 position of the purine ring [111]. In response to carbon catabolite repression, the expression levels of the genes in the aspartate biosynthetic pathway were not rendered low immediately but remained active through P2, being down-regulated in P3-P5. During P2, although *PYC1* was down-regulated, its active isoform *PYC2* was still up-regulated, enabling the formation of oxaloacetate. The synthesis of aspartate from pyruvate was rendered low through the simultaneous down-regulation of *PYC1* and *PYC2* through P3-P5. The down-regulation in the cytosolic aspartate aminotransferase, encoded by *AAT2,* and the up-regulation in the mitochondrial aspartate aminotransferase, specified by *AAT1*, indicated that L-aspartate biosynthesis from oxaloacetate was enabled through the mitochondrial route rather than the cytosolic route. However, the route for the production of homoserine and L-threonine from aspartate was rendered low through the down-regulation of *HOM2-HOM6* and *THR4*, respectively, throughout the experiment. The accumulated aspartate may be converted to fumarate by the up-regulated *ADE12* and *ADE13* (through adenylosuccinate), or by the up-regulated *ARG1* and *ARG4* (through L-argininosuccinate). Indeed, fumarate accumulation observed throughout the experiment also supports this hypothesis. Another possibility may be the conversion of L-aspartate to N-carboyl-L-aspartate through the up-regulated *URA2* towards pyrimidine metabolism. The cyclic interconversion between L-aspartate and L-asparagine through the equilibrium reaction catalysed by the product of the up-regulated *ASN1* and *ASN2* genes was observed to be active during P2-P5. *ASP1*, *ASP3-1*, *ASP3-2*, *ASP3-3* and *ASP3-4* mediating the conversion of L-asparagine to L-aspartate and ammonia lending a nitrogen atom for the purine ring was also found to be up-regulated during all

periods. The intracellular concentrations of L-aspartate, homoserine and L-threonine were all high. The blocked pathway from L-aspartate and homoserine towards L-threonine production was complemented by this intracellular accumulation (Figure Appendix D5 a1).

Nitrogen catabolite repression resulted in an up-regulation in L-aspartate biosynthetic pathway starting from pyruvate increasingly from P2 to P4. Either one of the isoforms; *PYC1* or *PYC2*, was active throughout all periods or L-aspartate production was enabled through either the mitochondrial or the cytosolic aspartate aminotransferase during P2-P4. In contrast to what has been observed during carbon catabolite repression, homoserine and L-threonine production was also up-regulated through *HOM3*, *HOM2*, *HOM6*, *THR1* and *THR4* during P2-P4. The intracellular concentrations of L-aspartate and homoserine were high whereas that of L-threonine was low. The up-regulation of the pathway from L-aspartate and homoserine towards L-threonine complemented this finding (Figure Appendix D5 b1).

L-glutamine delivers the nitrogen atoms at positions N3 and N9 of the purine ring [111]. L-glutamine biosynthesis initiates from a component of the TCA cycle, isocitrate. Isocitrate was converted to 2-oxoglutarate through the catalysis by the gene product of *IDP1*, which was selectively up-regulated throughout the carbon catabolite repression, diverting alpha-ketoglutarate to biosynthetic processes [115]. 2-oxoglutarate, together with NH_3 would then be converted into L-glutamate through the catalysis of the up-regulated *GDH1*, *GDH2* and *GDH3* and 2-oxoglutarate would be converted via the up-regulated *GLT1* in P2. This process was observed to be down-regulated during P3-P5. Ammonia utilization and the conversion into L-glutamine was not blocked through *GLN1* during P2 and P3, however, it was rendered low during P4 and P5 as a result of the down-regulation of the enzyme The intracellular concentrations of ammonium, 2-oxoglutarate, L-glutamate and L-glutamine were all high (Figure Appendix D5 a2).

In response to the addition of ammonium, the production of L-glutamate was observed to be low during P2-P4, which was also observed in the intracellular concentrations of the metabolite. Although *IDP1*, which mediates the conversion of isocitrate to 2-oxoglutarate, was up-regulated, *GDH1*, *GDH2* and *GDH3* were down-regulated in P2 and P3. The direct conversion of 2-oxoglutarate into L-glutamate was

rendered low by the down-regulation of *GLT1* in P2. L-glutamine production from L-glutamate was active as a response to nitrogen catabolite repression in P2-P3 and down-regulated in P4. *GLT1* was, on the other hand, up-regulated in P3 and P4. The intracellular concentrations of ammonium, 2-oxoglutarate and L-glutamine were all high (Figure Appendix D5 b2).

3.2.4. Study conclusions

The quantification of the dynamic changes in the transcriptome and the metabolome in response to an impulse-like perturbation in nutrient availability and the integration of these data with the partway information revealed long-term dynamic re-organization yeast cells.

The glycolytic and gluconeogenic pathways and the TCA cycle were found to be affected from an impulse-like shift of the nutritional availability and different isoforms of the genes constituting the central energy metabolism were observed to be active in different periods of time after the perturbation. The transcriptional response of the upper part of the glycolysis was immediate and these genes remained down-regulated for at least three hours, limiting glucose phosphorylation to avoid glucose-accelerated death. The most pronounced down-regulation of the TCA cycle genes was observed within the first hour following the glucose impulse, displaying a rather late response. The impulse-like addition of ammonium into the N-limited culture triggered an even later response in comparison to the addition of glucose. The response observed in the lower glycolytic pathway was found to be glucose-specific as an equivalent response was not observed during the ammonium perturbation. The fluxes towards the lower gluconeogenic pathway were limited through the down-regulation of genes encoding specific enzymes in both cases.

The initial steps of *de novo* synthesis of purine nucleotides were immediately activated as soon as glucose was introduced. Upon depletion of glucose, almost all of the pathway components were down-regulated and, with the activation of the TCA cycle, the necessary energy for survival and maintenance would again be supplied through that channel. The time-dependent changes observed in the purine salvage pathway provided additional evidence about the role and organization of this pathway to control energy

homeostasis and compensate for the sudden drop in the AXP pools. Further insight was provided into the accumulation of inosine, IMP and hypoxanthine that had been reported in previous studies. The *de novo* biosynthesis of pyrimidine ribonucleotides was also rendered low with the introduction of glucose into a C-limited culture. The salvage pathway of pyrimidine nucleotides was activated for the utilization of uracil, which is supplemented in the fermentation medium. The effect of the addition of ammonium into an N-limited culture was observed to cause similar, but less pronounced, changes in both the *de novo* synthesis of pyrimidine ribonucleotides and their salvage pathways to those observed in the response to the addition of glucose under C-limitation.

The folate interconversions donating 1C units in purine metabolism were active during the first hour following the introduction of glucose, being gradually down-regulated during the rest of the experiment. A very similar pattern of regulation to what had been observed for the carbon catabolite repression was encountered in the first three hours upon the addition of ammonium. The pathway gradually became inactive as the effect of the pulse began to cease.

In response to carbon catabolite repression, our integrative analysis of methionine biosynthesis indicated the importance of sulphur metabolism, rather than L-aspartate. The direction of flux was re-arranged such that the release of additional adenosine was facilitated. Genes in the salvage pathway of methionine were also observed to be up-regulated immediately. All of the upper methionine biosynthetic pathway genes were up-regulated in response to an ammonium perturbation. A similar up- and down regulation pattern was observed in the salvage pathway of methionine to that of the biosynthetic pathway with the exception that this pathway remains functional until the return to the initial steady-state condition. In response to carbon catabolite repression, the down-regulation of L-aspartate biosynthetic pathway genes was delayed, being prominent after the first minute. An accumulation of aspartate might have been relieved by its conversion to fumarate through various routes. Another possibility may have been its re-direction towards pyrimidine metabolism. In contrast, nitrogen catabolite repression resulted in an increasing up-regulation in the L-aspartate biosynthetic pathway. L-Glutamine production was up-regulated throughout the carbon catabolite repression phase, diverting alpha-ketoglutarate to biosynthetic processes, and was down-regulated throughout the nitrogen

catabolite repression.

This long-term integrative study revealed, that in addition to the dynamic re-organization of the *de novo* biosynthetic pathways, the salvage pathways appeared to be re-organized in a time-dependent manner by catabolite repression in the yeast. The transcriptional and the metabolic responses observed for nitrogen catabolite repression were not as severe as those for carbon catabolite repression. This may have been due to the fact that uracil, histidine and leucine were supplemented in the fermentation medium to satisfy the auxotrophic requirements of the strains employed. Selective up- or down regulation of different isoforms throughout the response to the relaxation from nutritional limitation in yeast requires further investigation to assign particular functions to the paralogs. Although this study provided additional information on inosine accumulation and recycling, it has also indicated the requirement of further studies to shed light into the specific situations that were encountered on the pathways, which were limiting the communication of the transcriptional message via the down-regulation of one or more genes in the pathway such as in the case of the relief from the accumulation of hypoxanthine or the down-regulation of *YNK1*, whose product phosphorylates XDP nucleotides to XTP.

Transcriptome and metabolome data were observed to complement each other, providing useful information whenever they were simultaneously available. Additional metabolite measurements and studies on the proteome and phosphoproteme level, complemented by accurate measurements of mRNA decay, may provide better information to shed light onto the time-dependent re-organization of yeast cells as a dynamic response to a changing nutritional environment and thus provide a quantitative understanding of cell behaviour. Similar integrative systems-level approaches would also provide a solid understanding of metabolic processes that control the respiro-fermentative transition in human cells.

3.3. A novel tool for the prediction of hidden genetic interactions embedded in dynamic gene expression data enriched with an a priori knowledge on network information

3.3.1. Background

Cellular processes are complex phenomena, which require the presence and the fine-tuning of simultaneous interactions among multiple events. This complexity also stems from the need for the dynamic evaluation of these multiple events, each of which may be considered as an individual stimulus for the event occurring at the following time point. It is therefore important to investigate cellular processes as they take place in time as a response to a perturbation in order to get a more comprehensive view of this complex coordination.

Monitoring the dynamic response of organisms has been the subject of many research studies including relatively small scale kinetics studies [116-118] as well as genome scale high-throughput studies including transcriptome [119, 120], proteome [121, 122], metabolome [123, 124] and interactome [125, 126]. The transient biological response of organisms ranging from simple bacteria [116, 122] to mammals [118, 124] including humans [120, 121] have been investigated in these studies.

One of the biggest challenges in systems biological applications is data integration [127]. Several methods have been developed in order to integrate data obtained from various sources to reach a better understanding of the overall view and to extract the hidden information within the collected data.

Partial least squares (PLS) regression has previously been suggested as a powerful tool for exploring the relationships among gene expression profiles in order to obtain biologically meaningful association data. Both simulated and original microarray data have been used in this analysis and the method has been shown to be effective as a screening procedure for the identification of gene-gene interactions [128]. In another study, Bayesian networks and Bayesian learning with Markov chain Monte Carlo has been used as a reverse engineering approach to infer interaction networks from simulated microarray data.

The results of this study indicated that the performance of network inference varied with the size of the training set, the degree of inadequacy of prior assumptions, and the inclusion of further information [129]. State space models have also been used such that they have been treated with variational Bayesian learning algorithms. Dynamic microarray data has been used to reconstruct genetic regulatory networks [130, 131]. Another framework has utilized Bayesian networks for the integration of various types of high-throughput data such as microarray data or two-hybrid screen data to predict gene function. Using two completely independent types of data meant that specificity did not have to be sacrificed, which is often an inevitable outcome of genome-scale data generation. Thus inaccuracies in the predictions would have been prevented. The method was tested on *Saccharomyces cerevisiae* using physical interaction data and microarray data set [132]. Yet another study makes use of a stochastic hybrid model enabling the abstraction and the controller design of the lactose regulation system in *Escherichia coli* due to the requirements imposed by the small size of the cell. The framework suggested the presence of a control mechanism that was based on a large number of Markov chains through the adjustment of the transition rates [133]. The statistical nature of Bayesian systems enables handling of challenging problems since they may account for the kinetic parameter uncertainty and incorporate environmental stochasticity [134].

Previously conducted studies indicate the necessity of integration of various types of information in order to increase the specificity of the information obtained from high-throughput studies. In this study, a novel integrative approach has been developed to extract hidden information from dynamic high- throughput data. The integration of different types of information has been utilized in such a way as to enable both an increase in the specificity of the obtained information and the identification of novel interactions and yet unknown associations among the genes. This hidden information was debugged from already known interactions and at the same time supported by high throughput dynamic data.

3.3.2. Methodology

The notion that the expression level of a gene at any time is determined as the result of multiple events that took place at that particular time as well as at discrete time points

that have proceeded that specific time point has been previously used in the literature. A useful approach for such applications is the utilization of linear algebra.

3.3.2.1. Construction of the linear model. Assuming that the expression level of a single gene at a particular time (t) depends on the expression of that particular gene at a preceding time point (t-1) as well as on the expression of the other genes constituting the gene expression vector at that preceding time point (t-1), then the following linear dependence could be given:

$$\bar{x}_t = A\bar{x}_{t-1} + \varepsilon \tag{2.1}$$

where $\bar{x}_t$ is the vector indicating the expression of all the genes available at time (t), $\bar{x}_{t-1}$ is the vector indicating the expression of all the genes available at time (t-1), A is the genetic association matrix and ε is the error term associated with the relation.

The objective function that needs to be minimized in this problem is the error[2] created by the prediction with an additional term to account for the sparsity of the matrix;

$$\sum_{t_i=2}^{T} \left\| x_t - Ax_{t-1} \right\|^2 + \lambda \sum_{ij} A_{ij} \tag{2.2}$$

with λ as a counting parameter and the second term of the objective function indicating the loose coupling of the system with relatively less number of interactions occurring within as reported in previous studies [135-137].

3.3.2.2. Segregation of the interaction matrix. The expression level of each gene may be thought of as a linear combination of several biological processes taking role in the cell. Therefore the interaction matrix can be partitioned such that the total expression level may be the linear combination of partial interaction matrices regarding various biological actions:

$$A = A_m + A_p + A_r + A_g + A_o \tag{2.3}$$

where the subscript m denotes the fraction of expression represented by the metabolic activity, p denotes the fraction of expression represented by being involved in a protein-protein interaction, r denotes the fraction of expression represented by being involved in a transcription factor-gene interaction, g denotes the fraction of expression represented by being involved in a genetic interaction and o denotes the fraction of expression represented by being involved in a yet unknown interaction or a post-translational modification. Not all genes are required to take a role in all of the available partitions.

The metabolic portion of the interaction matrix A_m, was obtained from the stoichiometric matrix such that any two genes that were sharing a common metabolite in their reactions were considered to be interacting. The extent of this sharing determined the strength of the interaction.

The protein-protein interaction sub-matrix A_p, and the transcription factor-gene interaction sub-matrix A_r, was directly obtained from the literature and the strength of this interaction was determined from the number of different resources that were used to confirm this interaction.

The epistatic interaction sub-matrix A_g, was directly obtained from the literature and similar to the previously discussed cases, the strength of this interaction was determined from the number of different resources that were used to confirm this interaction.

3.3.2.3. Model Network. In order to test the model, a subset of randomized expression profiles were used on the following hypothetical model network that was composed of the capital letter metabolites and small letter genes and gene products (Figure 3.11). Protein complexes and transcription factor-gene regulations are indicated in the figure with curved arrows. Currency metabolites functioning in more than one part of the metabolism (such as ADP and ATP in a realistic network) are also indicated by curved arrows. Feedback loops are included to make it more similar to a real network and transport reactions are denoted by the ^{o} superscript.

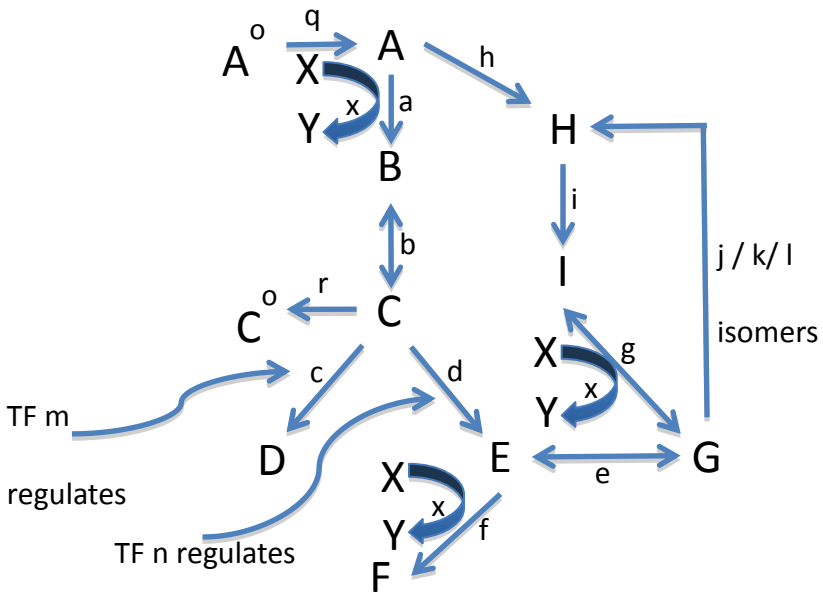

Figure 3.11. Hypothetical network

3.3.2.4. Test Model. The glycolysis and the tricarboxylic acid cycle in the yeast, *Saccharomyces cerevisiae* were selected as the test models. Both a linear and a cyclic pathway were selected for testing. The dynamic gene expression data following a perturbation were obtained from the literature [138]. The reactions were obtained from the Saccharomyces Genome Database [29], the genetic and the physical interactions regarding this set of genes were acquired from BioGRID [139] and the TF-gene interactions were obtained from three different sources [81, 140, 141].

3.3.2.5. Implementation of metabolic pathway information. The hypothetical metabolic pathway is converted into an electrical wiring diagram with time dependence characteristics. The metabolites were denoted as M and the enzymes catabolizing the reactions were denoted as x. The superscript (^{o}) indicated the extracellular metabolites. The effect of the contribution of previous metabolite concentrations affecting the available flux through a particular reaction at a particular time was included in the subscripts (t) and (t-1) thus enabling the implementation of time dependence into the metabolic pathway information. In this manner, it was made possible to represent the equilibrium reactions without dissecting the reaction into its forward and reverse components and analysing them separately (Figure 3.12). A deterministic logic table was prepared for this network. Then

the metabolites (M) were removed from the network, to be considered as hidden variables leaving only the enzymes (x) as the observable variables. With only the values of M^{o}_{1t} and M^{o}_{3t} known, the remaining hidden variables were assigned probabilities such that the observable variables would possess their assigned values as provided by their expressions. In order to keep the $\log_2$ expression values representing the flux through the corresponding enzymes, a prior was set such that the value of x varied between 2 and 14.

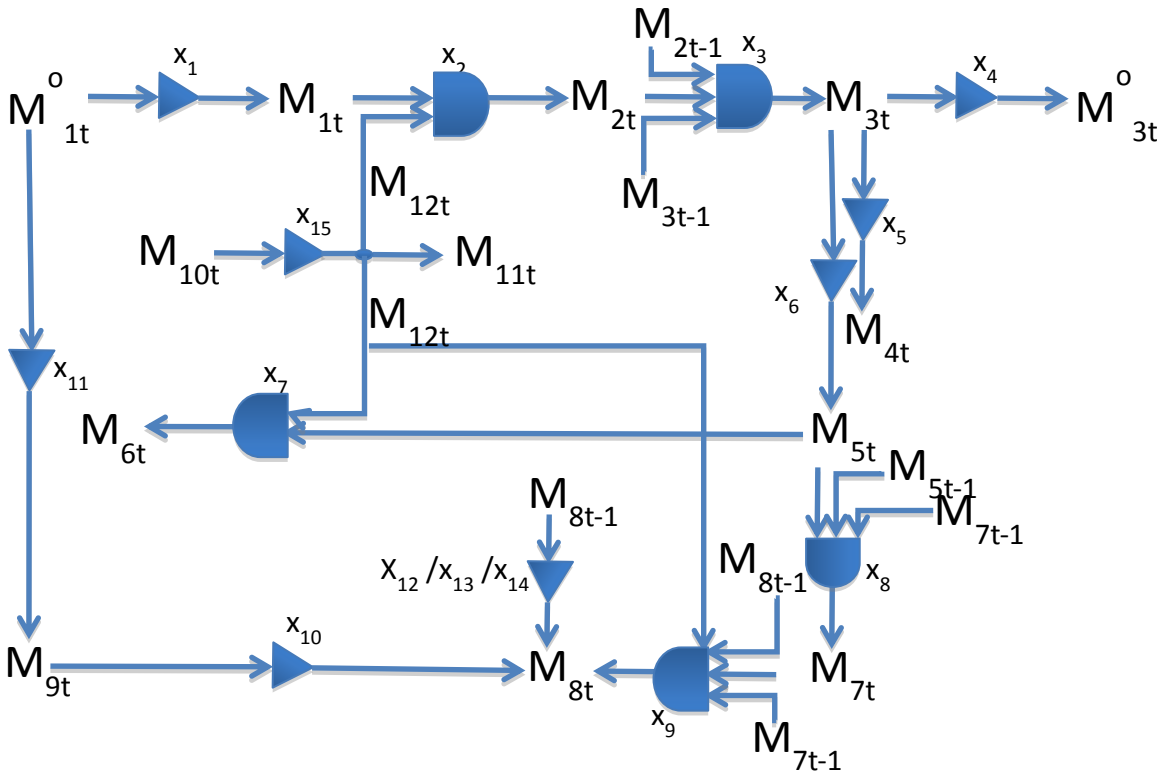

Figure 3.12. Electrical wiring diagram of the hypothetical metabolic network

3.3.2.6. Implementation of regulatory information. Hypothetical regulatory information on transcription factor-gene interactions (transcription factors denoted as y), protein-protein interactions (proteins denoted as z) and gene-gene interactions (genes denoted as w) was also provided in addition to the metabolic information. Providing the connection between the genes of the metabolic network based on the values provided for the observed variables.

3.3.3. Evaluation of the Applicability of the Test Model

The electrical wiring diagram was first converted into a simpler form, in which the observable and the hidden variables could clearly be separated from each other (Figure 3.13).

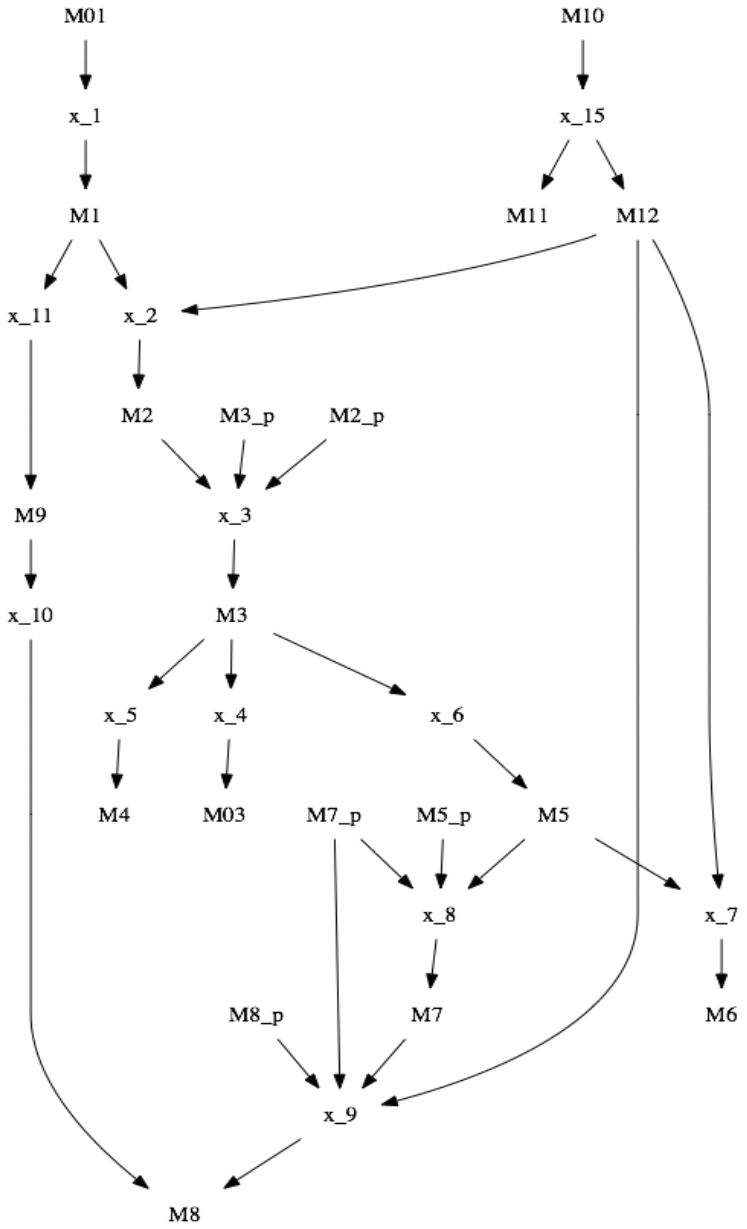

Figure 3.13. The finalized metabolic pathway with the observable variables x, and M0 and the hidden variables M

For each metabolic reaction taking place, the possibility of that event happening or not was determined through the help of a deterministic logical evaluation. For an individual reaction, the possibility of that reaction taking place in the absence or the presence of the metabolites and the enzyme catalysing the reaction were evaluated and deterministically stated as 1 if the reaction was concluded to occur and as 0 if under the stated conditions, it would be impossible for the reaction to take place (Figure 3.14).

M^0_{1} x_{1}, M_{1}															
0	0	0	1												
M_{10} x_{15}, M_{11}															
0	0	0	1												
M_{10} x_{15}, M_{12}															
0	0	0	1												
M_{1} M_{12} x_{2}, M_{2}															
0	0	0	0	0	0	0	1								
M_{12} x_{7}, M_{6}															
0	0	0	1												
M_{1} x_{11}, M_{9}															
0	0	0	1												
M_{8p} x_{12} x_{13} x_{14}, MM_{8}															
0	0	0	1	0	1	0	1	0	1	0	1	0	1	0	1
M_{12} M_{7p} M_{7} x_{9}, MMM_{8}															
0	0	0	0	0	0	0	0	0	1	1	1	1	1	1	1
M_{9} MM_{8} MMM_{8} x_{10}, M_{8}															
0	0	1	1	1	1	1	1	0	1	1	1	1	1	1	1
M_{2} M_{3p} M_{2p} x_{3}, M_{3}															
0	0	0	0	0	0	0	0	0	1	0	1	0	1	0	1
M_{3} x_{5}, M_{4}															
0	0	0	1												
M_{3} x_{4}, $M_^0_{3}$															
0	0	0	1												
M_{3} x_{6}, M_{5}															
0	0	0	1												
M_{5} x_{7}, M_{6}															
0	0	0	1												
M_{5} M_{7p} M_{5p} x_{8}, M_{7}															
0	0	0	0	0	0	0	0	0	1	0	1	0	1	0	1

Figure 3.14. Deterministic logical evaluation of the direction of flow for the metabolic information

The metabolites M01 and M03 as well as all x, y, w and z variables were identified as the observable variables since gene expression values or metabolite concentration values could be measured and provided as inputs into the software. The concentration of the remaining M metabolites was not determined and therefore, they were categorized as hidden variables. The interaction matrix among the observable variables x, y, w and z was constructed. The information regarding the interactions among the x enzymes were extracted from the hypothetical metabolic pathway (Figure 3.13). Any two x variables were determined to be interacting if they shared a common metabolite in the interactions that their enzyme products catalysed. The TF-gene interactions between y and x variables, the physical interactions between z and x variables as well as the epistatic interactions between w and x variables were arbitrarily assigned and again a deterministic table was formed (Figure 3.15).

	x_1	x_2	x_3	x_4	x_5	x_6	x_7	x_8	x_9	x_10	x_11	x_15	y_1	y_2	y_3	y_4	z_1	z_2	z_3	w_1	w_2
x_1	0	1	0	0	0	0	0	0	0	0	1	0	0	0	0	0	0	1	0	0	0
x_2	1	0	1	0	0	0	0	0	0	0	0	1	1	1	0	0	0	0	0	0	0
x_3	0	1	0	1	1	1	0	0	0	0	0	0	0	0	0	0	0	0	0	0	1
x_4	0	0	1	0	0	0	0	0	0	0	0	0	0	0	0	1	0	0	0	0	0
x_5	0	0	1	0	0	0	0	0	0	0	0	0	0	0	0	0	0	0	1	0	0
x_6	0	0	1	0	0	0	1	1	0	0	0	0	0	0	0	0	0	0	0	0	0
x_7	0	0	0	0	0	1	0	0	0	0	0	1	0	0	0	0	0	0	0	0	0
x_8	0	0	0	0	0	1	0	0	1	0	0	0	0	0	0	0	1	0	0	0	0
x_9	0	0	0	0	0	0	0	1	0	0	0	1	0	0	0	0	0	0	0	1	0
x_10	0	0	0	0	0	0	0	0	0	0	1	0	0	0	0	0	0	0	0	0	0
x_11	1	0	0	0	0	0	0	0	0	1	0	0	0	0	1	0	0	0	0	0	0
x_15	0	1	0	0	0	0	1	0	1	0	0	0	0	0	0	0	0	0	0	0	0
y_1	0	1	0	0	0	0	0	0	0	0	0	0	0	0	0	0	0	0	0	0	0
y_2	0	1	0	0	0	0	0	0	0	0	0	0	0	0	0	0	0	0	0	0	0
y_3	0	0	0	0	0	0	0	0	0	0	1	0	0	0	0	0	0	0	0	0	0
y_4	0	0	0	1	0	0	0	0	0	0	0	0	0	0	0	0	0	0	0	0	0
z_1	0	0	0	0	0	0	0	1	0	0	0	0	0	0	0	0	0	0	0	0	0
z_2	1	0	0	0	0	0	0	0	0	0	0	0	0	0	0	0	0	1	0	0	0
z_3	0	0	0	0	1	0	0	0	0	0	0	0	0	0	0	0	0	0	0	0	0
w_1	0	0	0	0	0	0	0	0	1	0	0	0	0	0	0	0	0	0	0	1	0
w_2	0	0	1	0	0	0	0	0	0	0	0	0	0	0	0	0	0	0	0	0	0

Figure 3.15. The interaction matrix

Arbitrary gene expression profiles and metabolite concentration profiles were generated for the observable M01, M03, x, y, w and z variables (Figure 3.16). The profiles were created for a similar condition to that introduced in the first two sections of this chapter. The concentrations and the expression levels were not completely randomly

assigned. Instead, a complementary or a synergetic relationship was assumed among some profiles whereas others were left as fluctuating samples. Some lag phases were introduced into the profiles of the genes that are functional along the same path, whose actions follow each other.

time	0	20''	40''	60''	8'	16'	24'	32'	1h	2h	3h	4h	5h	7h	Nh
observed metabolite concentrations															
M01	0.075	0.740	0.740	0.740	0.700	0.600	0.520	0.410	0.350	0.270	0.140	0.100	0.090	0.080	0.075
M03	0.03	0.03	0.03	0.03	0.04	0.08	0.07	0.10	0.20	0.30	0.28	0.15	0.05	0.04	0.03
gene expression levels for the metabolic pathway genes															
x_1	7.8	9.7	9.8	9.9	9.5	9.4	9.4	9.2	9.1	9.1	8.7	8.5	8.4	8.0	8.0
x_2	5.2	5.4	5.0	4.9	5.1	5.3	5.2	5.2	4.9	5.2	5.0	5.1	5.4	5.0	5.0
x_3	8.0	5.4	5.9	6.1	6.2	6.4	6.5	6.6	6.9	7.1	7.2	7.5	7.9	8.0	8.2
x_4	7.1	7.2	7.0	7.2	7.4	7.7	8.3	8.5	9.0	8.4	8.1	7.8	7.6	7.4	7.4
x_5	6.0	5.7	5.6	5.4	5.4	5.2	3.7	3.6	3.8	4.1	4.2	4.5	5.0	5.3	5.4
x_6	9.1	9.5	9.6	9.4	9.4	9.4	9.3	9.1	9.2	9.3	9.1	9.1	8.9	8.8	9.0
x_7	5.1	5.1	5.2	5.4	5.3	5.6	5.8	6.3	6.4	6.8	6.5	6.2	6.3	6.1	5.0
x_8	6.3	6.1	5.8	5.5	5.6	58	6.7	6.9	7.2	7.1	7.0	6.5	6.4	6.4	6.4
x_9	5.6	5.9	6.9	7.2	7.0	6.8	6.5	6.3	6.1	6.0	6.0	5.9	6.0	5.8	5.5
x_10	4.6	4.8	4.7	4.2	4.3	4.4	4.5	4.4	4.8	5.3	6.7	7.1	6.8	6.1	5.5
x_11	5.3	5.2	6.1	6.3	6.8	7.2	7.0	6.9	6.8	6.6	6.7	6.7	6.8	5.9	5.7
x_15	8.1	8.4	8.3	8.3	8.0	7.9	7.6	7.1	7.3	7.4	7.3	7.6	7.6	7.9	8.0
for the transcription factors regulating the metabolic pathway genes															
y_1	4.5	4.8	4.9	5.0	5.3	5.2	4.6	4.0	3.8	4.1	4.2	4.4	4.3	4.4	4.3
y_2	6.7	6.8	6.5	6.6	6.9	6.8	6.7	6.3	6.5	6.4	6.8	6.3	6.7	6.5	6.9
y_3	7.1	6.3	6.2	6.3	6.4	6.6	6.8	6.7	6.8	6.7	6.6	6.8	6.7	6.7	6.9
y_4	5.4	5.3	5.5	5.4	5.2	5.5	5.1	5.4	5.3	5.2	5.4	5.1	5.2	5.0	5.3
for the proteins that are interacting with the proteins from the metabolic pathway genes															
z_1	6.8	8.7	8.8	8.9	8.5	8.4	8.4	8.2	8.0	7.6	7.5	7.4	7.0	7.0	7.0
z_2	7.1	7.1	7.2	7.4	7.3	7.6	7.8	8.3	8.4	8.8	8.5	8.2	8.3	8.1	7.0
z_3	5.5	5.4	5.9	5.8	5.9	5.9	5.8	5.7	5.9	5.4	5.3	5.5	5.5	5.4	5.5
for the genes that are interacting with the metabolic genes															
w1	3.3	3.2	4.1	4.3	4.8	5.2	2.0	4.9	4.8	4.6	4.7	4.7	4.8	3.9	3.7
w2	8.4	8.1	8.0	7.6	7.0	6.8	6.6	6.7	7.1	7.2	7.6	8.0	8.3	8.4	8.2

Figure 3.16. Randomly assigned gene expression level and metabolite concentration profiles

Since the identification of novel interactions from gene expression profiles was targeted, two genes x_4 and z_2 were deliberately provided with similar expression profiles (Figure 3.17) and any interaction among them was not reported in the interaction matrix to be provided as input so that it was identified in the simulations being predicted as having an interaction.

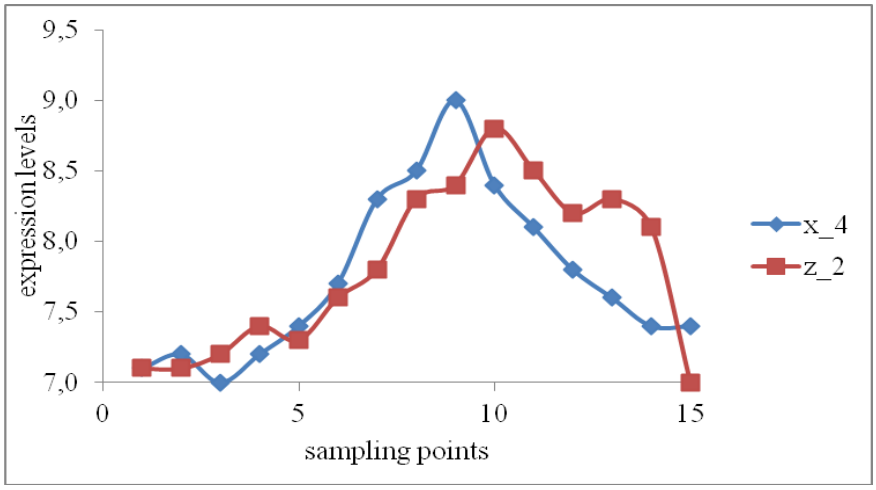

Figure 3.17. Similar expression profiles for x_4 and z_2 deliberately embedded into the data

3.3.4. Future Prospects

The implementation of metabolic networks and the regulatory networks into the interaction matrix for the hypothetical model system has been completed in this still on-going study. Following the implementation of gene-TF interaction network, protein-protein interaction network and gene-gene interaction network in the model, the system, on which information regarding transcript and metabolome levels was available, would gain enhanced predictive power for the identification of novel interactions at the same time taking plasticity into consideration. Upon application of this technique on the real small scale model system, the transient novel interactions hidden in the data, on which dynamic changes induced by an environmental perturbation was observed, would be determined and selected for *in vivo* verification. The model structure allows the implementation of the model on genome scale models in addition to the hypothetical test models and small-scale models. Therefore the next step would be extending the study through the application of the novel tool on genome scale information.

4. INVESTIGATION OF HOW GENETICALLY ALTERED YEAST STRAINS RESPOND TO DIFFERENT NUTRITIONAL ENVIRONMENTS

This chapter of the study is concerned with how yeast copes with the loss of drug resistance genes under different environmental conditions. The variations in the fermentation characteristics of two members of the DHA12 family and the pleiotropic drug resistance family were investigated in this chapter. The transcriptional and the metabolomic response of gene deletions of *QDR3* and *PDR3* under glucose or ammonium limitation in carefully controlled fermenters were investigated and presented in conjunction with the metabolic flux distribution predictions in the first section. The fitness effects of each member were investigated using a high throughput genomics approach and the genetic interactions between the query gene *QDR3* and the remaining members of these two families are currently being investigated using a chemical genomics approach.

4.1. Drug resistance in yeast: Is that all there is to it?

4.1.1. Background

Major metabolic pathways, DNA repair and cell cycle control regarding the functionality of the cell are conserved mechanisms throughout the evolution of the DNA within a range of eukaryotes from yeast to human [142]. The treatment of fungal infections has been much harder and the advances in developing therapies have been much slower than the case for bacterial infections with the use of antibiotics. Functional and structural similarity of the target cell to human cell lines is one of the main reasons of that outcome. Therefore, the obstacles presented in treating a fungal infection are similar to the problems that are faced in the treatment of the cancer cells [143].

Adaptation aims to maintain the integrity and the viability of the organism. Fungi populations are adaptable to changes in the environment through the development of drug resistance upon the introduction of an anti-fungal drug into the environment [144]. Drug resistance is a self-preservation technique to cope with external harmful chemical factors for survival. The organism may immediately resist to the presence of a harmful agent using

its necessary mechanisms or it may not have any coping mechanism, resulting in cellular death. In other cases, drug resistance can be developed through adaptation in a similar manner to what has been observed for patients developing resistance to chemotherapy drugs since chemical resistance mechanisms are highly conserved among eukaryotes. In both cases, many mechanisms of action involve the over-expression of multi-drug resistance pumps [143].

Development of drug resistance is desirable from the organism's point of view if the survival of the cell, which was exposed to the chemical agent, is aimed. On the other hand, it is a downfall if cells need to be destroyed using that particular agent as it is the case in fungal infections and in cancer therapy. Development of chemical resistance limits the therapeutic potential of both anti-fungal and anti-tumour drugs [145] and prevention of the development of a drug resistance will result in the efficient uptake and utilization of the drugs. The first step in the process is the target identification to prevent this resistance.

The similarity of yeast drug resistance mechanisms to that of human's makes it an ideal model for studying drug resistance. Moreover, the non-pathogenic nature of *Saccharomyces cerevisiae* makes it more attractive to use in this area of research. Several studies have been conducted where *S. cerevisiae* is used as a model organism for the identification of novel mechanisms of drug resistance, specifically, anti-tumour drug resistance. Schenk P. W. *et al.* have identified *NPR2* and *SKY1* genes in yeast to be epistatic in providing resistance to two anti-cancer agents; cisplatin and doxorubicin [97]. In a study, *IXR1* gene was identified as providing resistance to a chemotherapeutic agent; cisplatin [146]. Another study has been conducted using yeast and human ovarian carcinoma cell line in parallel identifying the *SKY1* gene in *S. cerevisiae* and its human homologue *SRPK1* gene to induce cisplatin resistance in the corresponding organisms [147]. High throughput technologies have also been used to identify genes that confer resistance to cisplatin such as *PDR2* and *ZDS2* [148].

The multiple drug resistance (MDR) in yeast is carried out via two major super-families of membrane transporters; the major facilitator super-family (MFS) and the ATP binding cassette (ABC) super-family. Both mechanisms work through the use of drug efflux pumps. The increased expression of these pump proteins allows the drugs to be

pumped out from the metabolism, hence the survival of the organism in the drugs' presence [149].

In *Saccharomyces cerevisiae*, the MFS comprises of the proton motive force-dependent multi-drug efflux system [150]. Most of the 23 genes of this system were thought to be involved in multi-drug resistance. The products of these genes consist of 12 and 14 predicted membrane–spanning segments and owing to that, they are called the DHA12 and DHA14 drug efflux families [151]. *QDR3*, the gene of interest in this study, is a member of the QDR family plasma membrane transporters in the DHA12 family. One of its close homologues Qdr1p confers resistance to the anti-fungal agents; ketoconazole and fluconazole as well as an isomer of quinine; quinidine [150]. Another close homolog, Qdr2p, is a resistance determinant for quinidine well as an anti-herbicide; barban [151]. The resistance range of Qdr3p, however, is much broader than its homologs, causing an increased tolerance to a range of inhibitory compounds that are structurally and functionally unrelated. Among these drugs are the anti-malarial drug; quinidine, the herbicide; barban and the anti-cancer drugs; cisplatin and bleomycin [152].

The other known associate of the MDR, the ABC super-family utilizes the ATP hydrolysis in order to drive drug extrusion and the factors that are required for all multi-drug transporters [150]. There are some 30 genes encoding the ABC proteins in yeast. A subset of these ABC transporters takes role in the mediation of pleiotropic drug resistance (PDR) that is very similar to the multi-drug resistance occurring in mammalian cells, parasites, fungal pathogens and bacteria. The PDR sub-family is reported to be the largest and the best characterized ABC sub-family in *S. cerevisiae* [153]. This PDR sub-family consists of transporter genes, also called the pleiotropic drug response elements (PDRE) [154]. Pdr1p and Pdr3p are the transcriptional regulators of the ABC transporter genes and either of them is able to mediate PDR although they are not directly responsible for the observed effects of drug resistance [155]. Pdr13p and Ngg1p are also thought to regulate Pdr1p and therefore, the function of the complex formed by Pdr1p and the self-regulatory Pdr3p is thought to be subject to regulation by other transcription factors [156]. Pdr1p and Pdr3p take interchangeable roles in regulating the PDRE, specifically Pdr5p that is responsible for the transport of drugs. However, Pdr3p is also involved in the retrograde response to activate Pdr5p [157].

This study aims to investigate how the metabolism copes with the loss of *QDR3* gene. Recent analyses (data not shown) have indicated a possible respiratory deficiency for the mutant lacking this gene in a manner that is dependent on the amount of glucose in the medium [14], which was different from what has been observed for the deletion mutants of two close orthologs with functional similarity; *QDR1* and *QDR2*. For this purpose homozygous diploid deletion mutant of *QDR3* was grown on carbon and nitrogen limited continuous cultures and transcriptome and endo- or exometabolome levels as well as the optimum metabolic solution space yielding the present phenotype was determined in comparison to *hoΔ/hoΔ* selected as control and *pdr3Δ/pdr3Δ* selected as drug resistance control strain from another well-characterized MDR family. Studies so far have been focusing on the drug and chemical resistance characteristics of that family [150, 151, 152] rather than concentrating on the system based changes observed in the metabolism. This is believed to be the first comprehensive study to investigate a member of the MDR major facilitator super-family; Qdr3p and its previously unpredicted respiratory performance in high-throughput terms with an integrative systems biological approach.

4.1.2. Methods

4.1.2.1. Strain, Growth Conditions and Sampling. Three homozygous deletion mutants; *Δho/Δho*, *Δqdr3/Δqdr3* and *Δpdr3/Δpdr3* of diploid BY4743 (MATa/MATα *his3Δ/his3Δ leu2Δ/leu2Δ* LYS2/*lys2Δ* MET15/*met15Δ ura3Δ/ura3Δ*; [23]) was cultivated in 2L fermenters (Applikon®) with 1L working volume under aerobic conditions in glucose- or ammonium-limited F1 media [24] in chemostat mode at a dilution rate of $0.1h^{-1}$. The fermentation conditions were given in Section 3.1.2.1. Samples for transcriptome, endo- and exometabolome analyses were taken after spending 5 residence times at steady state. Biomass was determined at the steady states gravimetrically.

4.1.2.2. Endo-metabolome and exometabolome sampling, endometabolome extraction, analytical methods for foot printing and fingerprinting. For metabolic foot printing, 1 ml samples were withdrawn from the fermentation broth on ice and centrifuged at 4^oC at 14 000 rpm for 4 minutes. The supernatant was stored at -80^oC until analysis. Sampling protocols for metabolic fingerprinting were described in Section 3.2.2.2. The protocols for metabolic foot printing and fingerprinting were described in Section 3.2.2.2. The

metabolome data is supplemented in Appendix E. Steady state exometabolic concentrations of glucose, ethanol, ammonium, acetate, acetaldehyde and succinate were determined enzymatically using Boehringer-Mannheim kits and they were further used in flux balance analysis.

4.1.2.3. Transcriptome sampling RNA isolation and transcriptome analysis. The complete protocol was carried out as described in Section 3.1.2.3.

4.1.2.4. Microarray data acquisition. The complete protocol was carried out as described in Section 3.1.2.4. In compliance with MIAME guidelines [72], the microarray data from this study has been submitted to ArrayExpress at the European Bioinformatics Institute under accession number [E-MTAB-707].

4.1.2.5. Data analysis. In order to identify transcripts whose expression significantly differed from wild type levels [74], the software package EDGE [75] was used. This set of significantly expressed transcripts for *QDR3* and *PDR3* deletions under glucose or ammonium limitation were evaluated using p-values, which were corrected for the false positives introduced by multiple testing using Bonferroni correction and 10^{-2} was selected as the cut-off threshold for p-values. The Benjamini-Hochberg method was used for the calculation of false discovery rates. The visualizations for the common subsets of genes were illustrated via the Venn Diagram generator (http://www.pangloss.com/seidel/Protocols/venn4.cgi). Hierarchical Clustering Explorer (HCE) 3.0 [77] was used for hierarchical clustering purposes. The significantly enriched functional categories and the process ontology terms of the genes falling into the same cluster were determined by AmiGO Term Finder tool [79]. The threshold p-value was selected as 10^{-3}. Transcription factors (TF) were taken from three sources; YEASTRACT [81, 158], Lee *et al.* [140], and Luscombe *et al.* [141]. Protein-protein interactions were taken from Yeast BIOGRID [139].

The optimum distributions of the fluxes under different genetic and environmental conditions were determined by linear optimization with the suitable biological objective functions by using the metabolic model constructed by Förster *et al.* [12]. The mapping of the transcriptome and the metabolome as well as the flux distributions on the biochemical

pathways was done by using the *Saccharomyces* Genome Database Pathway Tools Omics Viewer [53].

4.1.3. Results and discussion

The response to genetic perturbations resulting from the deletion of *QDR3* or *PDR3* genes from two separate multi-drug resistance families were investigated and compared using a system based integrative approach. Homozygous deletion mutants of *QDR3*, *PDR3* and *HO* genes were grown in glucose or ammonium limited continuous cultures. Transcriptome, endo- and exometabolome profiles at steady state as well as the distributions of the fluxes in the optimized solution space were compared to reveal the differences in the underlying mechanisms of action in drug resistance. The selection of the drug resistance control family was based on several criteria that needed to be taken into consideration simultaneously. The mutant of such a gene was selected that it would be respiratory proficient, not having close orthologs to replace the gene but with functional differences and not taking a role in the retrograde response from mitochondria. Since respiration related phenomena take place in the mitochondrion, a drug resistance mutant also unable to trigger retrograde signalling was selected as a control strain. The experimental setup was selected specifically to follow response to different amounts of glucose in fermentation medium aiming to clarify the yet unclear mechanisms put into action in the absence of *QDR3*.

4.1.3.1. Nutritional conditions determine the transcriptional and metabolic response of the deletion mutants. In order to identify the differences in the molecular mechanism of drug resistance in response to both genetic and environmental conditions, hierarchical organization of the transcriptome, endo- and exometabolome of the control strain and of the mutant strains; Δ*pdr3*/Δ*pdr3* and Δ*qdr3*/Δ*qdr3* were comparatively investigated under glucose and ammonium limitation.

A total of 1812 genes displayed a significantly altered expression levels (p-value=0.01) in either one or more of the experimental conditions. The hierarchical organization of both the transcriptome and the endometabolome obtained under glucose or ammonium limitation clustered as two separate subsets of one major cluster. Δ*pdr3*/Δ*pdr3*

was clustered together with the wild type under glucose limitation while Δ*qdr3/*Δ*qdr3* was then hierarchically associated with these two mutants. When ammonium was the limiting nutrient in the medium, Δ*qdr3/*Δ*qdr3* was in the same cluster with the control strain and Δ*pdr3/*Δ*pdr3* was more distant in terms of hierarchical organization. The clustering of exo-metabolome indicated the distinct behaviour of these strains under two different types of limitation conditions. Under ammonium limitation exo-metabolome for Δ*qdr3/*Δ*qdr3* was clustered together with the control strain and more distantly with Δ*pdr3/*Δ*pdr3* whereas the deletion mutants of the two drug resistance genes were clustered together further away from the control strain under glucose limitation (Figure 4.1a, b).

In light of the hierarchical organization of the strains obtained at different levels, the nutritional conditions were determined to be the dominant parameter in determining the cellular behaviour of these two deletion strains and these two strains were observed to display different and distinct behaviour under glucose or ammonium limitation.

4.1.3.2. Deletion and nutrition specific gene expression profiles reveal how yeast re-adjusts itself to its current condition. The investigation of the transcriptome profiles indicated that in total, 1523 genes were differentially up-regulated in at least one of the fermentations conducted using Δ*qdr3/*Δ*qdr3* and Δ*pdr3/*Δ*pdr3* under glucose or ammonium limitation whereas 1301 genes were differentially down-regulated (Figure 4.2, Tables 4.1 and 4.2).

The expression levels of 116 genes increased in response to all nutrient limitations and genetic perturbations and this subset of genes were significantly enriched for growth associated processes including gene expression, translation, ribosome biogenesis, regulation of gene expression and translation and non-coding RNA metabolism. On the other hand a subset of genes (62 genes) was constitutively down-regulated irrespective of the type of nutrient limitation or genetic perturbation that they were exposed to. This subset of genes was significantly enriched with cellular response to heat. Previous reports also indicated the up-regulation of similar growth associated processes irrespective of the type of environmental perturbation, in response to increasing growth rates and an accompanied down regulation of stress response genes including heat responsive genes [85, 86]. Interestingly it was observed that under nutrient limited conditions, the yeast cells

with a missing drug resistance gene responded in a similar manner to what has been observed under increasing growth rate conditions.

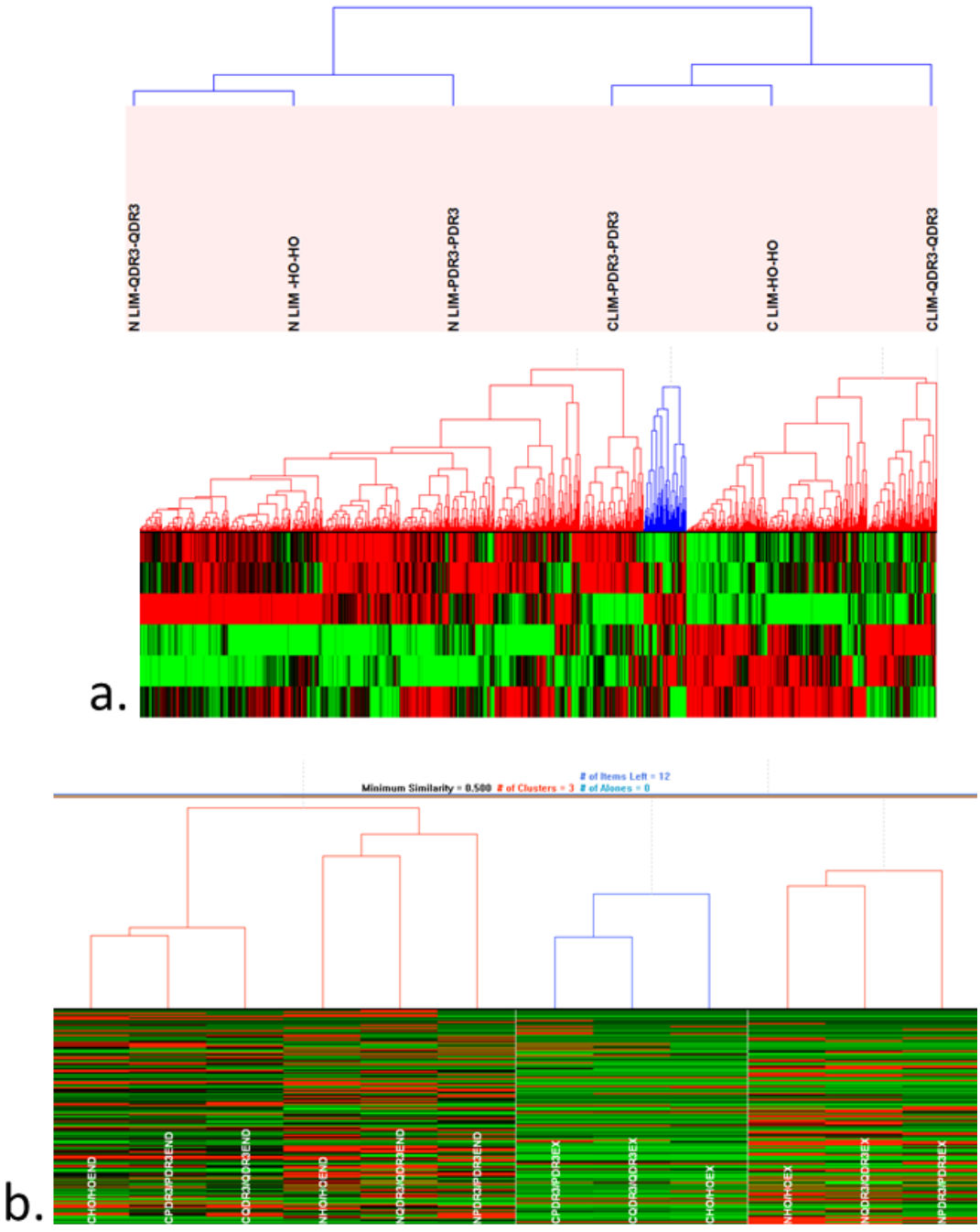

Figure 4.1. Hierarchical organization of transcriptome (a), and metabolome (b) with QDR3-QDR3: Δ*qdr3*/Δ*qdr3*, PDR3-PDR3: Δ*pdr3*/Δ*pdr3*, HO-HO: Δ*ho*/Δ*ho*

Table 4.1. Biological process GO terms significantly associated (p value < E-02) with differentially expressed transcripts under glucose limitation with U-R: up regulation, D-R: down regulation and non-significant associations denoted with *

Process GO Term	**Trend**	**P-value**	**Sample frequency**	**Background frequency**
Δ*qdr3*/Δ*qdr3*, glucose limitation				
oxidation reduction	U-R	1.47E-05	37/230	367/6355
ubiquitin-dependent protein catabolic process	U-R	3.45E-04	23/230	186/6355
carboxylic acid metabolic process	U-R	1.12E-03	35/230	397/6355
mitochondrion inheritance	U-R	1.24E-03	9/230	30/6355
proteolysis involved in cellular protein catabolic process	U-R	1.45E-03	26/230	248/6355
cellular ketone metabolic process	U-R	2.26E-03	35/230	409/6355
mitochondrion localization	U-R	3.04E-03	9/230	33/6355
amine biosynthetic process	U-R	4.98E-03	18/230	141/6355
potassium ion transport	D-R	1.11E-01*	3/61	11/6355
Δ*pdr3*/Δ*pdr3*, glucose limitation				
regulation of cell cycle	U-R	9.37E-01*	11/118	186/6358
mitochondrial ATP synthesis coupled electron transport	D-R	2.49e-08	12/206	28/6357
oxidative phosphorylation	D-R	3.40e-08	16/206	59/6357
respiratory electron transport chain	D-R	1.65e-07	12/206	32/6357
cell death	D-R	1.72e-05	13/206	55/6357
translation	D-R	4.67e-04	62/206	1042/6357
nucleobase, nucleoside and nucleotide metabolic process	D-R	1.26e-03	26/206	281/6357

The subset of genes that were up-regulated only in glucose limited conditions in the absence of the *QDR3* gene constituted a group of 231 genes.

Table 4.2. Biological process GO terms significantly associated (p value < E-02) with differentially expressed transcripts under ammonium limitation as well as at all times with U-R: up regulation, D-R: down regulation and non-significant associations denoted with *

Process GO Term	**Trend**	**P-value**	**Sample frequency**	**Background frequency**
Δ*qdr3*/Δ*qdr3*, ammonium limitation				
protein thiol-disulphide exchange	U-R	1.46E-01*	2/76	2/6358
glycerophospholipid catabolic process	U-R	8.60E-01*	2/76	4/6358
post-transcriptional regulation of gene expression	D-R	3.24e-04	18/134	206/6357
Δ*pdr3*/Δ*pdr3*, ammonium limitation				
ribosome biogenesis	U-R	8.66E-17	49/162	437/6355
rRNA processing	U-R	9.75E-08	31/162	321/6355
ncRNA processing	U-R	2.82E-07	35/162	419/6355
ribonucleoprotein complex assembly	U-R	9.24E-04	15/162	127/6355
maturation of SSU-rRNA from tricistronic rRNA transcript	U-R	7.88E-03	12/162	97/6355
glucose catabolic process	D-R	4.86E-09	14/128	57/6355
pyruvate metabolic process	D-R	4.83E-08	12/128	44/6355
glycolysis	D-R	1.17E-07	11/128	37/6355
alcohol metabolic process	D-R	6.00E-05	20/128	237/6355
gluconeogenesis	D-R	4.70E-03	7/128	33/6355
Up-regulated in all fermentations				
regulation of translation	U-R	2.21e-15	28/115	192/6357
ribosome biogenesis	U-R	1.84e-07	30/115	448/6357
gene expression	U-R	5.13e-06	71/115	2235/6357
regulation of gene expression	U-R	3.35e-05	39/115	878/6357
translation	U-R	4.23e-05	43/115	1042/6357
ncRNA metabolic process	U-R	1.34e-03	25/115	483/6357
Down-regulated in all fermentations				
cellular response to heat	D-R	3.56e-03	3/62	4/6357

This group of transcripts were significantly enriched with oxidation reduction, carboxylic acid metabolism, mitochondrion inheritance and mitochondrion localization, which are all related to the extent to which the organism uses its respiratory capacity, as well as other processes regarding the metabolic degradation processes including ubiquitin-dependent protein catabolism and proteolysis involved in cellular protein catabolism, cellular ketone metabolism and amine biosynthesis.Since the fermentation medium was limited in terms of its glucose content, the metabolism was observed to switch itself to perform respiratory functions as reported elsewhere [159, 160]. Genes that were involved in ubiquitination and proteolytic activity have previously been reported to be expressed at a higher level when the cells are growing by respiration, similar to the present findings [161].

All genes associated with protein thiol-disulphide exchange and half of the genes that were associated with glycerophospholipid catabolism were among the 76 transcripts that were up-regulated under ammonium limitation in Δ*qdr3*/Δ*qdr3* mutants. Protein thiol-disulphide exchange enzymes were previously reported to be strong oxidases [162]. The up-regulation in the expression levels of the oxidation-reduction enhancing genes, even in the presence of abundant glucose, might indicate that the absence of *QDR3* gene resulted in increased oxidative activity, which might put the cell at risk. Glycerophospholipid catabolism generates choline moieties to be reused in phosphaditylcholine synthesis as well as being involved in the utilization of glycerophosphocholines and glycerophosphoinositols as phosphate sources in yeast [163]. The up-regulation of this degradation pathway might indicate the necessity for additional phosphates made available through this route although this pathway is not reported as a major source of phosphates in the cell.

The group of genes that were differentially up-regulated when ammonium was limited in the absence of *PDR3* (162 genes), were significantly associated with growth related processes including ribosome biogenesis, rRNA and non-coding RNA processing, ribonucleoprotein complex assembly and the maturation of SSU-rRNA from tricistronic rRNA transcript. It would be possible to speculate that the yeast cells tried to cope with the loss of the drug resistance gene by trying to maintain their growth at optimum as much as the availability of the nitrogen source permitted.

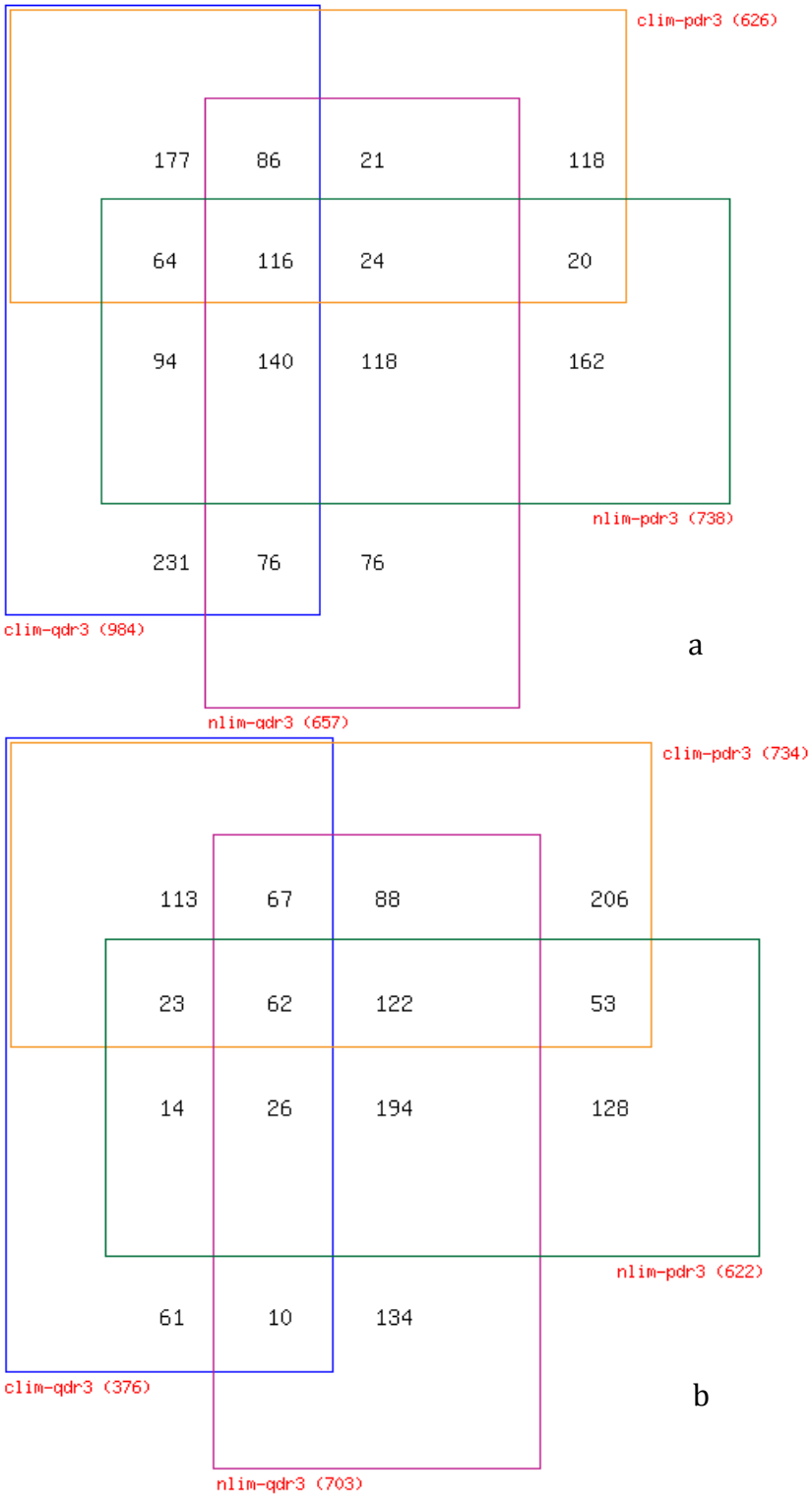

Figure 4.2. Distribution of the differentially up-regulated (a) and down-regulated (b) transcripts with Nlim: ammonium limitation, Clim: glucose limitation, pdr3: Δ*pdr3*/Δ*pdr* and qdr3: Δ*qdr3*/Δ*qdr* and the numbers indicating the number of genes in that set

The 118 genes that were up-regulated under glucose limitation in the absence of *PDR3* were associated with regulation of cell cycle. The control of glucose regulation on cell cycle genes, which were critical for the passage to G1 phase, was previously reported [164]. More of the cell cycle genes, including the previously reported *BCK2* and *GRR1*, would be affected from glucose limited conditions as a response to the absence of *PDR3*.

The 61 transcripts that were down-regulated under glucose limitation in the absence of *QDR3* gene were associated with potassium ion transport, though not significantly. The down-regulation of the genes that play role in the transport of potassium ion, which is the most abundant ion in the yeast cell, might have indicated alterations in the major determinant of electrical membrane potential modulating the ion homeostasis and toxicity in the cell created by the loss of function of the *QDR3* gene [165].

Another group of transcripts (134) were significantly down-regulated in the Δ*qdr3/*Δ*qdr3* population under ammonium limitation and they were associated with the post-transcriptional regulation of gene expression and the transcripts that were significantly down-regulated in the absence of the *PDR3* gene under ammonium limitation (128 genes) were significantly associated with glucose catabolism, pyruvate and alcohol metabolism, glycolysis, gluconeogenesis and monocarboxylic acid metabolism. Although the glucose supplied into the fermentation environment was sufficient, the genes active during fermentation were observed to be down-regulated in the absence of *PDR3*. Possibly, the ability of yeast cells to perceive the glucose level in the environment was altered in response to the loss of *PDR3*. The enzyme product of *PDR5* gene, whose transcription is directly controlled by Pdr3p, was reported previously to be physically interacting with the low affinity glucose transporter Hxt1p and the hexose transporter with a moderate affinity for glucose, Hxt5p (Table 4.3). The transport of glucose would thus be affected in the absence of *PDR3* and the metabolism might have lost its ability to efficiently uptake and utilize glucose through a loss of activity in Hxt1p and Hxt5p. Moreover, *HXT5* was previously reported to be induced by a decrease in growth rate [166]. This also agrees with the up-regulation of growth related transcripts observed under the same conditions.

Table 4.3. The expression levels of the physically interacting proteins for *QDR1*, *QDR2*, *QDR3*, and *PDR1*, *PDR3*, *PDR5* with the interactions within the DHA12 drug resistance family and the pleiotropic drug resistance family of the ABC transporters**

Family Name	**Gene Name***	**Significance (Y/N)**	**Case when significant***	**Interacting with**
The QDR sub-family	*QDR1*	N	-	*HSP82*
	QDR2	Y, d-r	C, QDR3	*PDR5, PDR12, HXT1, HXT5, HNM1, SFK1, SNQ1, SOS23, TPO1, UBI4*
	QDR3	N	-	*PDR12, HEK2*
The PDR sub-family	*PDR1*	N	-	*NGG1, PDR3, HEK2*
	PDR3	N	-	*HSP82, NGG1, PDR1, HEK2*
	PDR5	Y, d-r in C and N QDR3, u-r in N PDR3	All cases	*QDR2, PDR12, HXT1, HXT5, HNM1, SFK1, SNQ1, SOS23, TPO1, UBI4*
	TPO1	N	-	*QDR2, PDR12, PDR5, TPO3, TPO2, SNQ2*
	TPO2	Y, d-r	N, PDR3	*PDR12, TPO1, TPO3, SNQ2*
	TPO3	N	-	*SNQ2, TPO1, TPO2*
	TPO4	N	-	*PDR12, YOR1*
	NGG1	Y, u-r	C, PDR3	*PDR1, PDR3*
	PDR12	Y, d-r	Both QDR3 and C PDR3	*QDR2, QDR3, TPO4*
	SNQ2	Y, d-r	All cases	*PDR5, PDR12, QDR2, TPO1, TPO2, TPO3*
	YOR1	Y, d-r in C and N QDR3, u-r in N PDR3	All cases	*TPO4*

**Abbreviations: d-r = down-regulated, u-r = up-regulated, Y = yes, N = no, C = glucose limitation, N = ammonium limitation, QDR3 = Δ*qdr3*/Δ*qdr3*, PDR3 = Δ*pdr3*/Δ*pdr3*

The expression level of the transcripts that were significantly down-regulated in the absence of *PDR3* gene under glucose limitation (206) were significantly associated with

respiration related processes including mitochondrial ATP synthesis coupling electron transport, oxidative phosphorylation, respiratory electron transport chain, cell death, translation and nucleobase, nucleoside and nucleotide metabolic processes. This observation also supported the notion that the cells re-organized their glucose responsive respiration-fermentation switch metabolism during the loss of *PDR3* gene.

4.1.3.3. The expression levels of transcription factors were re-arranged to compensate for the loss of the drug resistance genes. The expression levels of 44 genes encoding transcription factors were significantly altered in response to the nutrient limitations and the genetic perturbations (Table 4.4). Four transcription factors (*GCN4, ASH1, HAP1* and *MET4*) were up-regulated in glucose limited conditions and down-regulated under ammonium limitation in both strains. The up-regulation of *GCN4* under glucose limitation might display its role in the energy metabolism, specifically in purine biosynthesis and its role as a general controller in response to nutrient stress whereas the presence of leucine, histidine and uracil supplemented in the medium to remove the strain's auxotrophy prevented the stress response induced by ammonium limitation, thus resulting in the down-regulation of the transcription factor [167]. The up-regulation of *HAP1* in aerobic conditions induced by the limited amount of glucose and its down-regulation in fermentative conditions induced by the presence of abundant glucose also agreed with the reported literature [168].

The gene encoding the haem-activated transcription factor, Hap4p, which is involved in the global control of respiratory gene expression, was down-regulated in the absence of *QDR3* whereas it was up-regulated in the absence of *PDR3* under both nutritional limitations. Despite the role of Hap4p as being active during growth on non-fermentable carbon sources [169, 170], its expression was low in Δ*qdr3*/Δ*qdr3* even under glucose limited conditions whereas the expression of the gene was high in Δ*pdr3*/Δ*pdr3* even during the presence of sufficient amounts of glucose to switch the metabolism to fermentation. This might possibly indicate the presence of a drug resistance mechanism associated with respiration by-passing the effect of the fermentable carbon source, glucose, through the respiration controlling transcription factor Hap4p.

Table 4.4. Differentially expressed genes encoding transcription factors (TFs)

	Trend* and significance of differential change (p-value)			
TF encoding gene	**Q –G****	**Q-A****	**P-G****	**P-A****
GCN4	u-r (1.10E-03)	d-r (1.01E-03)	u-r (1.01E-03)	d-r (1.06E-03)
GIS2	u-r (2.41E-02)	u-r (1.70E-02)	d-r (3.24E-02)	d-r (2.29E-02)
ASH1	u-r (2.89E-02)	d-r (3.52E-02)	u-r (2.06E-02)	d-r (3.82E-02)
ABF1	u-r (4.60E-02)	u-r (2.97E-02)	u-r (4.99E-02)	d-r (3.66E-02)
SIN3	u-r (2.90E-02)	d-r (2.96E-02)	d-r (2.98E-02)	d-r (3.04E-02)
CDC39	u-r (3.24E-02)	u-r (4.45E-02)	d-r (3.21E-02)	d-r (4.66E-02)
HAP1	u-r (3.54E-02)	d-r (1.24E-02)	u-r (4.39E-02)	d-r (2.03E-02)
RSF2	u-r (4.40E-02)	d-r (4.14E-02)	d-r (4.75E-02)	d-r (4.88E-02)
IXR1	u-r (5.47E-02)	u-r (5.64E-02)	u-r (5.60E-02)	u-r (5.40E-02)
MET4	u-r (5.99E-02)	d-r (5.07E-02)	u-r (4.22E-02)	d-r (4.93E-02)
HAP4	d-r (4.44E-02)	d-r (3.98E-02)	u-r (2.25E-02)	u-r (2.97E-02)
ZAP1	-	u-r (1.54E-02)	-	u-r (1.99E-02)
STP3	-	u-r (4.30E-02)	-	d-r (4.88E-02)
MIG2	-	u-r (4.61E-02)	-	u-r (5.81E-02)
IFH1	-	d-r (4.22E-02)	-	u-r (3.92E-02)
HAC1	-	d-r (1.26E-02)	-	u-r (1.83E-02)
STP2	-	d-r (4.96E-02)	-	d-r (4.23E-02)
RIM101	-	d-r (4.94E-02)	-	d-r (5.97E-02)
AFT1	-	d-r (4.56E-02)	-	d-r (5.52E-02)
CUP9	-	d-r(4.84E-02)	-	d-r (5.28E-02)
PHD1	u-r (3.72E-02)	-	u-r (3.65E-02)	-
CAT8	u-r (4.30E-02)	-	u-r (4.63E-02)	-
OPI1	u-r (4.76E-02)	-	u-r (4.25E-02)	-
ROX1	d-r (4.49E-02)	-	u-r (3.28E-02)	-
SUM1	d-r (5.36E-02)	-	u-r (2.29E-02)	-
GIS1	d-r (5. 94E-02)	-	d-r (5.08E-02)	-
ADR1	u-r (4.78E-02)	-	-	-

Table 4.4. Differentially expressed genes encoding transcription factors (TFs), cont.

	Trend* and significance of differential change (p-value)			
TF encoding gene	**Q –G****	**Q-A****	**P-G****	**P-A****
RPN10	u-r (5.42E-02)	-	-	-
MGA2	u-r (5.54E-02)	-	-	-
NRG2	-	u-r (4.60E-02)	-	-
TYE7	-	u-r (5.37E-02)	-	-
MIG1	-	u-r (5.71E-02)	-	-
UGA3	-	d-r (5.65E-02)	-	-
SPT23	-	d-r (5.96E-02)	-	-
HMRA2	-	-	u-r (2.86E-02)	-
LYS14	-	-	d-r (2.40E-02)	-
HAL9	-	-	d-r (5.31E-02)	-
RAP1	-	-	-	u-r (5.84E-02)
MTH1	-	-	-	d-r (4.94E-02)
SWI1	u-r (3.97E-02)	d-r (5.69E-02)	u-r (3.79E-02**)**	-
DOT6	-	u-r (3.09E-02)	u-r (3.85E-02)	d-r (3.53E-02)
RPN4	u-r (4.22E-02)	-	d-r (4.39E-02)	d-r (5.11E-02)
BAS1	-	u-r (4.93E-02)	u-r (5.52E-02)	u-r (4.90E-02)
RSC30	d-r (3.63E-02)	-	d-r (2.51E-02)	d-r (5.86E-02)

*u-r: up-regulated, d-r: down-regulated

**Q-G: Δ*qdr3*/Δ*qdr3* under glucose limitation, Q-A: Δ*qdr3*/Δ*qdr3* under ammonium limitation, P-G: Δ*pdr3*/Δ*pdr3* under glucose limitation, P-A: Δ*pdr3*/Δ*pdr3* under ammonium limitation

GIS2 and *CDC39* were found to be up-regulated in the absence of *QDR3* whereas it was down-regulated in the absence of *PDR3* under both environmental limitations. The absence of *GIS2* was previously reported to create decreased resistance to fenpropimorph; a morpholine fungicide and a reduction in the function of *CDC39* was reported to result in a decrease in the resistance to the antineoplastic drug, hydroxyurea [29]. The expression levels of these two transcription factors might be induced so as to compensate for the deficiency in drug resistance capacity that was created by the absence of *QDR3*. Such

compensation was not observed in the absence of *PDR3*, possibly due to the presence of *PDR1* superseding *PDR3*.

CAT8, *OPI1* were up-regulated and *GIS1* was down-regulated in both strains under glucose limitation. The decreased rapamycin resistance displayed by the null mutant of *CAT8*, the transcriptional activator necessary for de-repression of genes under non-fermentative growth conditions [171], as well as the decreased resistance to a variety of chemicals including sodium arsenite, CTBT, amiodarone, sulphanilamide, BPS, benomyl, calcium dichloride and wortmannin, displayed by *OPI1* might indicate that the up-regulation in these transcripts might have been triggered to compensate for the reduced chemical resistance induced by the deletion of the drug resistance genes [29]. An interesting point that requires further investigation was the down-regulation of *GIS1* in both mutant cultures under glucose limitation, which encodes a transcription factor involved in gene expression during nutrient limitation and also during transition to stationary phase [172, 173]. The haem-dependent repressor of hypoxic genes, *ROX1* and the transcriptional repressor required for the mitotic repression of middle sporulation specific genes, *SUM1* were down regulated in Δ*qdr3/*Δ*qdr3,* whereas they were up regulated in *Δpdr3/Δpdr3* under this condition. The down-regulation of *ROX1* might indicate that the yeast might have perceived its glucose limited and aerated environment as being insufficient in terms of the available oxygen in the absence of *QDR3* gene. On the other hand, *SUM1* might have been replacing functions during the absence of *PDR3* gene since its null mutant was previously reported to result in decreased resistance to streptomycin, amitrole, cycloheximide, fluconazole and sulfometuron methyl [29].

MIG2 was among the genes that were differentially expressed under ammonium limitation in both strains. Increased transcription of *MIG2* in both *Δqdr3/Δqdr3* and *Δpdr3/Δpdr3* under ammonium limitation could be attributed to the fact that in the presence of sufficient amounts of glucose, *MIG2* is required for the repression of the genes involved in the utilization of carbon sources other than glucose [174]. The loss of function of these transcription factors except for *MIG2* all cause decreased resistance to heavy metals, toxins or chemicals and their differential expression in the absence of drug resistance genes might attribute to their properties to overcome this limitation within the cell.

The *ADR1*, *RPN10* and *MGA2* were significantly up-regulated in Δ*qdr3/*Δ*qdr3,* whereas *HAL9* was among the genes whose expression was significantly down-regulated in *Δpdr3/Δpdr3* under glucose limitation. The protein encoded from *MGA2*, taking part in fatty acid desaturation, was involved in lipid biosynthetic activity which is controlled by a number of stimuli such as changes in the availability of lipid nutrients [175] and varying the available nutrient might be concluded to impose a change in the activity of the lipid biosynthetic pathways in the absence of *QDR3* but not of *PDR3*. *ADR1*, whose gene product is the carbon-source-responsive transcription factor involved in the expression of genes that are regulated by glucose repression, was up-regulated when the available amount of glucose was limited in the medium in the absence of *QDR3* [176]. Thus, in the absence of this gene, the metabolism tried to behave in such a way as to adjust itself to survive in glucose excess conditions. The absence of *RPN10* was reported to be associated with a decreased resistance to bleomycin, one of the anti-tumour drugs to which *QDR3* provides resistance [177]. Thus the up-regulation in *RPN10* might have been directly associated with the efforts to compensate for the absence of *QDR3*. Since the null mutation of *HAL9* causes increased nutrient utilization, the cellular mechanisms would have been adjusted in such a way in order to optimize the uptake of glucose under limited conditions in the absence of *PDR3* by decreasing the expression level of the *HAL9* transcription factor [29].

NRG2 and *MIG1* were among the genes that were found to be up-regulated, and *UGA3* and *SPT23* were down-regulated in the absence of *QDR3* under ammonium limitation. A significant up-regulation of *NRG2* gene whose product is a negative regulator of pseudohyphal growth was observed for *Δqdr3/Δqdr3* in N-source limitation [178]. On the other hand, this observation for *NRG2* was in accordance with its functional role of negative regulation of glucose-repressed genes [179] within the significant subset of *Δqdr3/Δqdr3* of ammonium limitation. Increased transcription of *MIG1* in *Δqdr3/Δqdr3* under ammonium limitation is in conjunction with its repressive function in the utilization of carbon sources other than glucose and in gluconeogenesis in the presence of glucose [174]. The cold responsive *SPT23,* which was significantly down-regulated in *Δqdr3/Δqdr3* under ammonium limitation, was also involved in lipid biosynthetic activity [175] and varying the available nutrient was again observed to impose a change in the activity of the lipid biosynthetic pathways in the absence of *QDR3* but not in *PDR3*.

Despite its role in nitrogen utilization, *UGA3* was down-regulated in the absence of *QDR3*, although under ammonium limited conditions the cells would have required an efficient utilization of the available nitrogen sources [180]. The expression of TF encoding genes was not significantly and exclusively affected in *Δpdr3/Δpdr3* under ammonium limitation (Table 4.3).

4.1.3.4. Alterations in glycerol metabolism to cope with the loss of drug resistance genes.

One of the most outstanding differences in intracellular metabolite levels was observed in the accumulation of glycerol and D-glucose. Therefore the glycerol production mechanism and related pathways of the central carbon metabolism in Δ*qdr3*/Δ*qdr3 or* Δ*pdr3*/Δ*pdr3* under glucose or ammonium limitation were investigated integratively using the information provided by the endometabolome and the transcriptome as well as the metabolic flux distributions. Differences in the distribution of metabolic fluxes in the deletion strains under glucose or ammonium limitation were determined by the predictions obtained from flux balance analysis. The reaction fluxes in the metabolic pathways were best predicted through the maximization of the oxygen uptake in glucose limited fermentations and of the ethanol production in ammonium limited fermentations with sufficient amount of glucose in the medium. The solution space was constrained by the exometabolite concentrations for each deletion under each nutrient limitation.

The absence of drug resistance mutants resulted in differences in the respiration – fermentation characteristics that would be expected to take place in wild-type yeast strains in the presence of abundant or limited amounts of glucose (Figure 4.3). The amount of intracellular glucose was higher in all cultures of mutant strains than what was observed for wild type, even though it was slightly lower in the case of the *QDR3* deletion under glucose limitation than the others, which would be an indicator of a more efficient route to glucose utilization by this mutant. Since *PDR3* would possibly be responsible for the functioning of the low-affinity hexose transporter Hxt1p and medium-affinity hexose transporter Hxt5p (as discussed above), Hxt3p (another low affinity hexose transporter) could replace the function of these proteins. The over-expression of *HXT3* in Δ*pdr3*/Δ*pdr3* under ammonium limitation supported this prediction. Interestingly, the expression levels of high affinity hexose transporters were not altered in comparison to their expression levels in wild-type strains under glucose limitation, although the intracellular accumulation

of glucose was apparent. The expression levels of both low-affinity hexose transporters *HXT1* and *HXT3* were up-regulated in Δ*qdr3*/Δ*qdr3* when glucose was abundant. A slight down-regulation of *HXT4* was observed under glucose limitation and this would be responsible for the slightly less accumulation of intracellular glucose under this condition.

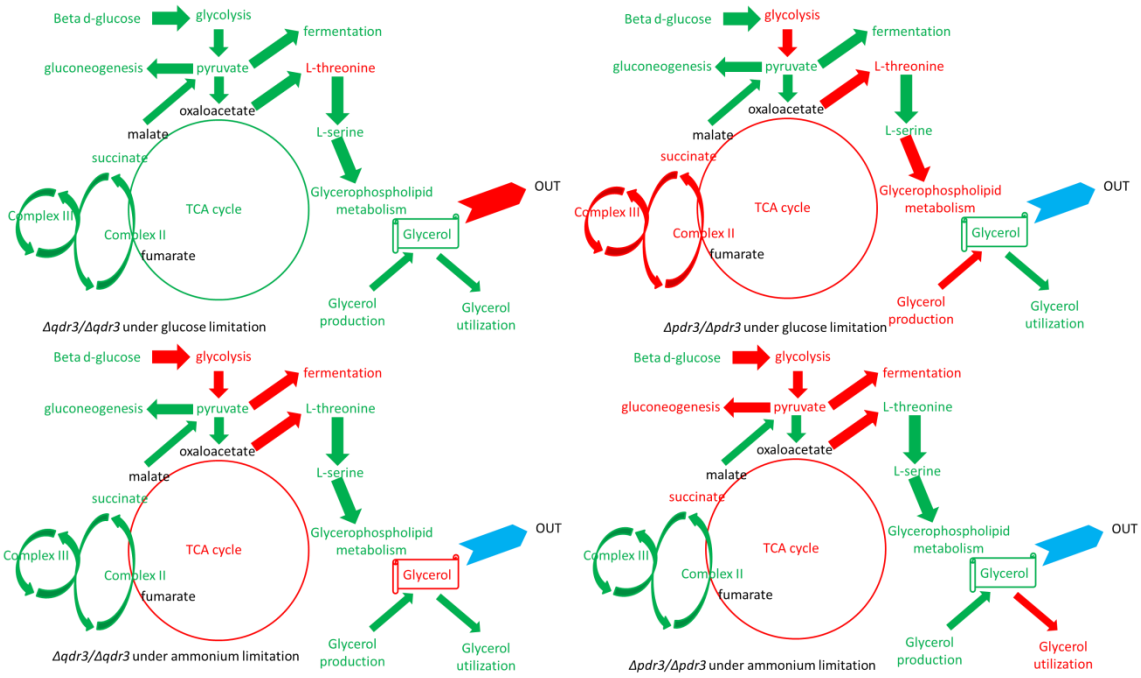

Figure 4.3. Differences in glycerol production mechanism for Δ*qdr3*/Δ*qdr* and Δ*pdr3*/Δ*pdr* under glucose or ammonium limitation. Green: up-regulation or increase, red: down-regulation or decrease, black: no data, blue: no significant change.

Not only the uptake, but also the mechanisms of formation of glucose were triggered in the loss of drug resistance mutants. Since the glucose transport mechanisms were active in all conditions, the increase in the expression of gluconeogenic pathway genes appeared slightly less expected. Δ*pdr3*/Δ*pdr3* mutant adjusted the expression levels of the gluconeogenic genes based on the availability of extracellular glucose, down regulating the expression of the genes whenever extracellular glucose was available. On the other hand, an up-regulation of gluconeogenic pathway genes was observed in glucose or ammonium limited cultures of Δ*qdr3*/Δ*qdr3*, regardless of the availability of glucose indicating the unresponsiveness of the genes from this pathway to either the intracellular or the extracellular glucose concentrations.

The expression levels of the genes involved in glycogen biosynthesis or catabolism were not significantly altered but slightly down-regulated to accompany the high concentrations of available intracellular glucose for either mutant strain under ammonium or glucose limitation indicating that high intracellular concentrations of glucose was not specifically directed towards the synthesis of glycogen, the storage carbohydrate, or neither was glycogen catabolised to supply additional glucose for the metabolism. The tendency of these mutants to re-arrange their metabolism for maintaining high levels of glucose in the cell would be considered as a means of enabling an anoxic fermentative environment to cope with the loss of drug resistance properties.

Glycerol production and the glycolytic flux pathways were previously reported to be related [181]. Despite differences in the availability of glucose, a fermentable carbon source, being present as the sole carbon source in these fermentations, the fluxes and the expression levels of the genes taking role in glycolysis, fermentation and the tricarboxylic acid cycle were constitutively up- or down-regulated without displaying a trade-off except for the case of the Δ*pdr3*/Δ*pdr3* mutant grown under glucose limitation, in which the response of the transcripts in the glycolytic pathway and the TCA cycle were similar to each other and different from those in fermentation. The genes in these pathways were down-regulated regardless of the amount of glucose available in the medium in the fermentation of the Δ*pdr3*/Δ*pdr3* mutants. However, the genes of the fermentation and gluconeogenesis pathways were up-regulated under glucose limitation and this was accompanied by the accumulation of intracellular pyruvate whereas these pathways were down-regulated under ammonium limitation when the available glucose was abundant accompanied by low intracellular pyruvate concentrations. The loss of *QDR3* gene resulted in the up-regulation of the genes taking role in glycolysis, fermentation and TCA cycle under glucose limitation while down-regulation was observed under ammonium limitation when the glucose was abundant.

A strong accumulation of glycerol was detected in all cases except for the Δ*qdr3*/Δ*qdr3* mutant grown under ammonium limitation. However, this accumulation was accompanied by the strong down-regulation of the glycerol exporter gene, *GUP2*, only in one case, and that was for the Δ*qdr3*/Δ*qdr3* mutant grown under glucose limitation. It was previously reported that yeast cells produced glycerol under anaerobic and glucose

repressing growth conditions in order to maintain a cytosolic redox state conducive to sustain glycolytic catabolism [182]. However, the present observation of glycerol accumulation in aerated glucose limited cultures of yeast cells would indicate an alteration in the yeast metabolism as a response to cope with the loss of drug resistance genes. Therefore *GUP2* would possibly be down-regulated to maintain high intracellular concentration of glycerol.

Although glycerol was previously reported to be a by-product of yeast ethanol fermentation [182], the loss of *PDR3* was observed to alter this coupling resulting in the two phenomena to become independent events under ammonium limitation both in terms of intracellular and/or extracellular metabolite concentrations as well as the expression levels of the genes involved in either one of the metabolisms.

The genes taking role in the utilization of glycerol were up-regulated except for the case of the Δ*pdr3/*Δ*pdr3* mutant grown under ammonium limitation. Although glycerol production and accumulation has previously been reported to be stimulated under stress conditions, these mechanisms are yet unclear in terms of providing explanatory information [181]. The stress conditions created by both the limitation of a macronutrient as well as the loss of a drug resistance gene both induced the production of glycerol through the up-regulation of the *GPD* genes and *RHR2* as well as the up-regulation of genes taking role in another route, glycerophospholipid metabolism, releasing glycerol as a by-product of cardiolipin production except for the Δ*pdr3/*Δ*pdr3* mutant grown under glucose limitation.

Despite the down-regulation of the expression levels of the TCA cycle enzymes, the expression levels of the genes involved in oxidation-reduction on the mitochondrial membrane were higher in Δ*pdr3/*Δ*pdr3* than their levels in wild type under ammonium limitation. The genes involved in the oxidation-reduction phenomenon taking role in the mitochondrial membrane in respiratory chain complexes II and III remained up-regulated in Δ*qdr3/*Δ*qdr3* mutants, regardless of the amount of glucose supplied into the environment. It was previously reported that the expression of *GPD2* taking role in glycerol production was induced by anoxic conditions [183]. The up-regulation observed in the expression level of this gene under ammonium limitation where abundant glucose

was available indicated that glycerol formation was facilitated to act as a redox sink to maintain the redox state under fermentative conditions. The high intracellular accumulation of glucose would possibly mimic the anoxic condition that the cells required in order to activate such mechanisms.

The intracellular accumulation of glycerol in Δ*pdr3*/Δ*pdr3* under glucose limitation despite the up-regulation of the genes taking role in its utilization and the down-regulation of the enzymes involved in its production remains unclear via any known routes of yeast and could only be explained through the presence of yet undisclosed alternative pathways. However, under ammonium limitation, the production of glycerol could not be facilitated through the glycerophospholipid pathways due to the down-regulation of the enzymes catalysing the production of L-threonine from oxaloacetate. Therefore, the glycerol accumulation could solely be attributed to the up-regulation of the genes involved in its production and the down-regulation of the genes taking part in its utilization.

The lower concentration of intracellular glycerol observed for the Δ*qdr3*/Δ*qdr3* mutant under ammonium limitation would be attributed to the abstinence to supply sufficient amounts of L-threonine that would be used for L-serine production, which in turn was required for the glycerophospholipid metabolism. Under these conditions, the glycerophospholipid metabolism would be identified as the more significant supplier of glycerol. As soon as the expression levels of the genes in this metabolic pathway were rendered low, the intracellular accumulation of glycerol was relieved.

4.1.4. Study Conclusions

The intracellular rearrangement of gene expression levels, metabolite concentrations and the predicted fluxes were integrated for the homozygous deletion mutants of drug resistance genes from two different families; *QDR3* from the multidrug resistance family and *PDR3* from the pleiotropic drug resistance family grown in aerated continuous fermentations under glucose or ammonium limitation. The availability of glucose was the dominant parameter in determining the hierarchical organization of transcriptome and endometabolome in the absence of these drug resistance genes. Yeast re-adjusted its metabolism to cope with the loss of drug resistance genes by inducing the expression of

growth associated genes whereas rendering the expression of heat response genes low mimicking a similar response to increasing the growth rate. In addition, transcriptional regulation was used as a mean to increase the yeast's resistance to external chemical factors through down- up-regulation of transcription factors involved in increased chemical resistance. Δ*qdr3/*Δ*qdr3* utilized potassium ion homeostasis as well as the re-adjustment of the expression levels of transcription factors in order to cope with its decreased resistance to external factors of toxicity.

Alterations in the mechanism of drug resistance either by ATP mediated transport or by proton pumps caused significant changes in the central carbon mechanism and glycerol related pathways. The mechanism was possibly associated with respiration, regardless of the availability and the amount of a fermentable carbon source in the medium through the respiration controlling transcription factor Hap4p. A strong accumulation of glucose and glycerol, even in glucose limited aerated cultures, as well as the decoupling of glycerol production and fermentation could be attributed to the re-arrangement of the metabolism to cope with the loss of drug resistance genes. The glycerophospholipid metabolism would be the more significant supplier of glycerol in the absence of *QDR3* whereas the increase in the amount of glycerol through its production pathway as well as its little utilization by the *PDR3* mutants under ammonium limitation could be attributed to the accumulation of glycerol. These re-arrangements enabled the maintaining of the redox state under the anoxic conditions dictated by the intracellular accumulation of glucose.

Alterations in the drug resistance mechanisms were shown to result in perturbations in sensing and rearrangement of the metabolism as well as switching on or off of several transcriptional regulatory mechanisms in response to the availability of glucose in the environment. Loss of *QDR3* gene could be related to the loss of resistance to chemical drugs from a wide range of applications including the chemotherapeutic agents; bleomycin and cisplatin. The anoxic conditions created by the presence of available glucose in the loss of *QDR3* gene and switching of the metabolism to accumulate intracellular glycerol to maintain the redox balance might imply that metabolic arrangements for the removal drug resistance would need to be evaluated carefully since the central carbon metabolism was completely affected by this change. Tumour cells prefer anoxic conditions for growth and development, which is similar to the conditions investigated in this study, and the

unexpected observations on the central carbon metabolism that were provided by this study indicated the necessity for the systems based evaluation of metabolism upon genetic manipulations conducted on drug resistance mechanisms. These arrangements were conducted to cope with the loss of drug resistance genes by helping to maintain the integrity of the cell, aiding in its survival and developing novel mechanisms to adapt to the newly encountered environmental conditions. These changes are yet unclear and require further investigation under the light of the present findings.

4.2. Prediction of genetic interactions from phenotype via chemical genomics and synthetic genetic arrays

4.2.1. Background

Phenomics is a field of study concerned with the characterization of phenotypes, which are characteristics of organisms that arise via the interaction of the genome with the environment. Phenotype analysis is used to ascertain gene function and it refers to any type of phenotypic analysis of genomic information to understand the relationship between genes and higher levels of organization in the cell. The development and implementation of genome-wide analytical techniques, which can be generally named under ‘omics’, provide information of mRNA, protein and metabolite levels in the whole cell. However, the operational unit of function in cells can more properly be seen fully as assembled biochemical networks and from their properties such as connectivity, interactions and dynamic properties [184].

With the advances in genome sequencing and large-scale genetic analyses, genetic interactions of large scale have been available for many organisms. These advances have proposed a new challenge on researchers to understand how genes function as networks to carry out and regulate cellular processes. *Saccharomyces cerevisiae* is a suitable model organism to gain insights into genetic interactions and networks due to the availability of powerful functional genomic tools to allow systematic analyses. This helps in understanding interacting components as well as key properties of the genetic networks in which they participate. Understanding genetic-interaction networks in yeast serve a higher purpose as similar networks are expected to underlie the relationship between genotype

and phenotype in outbred populations in which combinations of specific alleles determine the fitness of individuals. Moreover, complex genetic disorders with multiple effectors are largely unknown in higher organisms and understanding and mapping genetic networks in model organisms such as yeast provides a starting point in studying and understanding similar interactions in those organisms [38].

Genetic interactions tend to occur among functionally related genes, although for essential genes, interactions correspond to a broader functional range. Because of this reason, the set of genetic interactions observed for a particular query gene may suggest a function for that gene [38]. Synthetic lethal interactions identify pathways that buffer one another and therefore, genetic interaction maps are useful in identifying enzyme-substrate relationships. The upstream activators and downstream targets of specific enzymes might be identified from genetic identification profiles. The interaction relationships might also be used to identify proteins that are negatively regulated by specific enzymes [38].

Epistasis is defined as the interaction between different genes and it has been a growingly interesting topic in complex disease genetics. Complicating factors, such as an increased number of contributing loci and susceptibility alleles, penetrance and contributing environmental effects, cause the search for treatment of diseases with complex traits to be harder and the results to be less successful than simple Mendelian disorders. The presence of epistasis is particularly important if the effect of one locus is altered or masked by the effects at another locus and therefore the power to detect the first locus is reduced. Elucidation of the joint effects at the loci is hindered by their interaction [185].

Fitness, a class of phenotype is central to many genetic interaction studies. Fitness originally was a measure of population allele frequencies [186, 188, 188]. It can also be determined by using growth rates of isogenic microbial cultures.

In order to gain a thorough understanding of complex biological processes and functional relationships, small molecules can also serve as replacements of mutations. These molecules have the advantage of providing rapid and reversible modulation of gene activity. The use of such probes on a genome wide scale is generally termed as ‘chemical genomics’. Chemical genomics is based on the idea that deletion of a gene encoding the

target of an inhibitory compound should result in similar effects to inhibition of a target by drug treatment. In a chemical-genetic interaction, a deletion mutant is hypersensitive to a normally sub-lethal concentration of a growth inhibitory compound. The comparison of a chemical-genetic profile to a synthetic-lethality profile should identify pathways and targets that are inhibited by drug treatment (Figure 4.4). A comprehensive compendium of global genetic interaction profiles might allow the targets of growth-inhibitory compounds to be identified. For therapeutic intervention, gene-drug and drug-drug combinations inhibiting cellular systems should be investigated because most genes are non-essential and that cell function reflects interconnected robustness. Chemical genomics studies might enable identification of compounds that target specific pathways and selectively kill cells with defined mutant phenotypes to prevent and cure diseases [38].

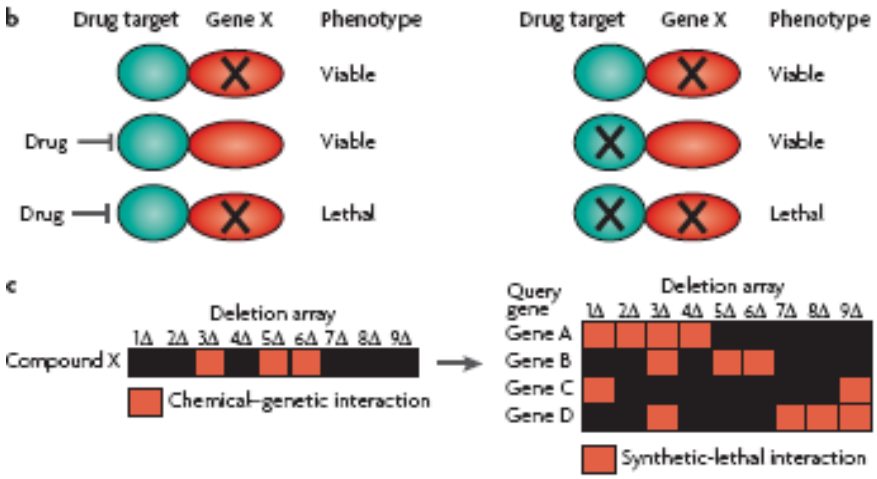

Figure 4.4 Chemical-genetic and synthetic lethal interactions [38]

In this study, the chemical genomics approach was used to investigate the yet undisclosed genetic relationships among two families of drug resistance genes; the DHA12 family from major facilitator superfamily and the PDR drug resistance family from the ABC drug transporters super-family in yeast. The query gene was selected as *QDR3*. The anti-malarial drug quinidine, the pesticide barban, the chemotherapeutic agents bleomycin and cisplatin were selected as the query drugs since *QDR3* gene provides resistance to these drugs. This study is believed to be the first study to investigate the resistance mechanisms and genetic interactions among these two drug resistance families using this approach.

4.2.2. Methods

4.2.2.1. Selection of drug resistance mutants. The deletion strains were selected from BY4742 (MATα *his3*Δ*1 leu2*Δ*0 lys2*Δ*0 ura3*Δ*0*) background [23]. The deletion strains that were used are Δ*ho* as control, Δ*aqr1*, Δ*flr1*, Δ*qdr1*, Δ*qdr2*, Δ*qdr3*, Δ*dtr1*, Δ*hol1*, Δ*yhk8*, Δ*tpo1*, Δ*tpo2*, Δ*tpo3*, and Δ*tpo4* from the DHA12 drug resistance family and Δ*pdr1*, Δ*pdr3*, Δ*pdr5*, Δ*pdr8*, Δ*pdr10*, Δ*pdr11*, Δ*pdr12*, Δ*pdr13*, Δ*pdr15*, Δ*snq2*, Δ*aus1*, Δ*ngg1*, Δ*yor1*, Δ*war1*, Δ*yrr1*, Δ*yap1*, Δ*yap8*, Δ*rdr1*, Δ*msn2*, and Δ*yrm1* from the PDR family. The deletions in the strains were confirmed by diagnostic PCR.

4.2.2.2. Determination of drug dosages. All drugs were purchased from Sigma; Bleomycin sulphate from *Streptomyces verticillus* B5507, cis-Diamineplatinum (II) dichloride P4394, quinidine Q3625, barban PS540 and G418 disulphate salt G5013. The drug stock solutions were prepared as described elsewhere [152]. The stock solutions were; 40 mM barban in acetone, 8.44 mM cisplatin in saline solution, 1.26 mg/ml bleomycin in water and 10 mM quinidine in 70% ethanol. All solutions were kept refrigerated and used within a month of preparation. In the growth media following the addition of the solutions, care was taken to keep the ethanol concentration below 1.4% (v/v) and the acetone concentration below 0.3% (v/v) in order to avoid growth inhibition due to the presence of the solvents. Lethal concentrations of the drugs were determined by growing Δ*ho* and Δ*qdr3* mutants in micro-aerated YPD+geneticin (200µg/l) environment supplemented by the drugs. The lethal concentrations were determined as being above 0.08 mM for barban, 1.2 mM for quinidine, 38 mg/ml for bleomycin and 5.91 mM for cisplatin.

4.2.2.3. Randomization of strains on pinning plates and wells, pinning and replication. The positioning of cells on the pinning plates were randomized such that on a 96-well or 96-pin plate, 3 randomly selected strains were present as duplicates and the remaining 30 strains were present as triplicates. Among the replicates, it was ensured that at least one pinning was done on the inner portion of the plate rather than the sides to eliminate the edge effects. The master plate was prepared in a 96-well plate using liquid medium (YPD + geneticin (200µg/l)). The agar plates of the same medium were prepared in triplicates and except for the control plates, the drugs were added to attain the desired concentrations. Plate inoculations and replications were carried out using Singer Instruments Rotor HDA.

4.2.2.4. Colony visualizations, size determination and calculation of significance and epistasis. The visualization of the colonies and the colony perimeter/area/volume determinations were carried out using the software provided by the gel documentation equipment; UVITec transilluminator Fire Reader v. 15.08 for Windows. The significance analysis was carried out using Student's t-test as the statistic and the significance threshold was determined as 10^{-3}. Product formulation was used for the determination of epistasis from colony areas as described in Section 2.2.2.2. Average colony areas were used in the calculations.

4.2.3. Study results

4.2.3.1. Growth defects. The DHA12 and ABC transporter family mutants have been screened for their growth performances using quinidine in the chemical screens. The maximum available non-lethal concentration of quinidine (1.2 mM) was used in the screens. Both control and drug treated plates were grown on geneticin. The control triplicates and the drug-treated triplicates are presented in Figure 4.5. The colony sizes determined from pixel counts are provided in Appendix F. The interplate differences among the replicates were determined to be insignificant (p-value < 10^{-3}) in both treated and untreated pinnings.

The measure of growth was determined in terms of colony areas. Growth of Δ*qdr3* and Δ*pdr5* mutants indicated that a fitness defect was not observed for these two mutants on untreated environment in comparison to the growth of Δ*ho* (p-value < 10^{-3}). On the other hand, Δ*ngg1* had a significant decrease in growth (p-value < 10^{-5}) even on the control environment. The fitness of both Δ*ngg1* and Δ*pdr5* mutants was decreased significantly (< 10^{-5} and < 10^{-4}, respectively) in the treated samples in comparison to the growth performance of Δ*ho* whereas no significant change was observed for Δ*qdr3*. The quinidine treatment on the other hand directly affected the fitness of Δ*pdr5* (p-value < 10^{-5}) whereas a significant difference could not be observed for the other strains.

4.2.3.2. Determination of epistasis. The statistical evaluation of the growth defect in both Δ*ngg1* and Δ*pdr5* mutants indicated that the growth of these mutants was significantly

altered in response to the treatment by the drug quinidine replacing the loss of function by *QDR3*. The extent of epistasis was calculated using the product rule (Table 4.5).

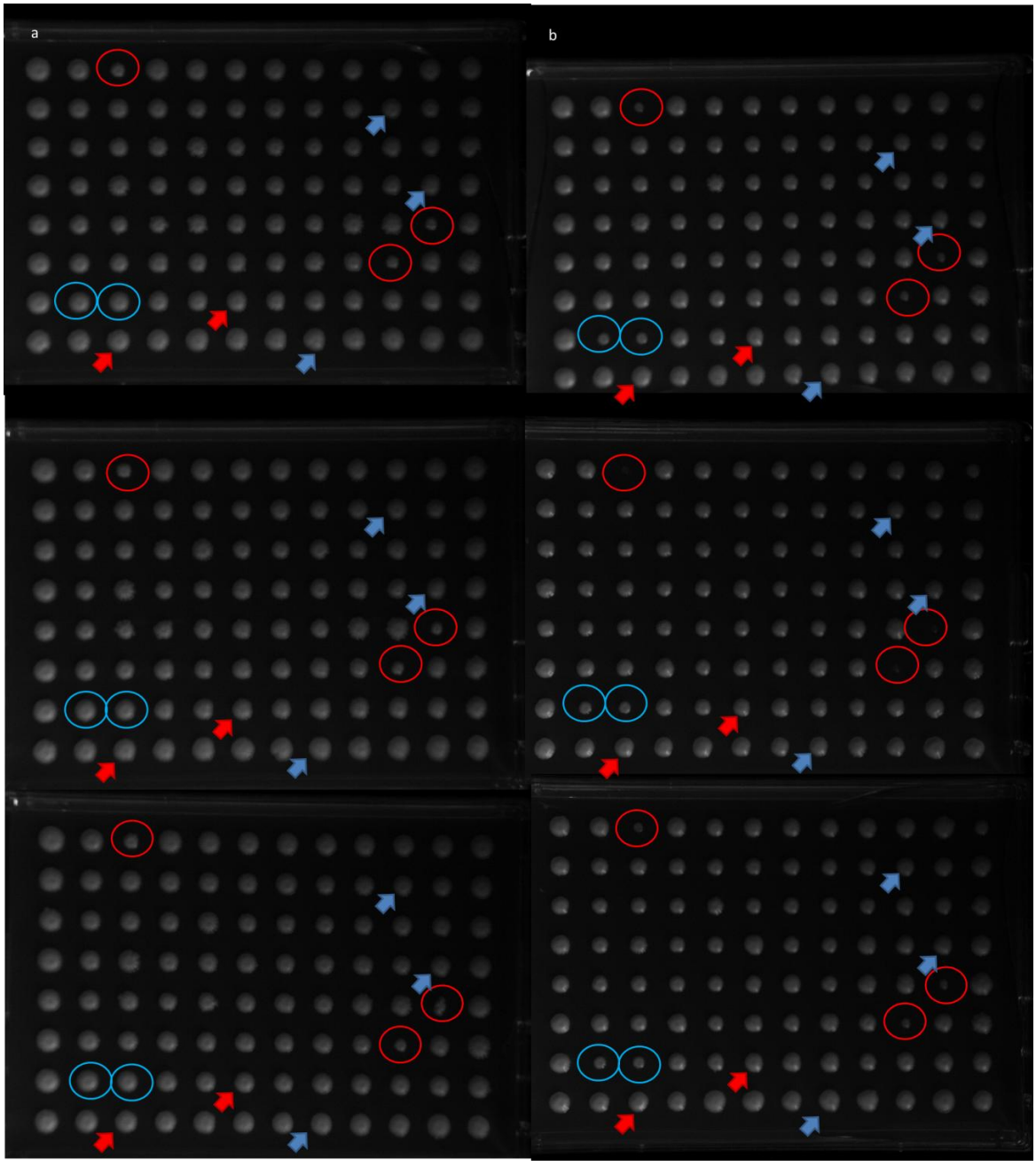

Figure 4.5. Drug screens for the replicates (in red or in blue) in quinidine untreated (a) and quinidine treated (b) strains with Δ*qdr3* indicated by blue arrow, Δ*ho* indicated by red arrow, Δ*ngg1*indicated by red circles and Δ*pdr5* indicated by blue circles

A strong epistasis was observed for both gene pairs; *QDR3-NGG1* and *QDR3-PDR5*. Both of the proposed interactions were previously not reported. However, in previous

studies, *PDR5* was observed to be down regulated in the absence of *QDR3* gene and *NGG1* was slightly up-regulated in the absence of *QDR3* (Section 4.1.3). *PDR5* was previously reported as a multi-drug transporter with a decreased resistance to several anti-fungal and chemotherapeutic agents [154, 156]. The epistatic interaction that was observed between the two multi-drug transporters would indicate complementary roles in drug resistance in terms of ATP mediated and proton pump transfer of toxic chemicals out of the cell. The amino terminal domain of *NGG1*, a transcriptional regulator involved in glucose repression, was shown to interact with *PDR1* and *PDR3* transcriptional domains and it was also reported to take role in retrograde transport although no physical or chemical interactions with any of the QDR family genes were reported and further investigation of this interaction might lead towards novel findings on drug resistance –glucose regulation relationship, which was discussed in Section 4.1.3 [189, 190].

Table 4.5. Determination of epistasis between *QDR3 – NGG1* and *QDR3 – PDR5* gene pairs

Average colony areas	**untreated**	**treated**
Δ*ho*	414	430
Δ*qdr3*	543	472
Δ*ngg1*	234	110
Δ*pdr5*	413	183
Growth ratios with respect to Δ*ho*	**untreated**	**treated**
Δ*qdr3*	1.310789	1.097325
Δ*ngg1*	0.566023	0.254879
Δ*pdr5*	0.997182	0.425746
Multiplicative epistatic effect	**observed**	**calculated**
QDR3-NGG1	0.254879	0.741936
QDR3-PDR5	0.425746	1.307095

4.2.2. Future prospects

This on-going study shed light onto the identification of novel genetic interactions, which were proposed by chemical genomics studies. A single drug, quinidine was sufficient to identify two novel interactions involving *NGG1* and *PDR5* with *QDR3*.

Colony formation was amorphous in the presence of barban as the treatment drug (data not shown). Further dosage optimization studies would be needed to confirm this colony deformation and cell morphologies would be investigated in conjunction with the drug treatment studies. Further analyses would be carried out using the chemotherapeutic agents; bleomycin and cisplatin. The proposed novel interactions would be confirmed by synthetic genetic arrays creating double mutants and the fitness of the drug resistance mutants would further be investigated through competition experiments using yeast TAG microarrays with universal molecular barcodes.

5. CONCLUSION

Prediction of phenotype from genome-scale high-throughput network and component information still remains a challenge for systems based approaches in biological research. The aim of this thesis was to identify the effect of plasticity on the prediction of novel genetic interactions leading to a decrease in fitness and causing synthetic sickness or lethality within the network of yeast in a quantitative manner. The conditional fitness of yeast cells, which were subject to changes in their physiology, was investigated taking the concept of plasticity into consideration.

In the first part of this study, in order to improve the predictive power of Flux Balance Analysis for epistatic interactions, the effect of variations in the composition of biomass constituents on flux distributions was investigated. This study revealed the importance of plasticity and the biomass composition in predicting flux distributions. Biomass formation can be predicted with less than only 10% discrepancy, only for the mid-exponential phase, during which a quasi-steady state would be assumed, but not for the early or the late exponential phase. The distribution of fluxes indicated that the amino acid production and utilization pathways would be a suitable choice for monitoring fitness through manipulations in metabolic fluxes. The changes in the biomass composition were found to affect different parts of the metabolism under different environmental conditions. Thus, the results of this chapter of the study indicated that the predictive power of flux balance analysis could be enhanced by taking the effect of the environment on the metabolism and its regulation (plasticity) into consideration.

In the second and third parts of this thesis, the effect of environmental and genetic perturbations on the metabolism and its regulation in yeast was investigated.

Dynamic re-organization of yeast metabolism in response to two nutritional perturbations involving glucose or ammonium was analysed by monitoring the short- and long-term transient changes at both transcriptome and metabolome levels using a systems based approach. The time scale of the investigation ranged from seconds to hours, allowing the elucidation of both the metabolic and regulatory switches that enable yeast cells to

adapt to, and recover from a transient change in the nutritional environment. The experimental design was such that the specific perturbation was uniquely introduced into an otherwise carefully controlled environment. A glucose impulse was injected into a steady-state glucose limited culture and an ammonium impulse into a corresponding ammonium –limited steady state culture. The quantification of the dynamic changes in the transcriptome and the metabolome in response to an impulse-like perturbation in nutrient availability and the integration of these data with the pathway information revealed long-term dynamic re-organization yeast cells. Metabolic processes, which were affected at distinct time scales as a response to the relaxation from nutritional limitations, were identified. The changes in expression levels of transcripts following the glucose perturbation were more pronounced and sudden when compared to the relaxation from ammonium limitation. The dynamic re-programming of the cell in response to carbon catabolite repression displayed a more complex behaviour than what was observed for the nitrogen catabolite repression. The transcriptional and the metabolic responses observed for nitrogen catabolite repression were not as severe as those for carbon catabolite repression. The molecular basis of the changes in energy homeostasis as a response to the impulse-like perturbations was clarified. A novel integrative approach to extract hidden information from dynamic high-throughput data was developed to improve the predictions of genetic interactions from these data.

The response to genetic perturbations from deletions of *QDR3* or *PDR3* genes, which are members of two separate multi-drug resistance families, were investigated and compared using a system based integrative approach. The homozygous deletion mutants of *QDR3, PDR3* and *HO* genes were grown in glucose or ammonium limited continuous cultures. Transcriptome, endo- and exometabolome profiles at steady state as well as the flux distributions in the optimized solution space were compared to understand the molecular basis of the drug resistance and the changes induced by the deletion of these genes in two different environmental conditions. The availability of glucose was the dominant parameter in determining the hierarchical organization of the transcriptome and the endometabolome in the absence of these drug resistance genes. Yeast re-adjusted its metabolism to cope with the loss of drug resistance genes by inducing the expression of growth associated genes whereas rendering the expression of heat response genes low mimicking a similar response to increasing the growth rate. The molecular basis of the

changes induced by the genetic alterations in drug resistance either by ATP mediated transport or by proton pumps was clarified by using a system based approach. A chemogenomic approach was also developed to predict lethal drug-gene interactions using drug treatment as bait; and the deletion mutants of two drug resistance families, namely *QDR3* or *PDR3* were screened against drugs. Two novel interactions involving *NGG1* and *PDR5* with *QDR3* were identified by chemical genomics studies.

In conclusion, flux balance analysis should be considered for the prediction of phenotypic information and genetic interactions through implementation of regulatory information and plasticity information provided from the response of organisms to environmental perturbations. The results obtained from different levels of the systems based study should be integrated with chemogenomic information and through implementation of novel tools.

In a broader perspective, the enhancement of our power of prediction of phenotype information would help unravel the complete quantitative genetic interaction network, which in turn would provide the link between genotype and phenotype. This would then enable reaching direct deductions about phenotype just with the knowledge of genotypic information on functional relationships and in return, might set a milestone for construction of quantitative genetic interaction networks of higher organisms including *Homo sapiens* as well as providing clues as to open reading frames encoding human genetic disorders through the use of their homologues in a model organism.

REFERENCES

1. Mustacchi, R., S. Hohmann, and J. Nielsen, "Yeast systems biology to unravel the network of life", *Yeast*, 23, pp. 227-238, 2006.

2. Goffeau, A., B. G. Barrell, H. Bussey, R. W. Davis, B. Dujon, H. Feldmann, F. Galibert, J. D. Hoheisel, C. Jacq, M. Johnston, E. J. Louis, H. W. Mewes, Y. Murakami, P. Philippsen, H. Tettelin, and S. G. Oliver, "Life with 6000 genes", *Science*, 274, 563-567, 1996.

3. Kellis, M., N. Patterson, M. Endrizzi, B. Birren, and E. S. Lander, "Sequencing and comparison of yeast species to identify genes and regulatory elements", *Nature*, 423, 241-254, 2003.

4. Wood, V., R. Gwilliam, M. A. Rajandream, M. *et al*., "The genome sequence of *Schizosaccharomyces pombe*", *Nature*, 415, 871-880, 2002.

5. Joyce, A. R., and B. O. Palsson, "The model organism as a system: integrating 'omics' data sets", *Nature Reviews*, 7, pp. 198-210, 2006.

6. Kemmeren, P., T. T. J. P. Kockelkorn, T. Bijma, R. Donders, and F. C. P. Holstege, "Predicting gene function through systematic analysis and quality assessment of high-throughput data", *Bioinformatics*, 21, pp. 1644-1652, 2004.

7. Oliver, S. G., "From DNA sequence to biological function", *Nature*, 379, pp. 597-600, 1996.

8. Oliver, S. G., "A network approach to the systematic analysis of yeast gene function", *Trends in Genetics*, 12, pp. 241-242, 1996.

9. Tong, A. H. Y., M. Evangelista, A. B. Parsons, *et al*., "Systematic genetic analysis with ordered arrays of yeast deletion mutants", *Science*, 294, pp. 2364, 2001.

10. Edwards, J. S., and B. O. Palsson, "The *Escherichia coli* MG1655 *in silico* metabolic genotype: Its definition, characteristics, and capabilities", *PNAS*, 97:10, pp. 5528-5533, 2000.

11. Dobson, P. D., K. Smallbone, D. Jameson, *et al*., "Further developments towards a genome-scale metabolic model of yeast", *BMC Systems Biology*, 4:145, 2010.

12. Förster, J, I. Famili, P. Flu, B. O. Palsson, and J. Nielsen, "Genome-Scale Reconstruction of the *Saccharomyces cerevisiae* Metabolic Network", *Genome Research*, 13, pp. 244-253, 2003.

13. Edwards, J. S., R. U. Ibarra, and B.O. Palsson, "*In silico* predictions of *Escherichia coli* metabolic capabilities are consistent with experimental data", *Nature Biotechnology*, 19, pp. 125-130, 2001.

14. Dikicioglu, D, P. Pir, Z. I. Onsan, K. O. Ulgen, B. Kirdar, and S. G. Oliver, "Integration of Metabolic Modeling and Phenotypic Data in Evaluation and Improvement of Ethanol Production Using Respiration-Deficient Mutants of *Saccharomyces cerevisiae*", *Applied and Environmental Microbiology*, 74, 18, pp. 5809-5816, 2008.

15. Harrison R., B. Papp, C. Pal, S. G. Oliver, and D. Delneri, "Plasticity of genetic interactions in metabolic networks of yeast", *Proceedings in the National Academy of Sciences, USA*, 104, pp. 2307-2312, 2007.

16. Gombert, A. K., and J. Nielsen, "Mathematical modeling of metabolism", *Current Opinion in Biotechnology*, 11, pp. 180-186, 2000.

17. Kauffman, K. J., P. Prakash, and J. S. Edwards, "Advances in Flux Balance Analysis", *Current Opinion in Biotechnology*, 14:5, pp. 491-496, 2003.

18. Bonarius, H. P. J., G. Schmid, and J. Tramper, "Flux analysis of underdetermined metabolic networks: The quest for the missing constraints", *Trends in Biotechnology*, 15, pp. 308-314, 1997.

19. Ibarra, R. U., J. S. Edwards, and B. O. Palsson, "*Escherichia coli* K-12 undergoes adaptive evolution to achieve *in silico* predicted optimal growth", *Nature*, 420, pp. 186-189, 2002.

20. Fong, S. S., A. Nanchen, B. O. Palsson, and U. Sauer, "Latent pathway activation and increased pathway capacity enable *Escherichia coli* adaptation to loss of key metabolic enzymes", *Journal of Biological Chemistry*, 281, pp. 8024-8033, 2006.

21. Burgard, A. P., and C. D. Maranas, "Optimization-based framework for inferring and testing hypothesized metabolic objective functions", *Biotechnology and Bioengineering*, 82, pp. 670-677, 2003.

22. Raghunathan, A. U., J. R. Perez-Correa, and L.T. Bieger, "Data reconciliation and parameter estimation in flux-balance analysis", *Biotechnology and Bioengineering*, 84, pp. 700-709, 2003.

23. Brachmann, C. B., A. Davies, G. J. Cost, E. Caputo, J. Li, P. Hieter, and J. D. Boeke, "Designer deletion strains derived from *Saccharomyces cerevisiae* S288C: a useful set of strains and plasmids for PCR-mediated gene disruption and other applications", *Yeast*, 14, pp. 115-32, 1998.

24. Baganz, F., A. Hayes, D. Marren, D. C. J. Gardner, and S. G. Oliver, "Suitability of replacement markers for functional analysis studies in *Saccharomyces cerevisiae*", *Yeast*, 13, pp. 1563-1573, 1997.

25. Mahadevan, R., and C. H. Schilling, "The effects of alternate optimal solutions in constraint-based genome-scale metabolic models", *Metabolic Engineering*, 5, pp. 264–276, 2003.

26. Bonarius, H. P. J., V. Hatzimanikatis, K. P. H. Meesters, C. D. de Gooijer, G. Schmid, and J. Trasmper, "Metabolic flux analysis of hybridoma cells in different culture media using mass balances", *Biotechnology and Bioengineering*, 50(3), pp. 299-318, 1996.

27. Ooi, S. L., X. Pan, B. D. Peyser, P. Ye, P. B. Meluh, D. S. Yuan, R. A. Irizzary, J. S. Bader, F. A. Spencer, and J. D. Boeke, "Global synthetic-lethality analysis and yeast functional profiling", *Trends in Genetics* 22, 1, pp. 56-63, 2006.

28. Grate, L., and M. Ares, Jr., "Searching yeast intron data at Ares lab Web site", *Methods in Enzymology*, 350, pp. 380-392, 2002.

29. The SGD project. "Saccharomyces Genome Database" (14/02/2011), www.yeastgenome.org.

30. Crow, J. A., and M. J. Simmons, "The mutation load in *Drosophila. The Genetics and Biology of Drosophila*", 3, pp. 1-35. London: Academic Press, 1983.

31. Wright, S., "Physiological and evolutionary theories of dominance", *American Naturalist*, 68, pp. 25-53, 1934.

32. Kacser, H., and J. A. Burns, "The molecular basis of dominance", *Genetics*, 97, pp. 639-666, 1981.

33. Mayo, O., and R. Bürger, "The evolution of dominance: a theory whose time has passed?", *Biological Reviews*, 72, pp. 97-110, 1997.

34. Bourguet, D., "The evolution of dominance", *Heredity*, 83, pp. 1-4, 1999.

35. Muller, H. J., "Our load of mutations" *American Journal of Human Genetics*, 2, pp. 11-176, 1950.

36. Szafraniec, K., D. M. Wloch, P. Sliwa, R. H. Borts, and R. Korona, "Small fitness defects and weak genetic interactions between deleterious mutations in heterozygous loci of the yeast *Saccharomyces cerevisiae*", *Genetics Research*, 82, pp. 19-31, 2003.

37. Tong A. H. Y., G. Lesage, G. D. Bader, *et al*., "Global mapping of the yeast genetic interaction network", *Science*, 303, pp. 808-813, 2004.

38. Boone, C., H. Bussey, and B. J. Andrews, “Exploring genetic interactions and networks with yeast”, *Nature Reviews*, 8, pp. 437-449, 2007.

39. Giaever, G., A. M. Chu, L. Ni, C. Connelly, *et al*., “Functional profiling of the *Saccharomyces cerevisiae* genome”, *Nature*, 418, pp. 387-391, 2002.

40. Winzeler E. A., D. D. Shoemaker, A. Astromoff, *et al*., “Functional characterization of the *S. cerevisiae* genome by gene deletion and parallel analysis”, *Science*, 285, pp. 901-906, 1999.

41. Deutschbauer, A. M., D. F. Jaramillo, M. Proctor, J. Kumm, M. E. Hillenmeyer, R. W. Davis, C. Nislow, and G. Giaever, “Mechanisms of haploinsufficiency revealed by genome-wide profiling in yeast”, *Genetics*, 169, pp. 1915-1925, 2005.

42. Hartman, L. J., B. Garvik, and L. Hartwell, “Principles for the buffering of genetic variation”, *Science*, 291, pp. 1001-1004, 2001.

43. Guarente, L., “Synthetic enhancement in gene interaction: a genetic tool come of age”, *Trends in Genetics*, 9, pp. 362-366, 1993.

44. Pan, X., P. Ye, D. S. Yuan, X. Wang, J. S. Bader, J. D. Boeke, “A DNA integrity network in the yeast *Saccharomyces cerevisiae*”, *Cell*, 124, pp. 1069-1081, 2006.

45. Kelley, R. and T. Ideker, “Systematic interpretation of genetic interactions using protein networks”, *Nature Biotechnology*, 23, pp. 561-566, 2005.

46. Ihmels, J., S. R. Collins, M. Schıldiner, N. J. Krogan, J. S. Weissman, “Backup without redundancy: genetic interactions reveal the cost of duplicate gene loss”, *Molecular Systems Biology*, 3, 86, 2007.

47. Elena, S. F., and R. E. Lenski, “Test of synergistic interactions among deleterious mutations in bacteria”, *Nature*, 390, pp. 395-398, 1997.

48. Segre, D., A. DeLuna, G. M. Church, and R. Kishony, "Modular epistasis in yeast metabolism", *Nature Genetics*, 37, pp. 77-83, 2005.

49. St. Onge, R. P., R. Mani, J. Oh, M. Proctor, E. Fung, R. W. Davis, C. Nislow, F. P. Roth, and G. Giaever, "Systematic pathway analysis using high resolution fitness profiling of combinatorial gene deletions", *Nature Genetics*, 39, pp. 199-206, 2007.

50. Almaas E., Z. N. Oltvai, and A.-L. Barabasi, "The activity reaction core and plasticity of metabolic networks", *PLOS Computational Biology*, 1(7)-e68, pp. 557-563, 2005.

51. Chiu, H.-C., and D. Segré, "Comparative determination of biomass composition in differentially active metabolic states", Genome Informatics, 20, pp. 171-182, 2008.

52. Allen, J., H. M. Davey, D. Broadhurst, J. K. Heald, J. J. Rowland, S. G. Oliver, and D. B. Kell, "High-throughput classification of yeast mutants for functional genomics using metabolic footprinting", Nature Biotechnology, 21, 6, pp. 692-696, 2003.

53. The *Saccharomyces* Genome Database Pathway Tools Omics Viewer, (http://pathway.yeastgenome.org/expression.html).

54. Shin, D.Y., K. Matsumoto, H. Iida, I. Uno, and T. Ishikawa, "Heat shock response of *Saccharomyces cerevisiae* mutants altered in cyclic AMP-dependent protein phosphorylation", *Mol Cell Biol*, 7:1, pp. 244-250, 1987.

55. Viladevall, L., R. Serrano, A. Ruiz, G. Domenech, J. Giraldo, A. Barcelo, and J. Arino, "Characterization of the Calcium-mediated response to alkaline stress in *Saccharomyces cerevisiae*", *J Biol Chem*, 279:42, pp. 43614-43624, 2004.

56. Kresnowati, M.T.A.P., W. A.van Winden, M. J. H. Almering, A. ten Pierick, C. Ras, T. A. Knijnenburg, P. Daran-Lapujade, J. T. Pronk, J. J. Heijnen, and J. M. Daran, "When transcriptome meets metabolome: fast cellular responses of yeast to sudden relief of glucose limitation", *Mol Syst Biol*, 2:49, 2006.

57. Ronen, M., and D. Botstein, “Transcriptional response of steady-state yeast cultures to transient perturbations in carbon source”, *P Natl Acad Sci USA*, 103: 2, pp. 389-394, 2006.

58. Causton, H. C., B. Ren, S. S. Koh, C. T. Harbison, E. Kanin, E. G. Jennings, T. I. Lee, H. L. True, E. S. Lander, and R. A. Young, “Remodelling of yeast genome expression in response to environmental changes”, *Mol Biol Cell*, 12, pp. 323-337, 2001.

59. Moriya, H., and M. Johnston, “Glucose sensing and signaling in *Saccharomyces cerevisiae* through the Rgt2 glucose sensor and casein kinase I”, *P Natl Acad Sci*, 101:6, pp. 1572-1577, 2004.

60. Meijer, M. C. M., J. Boonstr, A. J. Verkleij, C. T. Verrips, “Glucose repression in *Saccharomyces cerevisiae* is related to the glucose concentration rather than the glucose flux”, *J Biol Chem*, 273:37, pp. 24102-24107, 1998.

61. Gancedo, J.M. “Yeast carbon catabolite repression”, *Microbiol Mol Biol R*, 62:2, pp. 334-361, 1998.

62. Foat, B. C., S. S. Houshmandi, W. M. Olivas, and H. J. Bussemaker, “Profiling condition specific, genome-wide regulation of mRNA stability in yeast”, *P Natl Acad Sci*, 102, 49, pp. 17675-17680, 2005.

63. Kim, S. Y., A. Herbst, K. A. Tworkowski, S. E. Salghetti, and W. P. Tansey, “Skp2 regulates Myc protein stability and activity”, *Mol Cell*, 11, pp. 1177-1188, 2003.

64. Magasnik, B., “Ammonia assimilation by *Saccharomyces cerevisiae*”, *Eucaryot Cell*, 2:5, pp. 827-829, 2003.

65. Magasnik, B., and C. A. Keiser, “Nitrogen regulation in *Saccharomyces cerevisiae*”, *Gene*, 290, pp.1-18, 2002.

66. ter Schure, E. G., H. H. W. Sillje, E. E. Vermeulen, J. W. Kalhorn, A. J. Verkleij, J. Boonstra, and C. T. Verrips, “Repression of nitrogen catabolic genes by ammonia and

glutamine in nitrogen-limited continuous cultures of *Saccharomyces cerevisiae*", *Microbiology*, 144, pp. 1451-1462, 1998.

67. Saldanha, A. J., M. J. Brauer, and D. Botstein, "Nutritional homeostasis in batch and steady-state culture of yeast", *Mol Biol Cell*, 15:9, pp. 4089-4104, 2004.

68. Hayes, A., N. Zhang, J. Wu, P. R. Butler, N. C. Hauser, J. D. Hoheisel, F. L. Lim, A. D. Sharrocks, and S. G. Oliver, "Hybridization array technology coupled with chemostat culture: Tools to interrogate gene expression in *Saccharomyces cerevisiae*", *Methods*, 26, pp. 281-290, 2002.

69. Wishart, J. A., A. Hayes, L. Wardleworth, N. Zhang, and S. G. Oliver, "Doxycycline, the drug used to control the tet-regulatable promoter system, has no effect on global gene expression in *Saccharomyces cerevisiae*", *Yeast*, 22, pp. 565-569, 2005.

70. Li, C., and W. H. Wong, "Model-based analysis of oligonucleotide arrays: Expression index computation and outlier detection", *Proc Natl Acad Sci*, 2001a, 98, pp. 31-36, 2001.

71. Bolstad, B. M., R. A. Irizarry, M. Astrand, and T. P. Speed, "A comparison of normalization methods for high density oligonucleotide array data based on bias and variance", *Bioinformatics*, 19:2, pp. 185-193, 2003.

72. Brazma, A., P. Hingamp, J. Quackenbush, G. Sherlock, P. Spellman, C. Stoeckert, J. Aach, W. Ansorge, C. A. Ball, H. C. Causton, T. Gaasterland, P. Glenisson, F. P. C. Holstege, I. F. Kim, V. Markowitz, J. C. Matese, H. Parkinson, A. Robinson, U. Sarkans, S. Schulze-Kremer, J. Stewart, R. Taylor, J. Vilo, and M. Vingron, "Minimum information about a microarray experiment (MIAME) – toward standards for microarray data", *Nat Genet*, 29, pp. 365-371, 2001.

73. Storey, J. D., W. Xiao, J. T. Leek, R. G. Tompkins, and R. W. Davis, "Significance analysis of time course microarray experiments", *P Natl Acad Sci*, 102, pp. 12837-12842, 2005.

74. Storey, J. D., J. Y. Dai, and J. T. Leek, "The optimal discovery procedure for large-scale significance testing, with applications to comparative microarray experiments", *Biostatistics*, 8, pp. 414-432, 2007.

75. Leek, J. T., E. C. Monsen, A. R. Dabney, and J. D. Storey, "EDGE: Extraction and analysis of differential gene expression", *Bioinformatics*, 22, pp. 507-508, 2006.

76. Reich, M., K. Ohm, P. Tamayo, M. Angelo, and J. P. Mesirov, "GeneCluster 2.0: An advanced toolset for bioarray analysis", *Bioinformatics*, 20:11, pp. 1797-1798, 2004.

77. Seo, J., M. Bakay, Y. W. Chen, S. Hilmer, B. Shneiderman, and E. P. Hoffman, "Interactively optimizing signal-to-noise ratios in expression profiling: project-specific algorithm selection and detection p-value weighting in Affymetrix microarrays", *Bioinformatics*, 20, pp. 2534-2544, 2004.

78. "Saccharomyces Genome Database GO Term Finder", http://db.yeastgenome.org/cgi-bin/GO/goTermFinder.pl, 2011.

79. Carbon, S., A. Ireland, C. J. Mungall, S. Shu, B. Marshall, and S. Lewis, "The AmiGO Hub; the Web Presence Working Group. AmiGO: online access to ontology and annotation data", *Bioinformatics*, 2008.

80. Matys, V., E. Fricke1, R. Geffers, *et al*., "TRANSFAC: transcriptional regulation, from patterns to profiles", *Nucleic Acids Res*, 1:31:1, pp. 374-378, 2003.

81. Teixeira, M. C., P. Monteiro, P. Jain, S. Tenreiro, A. R. Fernandes, N. P. Mira, M. Alenquer, A. T. Freitas, A. L. Oliveira, and I. Sá-Correia, "The YEASTRACT database: a tool for the analysis of transcription regulatory associations in *Saccharomyces cerevisiae*", *Nucleic Acids Res*, 34, pp. 446-451, 2006.

82. Ernst, J., O. Vainas, C. T. Harbison, I. Simon, and Z. Bar-Josef, "Reconstructing dynamic regulatory maps", *Mol Syst Biol*, 3:74, 2007.

83. Harbison, C.T., D. B. Gordon, T. I. Lee, *et al*., "Transcriptional regulatory code of a eukaryotic genome", *Nature*, 431, pp. 99-104, 2004.

84. MacIsaak, K.D., T. Wang, D. B. Gordon, D. K. Gifford, G. D. Stormo, and E. Fraenkel, "An improved map of conserved regulatory sites for *Saccharomyces cerevisiae*", *BMC Bioinformatics*, 7, 113, 2006.

85. Castrillo, J.I., L. A. Zeef, D. C. Hoyle, N. Zhang, A. Hayes, D. J. C. Gardner, M. J. Cornell, J. Petty, L. Hakes, L. Wardleworth, B. Rhash, M. Brown, W. B. Dunn, D. Broadhurst, K. O'Donoghue, S. S. Hester, T. P. J. Dunkley, S. R. Hart, N. Swainston, P. Li, S. J. Gaskell, N. W. Paton, K. S. Lilley, D. B. Kell, and S. G. Oliver, "Growth control of the eukaryote cell: a systems biology study in yeast", *Journal of Biology*, 6,4, 2007.

86. Gutteridge, A., P. Pir, J. I. Castrillo, P. D. Charles, K. S. Lilley, and S. G. Oliver, "Nutrient control of eukaryote cell growth: a systems biology study in yeast", *BMC Biol*, 8:68, 2010.

87. Tamayo, P., D. Slonim, J. Mesirov, Q. Zhu, E. Dmitrovsky, E. S. Lander, and T. R. Golub, "Interpreting gene expression with self-organizing maps: Methods and application to hematopoeitic differentiation", *P Natl Acad Sci*, 96, pp. 2907-2912, 1999.

88. Beilharz, T.H., and T. Preiss, "Widespread use of poly-A tail length control to accentuate expression of the yeast transcriptome", *RNA*, 13, pp. 982-997, 2007.

89. Carlini, D.B., "Context-dependent codon bias and mRNA longevity in the yeast transcriptome", *Math Biosci Eng*, 22:6, pp. 1403-1411, 2005.

90. Lang T., E. Schaeffeler, D. Bernreuther, M. Bredschneider, D. H. Wolf, and M. Thumm, "Aut2p and Aut7p, two novel microtubule-associated proteins are essential for delivery for autophagic vesicles to the vacuole", *EMBO J*, 17, pp. 3597-3607, 1998.

91. Ohashi, Y., and S. Munro, "Membrane delivery to the yeast autophagosome from the Golgi-endosomal system", *Mol Biol Cell*, 15; 21(22), pp. 3998-4008, 2011.

92. Braun, E., and N. Brenner, “Transient responses and adaptation to steady state in a eukaryotic gene regulation system”, *Physical Biology*, 1, pp. 67-76, 2004.

93. van den Brink, J., P. Daran-Lapujade, J. T. Pronk, and J. H. de Winde, “New insights into the *Saccharomyces cerevisiae* fermentation switch: Dynamic transcriptional response to anaerobicity and glucose-excess”, *BMC Genomics*, 9:100, 2008.

94. Gasch, A. P., P. T. Spellman, C. M. Kao, O. Carmel-Harel, M. B. Eisen, G. Storz, D. Botstein, and P. O. Brown, “Genomic expression programs in the response of yeast cells to environmental changes”, *Molecular Biology of the Cell*, 11, pp. 4241-4257, 2000.

95. Zaman, S., S. I. Lippman, L. Schneper, N. Slonim, and J. R. Broach, “Glucose regulates transcription in yeast through a network of signalling pathways”, *Molecular Systems Biology*, 5:245, 2009.

96. Walther, T., M. Novo, K. Rössger, F. Létisse, M.O. Loret, J. C. Portais, and J. M. François, “Control of ATP homeostasis during the respire-fermentative transition in yeast”, *Molecular Systems Biology*, 6:344, 2009.

97. Castrillo, J. I., A. Hayes, S. Mohammed, S. J. Gaskell, and S. G. Oliver, “An optimized protocol for metabolome analysis in yeast using direct infusion electrospray mass spectrometry”, *Phytochemistry*, 62, pp. 929-937, 2003.

98. Pope, G. A., D. A. MacKenzie, M. Defemez, M. A. M. M. Aroso, L. J. Fuller, F. A. Mellon, W. B. Dunn, M. Brown, R. Goodacre, D. B. Kell, M. E. Marvin, E. J. Louis and I. N. Roberts, “Metabolic footprinting as a tool for discriminating between brewing yeasts”, *Yeast*, 24, pp. 667-679, 2007.

99. Kanehisa, M. and S. Goto, “KEGG: Encyclopedia of Genes and Genomes”, *Nucleic Acids Research*, 28,1, pp. 27-30, 2000.

100. Yoo, S. H., F. S. Genbauffe, and T. G. Cooper, "Identification of the ureidoglycolte hydrolase gene in the DAL gene cluster of *Saccharomyces cerevisiae*", *Molecular and Cellular Biology*, 5, 9, pp. 2279-2288, 1985.

101. Boles, E., P. de Jong-Gubbels, and J. T. Pronk, "Identification and characterization of *MAE1*, the *Saccharomyces cerevisiae* structural gene encoding mitochondrial malic enzyme", *Journal of Bacteriology*, 180, 11, pp. 2875-2882, 1998.

102. Hung, G.-C., C. R. Brown, A. B. Wolfe, J. Liu, and H.-L. Chiang, "Degradation of the gluconeogenic enzymes fructose-1,6-biphosphatase and malate dehydrogenase is mediated by distinct proteolytic pathways and signalling events", *The Journal of Biological Chemistry*, 279, 47, pp. 49138-49150, 2004.

103. van den Berg, M. A., P. de Jong-Gubbels, and H. yde Steensma, "Transient mRNA responses in chemostat cultures as a method of defining putative regulatory elements: Application to genes involved in *Saccharomyces cerevisiae* Acetyl-coenzyme A metabolism", *Yeast*, 14, pp. 1089-1104, 1998.

104. Kunze, M., I. Pracharoenwattana, S. M. Smith, A. Hartig, "A central role for the peroxisomal membrane in glyoxylate cycle function", *Biochimica et Biophysica Acta*, 1763, pp. 1441-1452, 1998.

105. Schricker, R., V. Magdolen, A. Kaniak, K. Wolf, and W. Bandlow, "The adenylate kinase family in yeast: identification of *URA6* as a multicopy suppressor of deficiency in major AMP kinase", *Gene*, 122-1, pp. 111-118, 1992.

106. Kaneisha, M, M. Araki, S. Goto, M. Hattori, M. Hirakawa, M. Itoh, T. Katayama, S. Kawashima, S. Okuda, T. Tokimatsu, and Y. Yamanishi, "KEGG for linking genomes to life and environment", *Nucleic Acids Research*, 36, pp. D480-D484, 2008.

107. Fluri, R. and J. R. Kinghorn, "Induction control of purine catabolism in *Schizosachharomyces pombe*", *Current Genetics*, 9, pp. 573-578, 1985.

108. Fernandez, E., M. Fernandez, and R. Rodicio, "Two structural genes are encoding malate synthase isoenzymes in *Saccharomyces cerevisiae*", *FEBS Letters*, 320, 3, pp. 271-275, 1993.

109. Kurtz, J.-E., F. Exinger, P. Erbs, and R. Jund, "The *URH1* uridine ribohydrolase of *Saccharomyces cerevisiae*", *Current Genetics*, 41, pp. 132-141, 2002.

110. Christensen, K. E. and R. E. MacKenzie, "Mitochondrial one-carbon metabolism is adapted to the specific needs of yeast, plants and mammals", *BioEssays*, 28, pp. 595-605, 2006.

111. Griffin, D. H., *Fungal Physiology*, 1996. 2nd edition, Wiley.

112. Cherest, H., D. Thomas, and Y. Surdin-Kerjan, "Polyglutamylation of folate coenzymes is necessary for methionine biosynthesis and maintenance of intact mitochondrial genome in *Saccharomyces cerevisiae*", *The Journal of Biological Chemistry*, 275, 19, pp. 14056-14063, 2000.

113. Bowman S. B., Z. Zaman, L. P. Collinson, A. J. Brown, and I. W. Dawes. 1992. Positive regulation of the *LPD1* gene of *Saccharomyces cerevisiae* by the *HAP2*/*HAP3*/*HAP4* activation system. Molecular and General Genetics, 231, 2: 293-303.

114. Subhi, A. L., P. Diegelman, C. W. Porter, B. Tang, Z. J. Lu, G. D. Markham, and W. D. Kruger, "Methylthioadenosine phosphorylase regulates ornithine decarboxylase by production of downstream metabolites", *Journal of Biological Chemistry* 278(50), pp. 49868-49873, 2003.

115. Haselbeck, R. J. and L. McAlister-Henn, "Function and expression of yeast mitochondrial NAD- and NADP-specific isocitrate dehydrogenase", *The Journal of Biological Chemistry*, 268, 16, pp. 12116-12122, 1993.

116. Corradini, M. G., and M. Peleg, "Dynamic model of heat inactivation kinetics for bacterial adaptation", *Applied and Environmental Microbiology*, 75, 8, pp. 2590-2597, 2009.

117. Ortiz-Muniz, B, O. Carvajal-Zarrabal, B. Torrestiana-Sanchez, and M. G. Aguilar-Uscanga, "Kinetic study on ethanol production using *Saccharomyces cerevisiae* ITV-01 yeast isolated from sugar cane molasses", *Journal of Chemical Technology and Biotechnology*, 85, pp. 1361-1367, 2010.

118. Picard, C, L. Lambotte, P. Starkel, C. Sempoux, A. Saliez, V. van den Berge, C. de Saeger, and Y. Horsmans, "Retrorsine: a kinetic study of its influence on rat liver regeneration in the portal branch ligation model", *Journal of Hepatology*, 39, pp. 99-105, 2003.

119. Dutrow, N., D. A. Nix, D. Holt, B. Milash, B. Dalley, E. Westbrock, T. J. Parnell, and B. R. Cairns, "Dynamic transcriptome of *Schizosaccharomyces pombe* shown by RNA-DNA hybrid mapping", *Nature Genetics*, 40, 8, pp. 977-986, 2008.

120. Volpe, E, G. Cappelli, M. Grassi, A. Martino, A. Serafino, V. Colizzi, N. Sanarico, and F. Mariani, "Gene expression profiling of human macrophages at late time of infection with *Mycobacterium tuberculosis*", *Immunology*, 118, pp. 449-460, 2006.

121. Helmerhorst, E. J., and F. G. Oppenheim, "Saliva: a dynamic proteome", *Journal of Dental Research*, 86 (8), pp. 680-693, 2007.

122. Zhu, L., X.-K. Liu, Y.-D. Zhi, X. Bu, T.-Y. Ying, E.-L. Feng, J. Wang, X.-M. Zhang, P.-T. Huang, and H.-L. Wang, "Dynamic proteome changes of *Shigella flexneri* 2a during transition from exponential growth to stationary phase", *Genomics, Proteomics & Bioinformatics*, 5, 2, p. 111-120, 2007.

123. Wu, L., J. van Dam, D. Schipper, M. T. A. P. Kresnowati, A. M. Proell, C. Ras, W. A. van Winden, W. M. van Gulik, and J. J. Heijnen, "Short-term metabolome dynamics and carbon, electron and ATP balances in chemostat-grown *Saccharomyces cerevisiae*

CEN.PK 113-7D following a glucose pulse", *Applied and Environmental Microbiology*, 72, 5, pp. 3566-3577, 2006.

124. Kaplan, K., P. Dwivedi, S. Davidson, Q. Yang, P. Tso, W. Siems, and H. H. Hill, Jr, "Monitoring dynamic changes in lymph metabolome of fasting and fed rats by electrospray ionization-ion mobility mass spectrometry (ESI-IMMS)", *Analytical Chemistry*, 81, 19, pp. 7944-7953, 2009.

125. Ni, L., C. Bruce, C. Hart, J. Leigh-Bell, D. Gelperin, L. Umansky, M. B. Gerstein, and M. Snyder, "Dynamic and complex transcription factor binding during an inducible response in yeast", *Genes&Development*, 23, pp. 1531-1363, 2009.

126. Alexeyenko, A., D. M. Wassenberg, E. K. Lobenhofer, J. Yen, E. Linney, E. L. L. Sonnhammer, and J. N. Meyer, "Dynamic zebrafish interactome reveals transcriptional mechanisms of dioxin toxicity", *PLOS One*, 5, 5: e10465.

127. Sullivan, D. E., J. L. Gabbard, M. Shukla, and B. Sobral, "Data integration for dynamic and sustainable systems biology resources: challenges and lessons learned", *Chemical Biodiversity*, 7 (5), pp. 1124-1141, 2010.

128. Pihur, V., S. Datta, and S. Datta, "Reconstruction of genetic association networks from microarray data: a partial least squares approach", *Bioinformatics*, 24, 4, pp. 561-568, 2008.

129. Husmeier, D., "Sensitivity and specificity of inferring genetic regulatory interactions from microarray experiments with dynamic Bayesian networks", *Bioinformatics*, 19, 17, pp. 2271-2282, 2003.

130. Beal, J. M., F. Falciani, Z. Ghahramani, C. Rangel, and D. L. Wild, "A Bayesian approach to reconstructing genetic regulatory networks with hidden factors", *Bioinformatics*, 21, 3, pp. 349-356, 2005.

131. Ghaharamani, Z., and M. J. Beal, “Propagation algorithms for variational Bayesian learning”, *Advances in Neural Information Processing Systems* 13, eds. T K Leen, T Dietterich, V Tresp, MIT Press, 2001.

132. Troyanskaya, O. G., K. Dolinski, A. B. Owen, and D. Botstein, “A Bayesian framework for combining heterogeneous data sources from gene function prediction (in *Sachharomyces cerevisiae*)”, *Proceedings of the National Academy of Sciences*, 100, 14, pp. 8348-8353, 2003.

133. Julius, A. A., A. Halasz, M. S. Sakar, H. Rubin, V. Kumar, and G. J. Pappas, “Stochastic modelling and control of biological systems: The lactose regulation system of *Escherichia coli*”, *IEEE Special Issue on Systems Biology*, 2008.

134. Barnes, C., D. Silk, X. Sheng, and M. P. H. Stumpf, “Bayesian design of synthetic biological systems”, *arXiv*:1103.1046v1 [q-bio.MN], 2011.

135. Davidson, E. H., “Genomic Regulatory Systems”. *Academic Press*, New York, USA 2001.

136. Song, L., M. Kolar, and E. P. Xing, “KELLER: estimating time-varying interactions between genes”, *Bioinformatics*, 25, pp. 128-136, 2009.

137. Dikicioglu, D., M. E. Karabekmez, B. Rash, P. Pir, B. Kirdar, and S. G. Oliver, “A comparison of how yeast re-programmes its transcriptional profile in response to different nutrient impulses”, *manuscript in submission*.

138. Stark, C., B.-J. Breitkreutz, T. Reguly, L. Boucher, A. Breitkreutz, and M. Tyers, “BioGRID: a general repository for interaction datasets”, *Nucleic Acids Research*, 34, pp. D535-D539, 2006.

139. Lee, T. I., N. J. Rinaldi, F. Robert, *et al*., “Transcriptional regulatory networks in *Saccharomyces cerevisiae*”, *Science*, 298, pp. 799-804, 2002, data update Dec 5th, 2003.

140. Luscombe, N. M., M. M. Babu, H. Yu, M. Snyder, S. A. Teichmann, and M. Gerstein, "Genomic analysis of regulatory network dynamics reveals large topological changes", *Nature*, 431: doi:10.1038/nature02782, 2004.

141. Kurtz, J. E., P. Dufour, J. P. Bergerat, and F. Exinger, "*Saccharomyces cerevisiae* as a genetic model in anticancer therapy", *Current Pharmacogenomics*, 3:1-7, 2005.

142. Cardenas, M. E., M. C. Cruz, M. del Poeta, N. Chung, J. R. Perfect, and J. Heitman, "Antifungal activities of antineoplastic agents: *Saccharomyces cerevisiae* as a model system to study drug action", *Clinical Microbiology Reviews*, 12,4, pp. 583-611, 1999.

143. Anderson, J. B., "Evolution of antifungal drug resistance: Mechanisms and pathogen fitness", *Nature Reviews, Microbiology*, 3, pp. 547-556, 2005.

144. Schenk, P. W., M. Brok, A. W. M. Boersma, J. A. Brandsma, H. den Dulk, H. Burger, G. Stoter, J. Brouwer, and K. Nooter, "Anticancer drug resistance induced by disruption of the Saccharomyces cerevisiae NPR2 gene: a novel component involved in cisplatin- and doxorubicin-provoked cell kill", *Molecular Pharmacology*, 64, 2, pp. 259-268, 2003.

145. Brown, S. J., P. J. Kellett, and S. J. Lippard, "Ixr1, a yeast protein that binds to platinated DNA and confers sensitivity to cisplatin", *Science*, 261(5121), pp. 603-605, 1993.

146. Schenk, P. W., A. W. M. Boersma, J. A. Brandsma, H. den Dulk, H. Burger, G. Stoter, J. Brouwer, and K. Nooter, "*SKY1* is involved in cisplatin-induced cell kill in *Saccharomyces cerevisiae*, and inactivation of its human homolog, SRPK1, induces cisplatin resistance in a human ovarian carcinoma cell line", *Cancer Research*, 6, pp. 6982-6986, 2001.

147. Burger, H., A. Capello, P. W. Schenk, G. Stoter, J. Brouwer, and K. Nooter, "A genome-wide screening in Saccharomyces cerevisiae for Genes that confer resistance to

the anticancer agent cisplatin", *Biochemical and Biophysical Research Communications*, 269, pp. 767-774, 2000.

148. Akache, B., S. MacPherson, M.-A. Sylvain, and B. Turcotte, "Complex interplay among regulators of drug resistance genes in *Saccharomyces cerevisiae*", *The Journal of Biological Chemistry*, 279, 27, pp. 27855-27860, 2004.

149. Nunes, P. A., S. Tenreiro, and I. Sa-Correia, "Resistance and adaptation to quinidine in *Saccharomyces cerevisiae*: Role of QDR1 (YIL120w), encoding a plasma membrane transporter of the major facilitator super-family required for multi-drug resistance", *Antimicrobial Agents and Chemotherapy*, 45, 5, pp. 1528-1534, 2001.

150. Vargas, R. C., S. Tenreiro, M. C. Teixeira, A. R. Fernandes, and I. Sa-Correia, "*Saccharomyces cerevisiae* multi-drug transporter Qdr2p (Yil121wp): Localization and function as a quinidine resistance determinant", *Antimicrobial Agents and Chemotherapy*, 48,7, pp. 2531-2537, 2004.

151. Tenreiro, S., R. C. Vargas, M. C. Teixeira, C. Magnani, I. Sa´-Correia, "The yeast multidrug transporter Qdr3 (Ybr043c): localization and role as a determinant of resistance to quinidine, barban, cisplatin, and bleomycin", *Biochemical and Biophysical Research Communications*, 327, pp. 952–959, 2005.

152. Wolfger, H., Y. M. Mamnun, and K. Kuchler, "Fungal ABC proteins: pleiotropic drug resistance, stress response and cellular detoxification", *Research in Microbiology*, 152, pp. 375-389, 2001.

153. Ernst, R., R. Klemm, L. Schmitt, and K. Kuchler, "Yeast ATP-binding cassette transporters:: Cellular cleaning pumps", *Methods in Enzymology*, Vol. 400, pp. 460-484, 2005.

154. Moye Rowley, W. S., "Retrograde regulation of multi-drug resistance in *Saccharomyces cerevisiae*", *Gene*, 354, pp. 15-21, 2005.

155. Bauer, B. E., H. Wolfger, and K. Kuchler, “Inventory and function of yeast ABC proteins: about sex, stress, pleiotropic drug and heavy metal resistance”, *Biochimica et Biophysica Acta*, 14f61, pp. 217-236, 1999.

156. Devaux, F., E. Carvajal, S. Moye-Rowley, and C. Jacq, “Genome-wide studies on the nuclear PDR3-controlled response to mitochondrial dysfunction in yeast”, *FEBS Letters*, 515, pp.25-28, 2001.

157. Monteiro, P. T., N. Mendes, M. C. Teixeira, S. d'Orey, S. Tenreiro, N. Mira, H. Pais, A. P. Francisco, A. M. Carvalho, A. Lourenço, I. Sá-Correia, A. L. Oliveira, and A. T. Freitas, “YEASTRACT-DISCOVERER: new tools to improve the analysis of transcriptional regulatory associations in *Saccharomyces cerevisiae*”, *Nucleic Acids Research*, 36, pp. D132-D136, 2008.

158. Postma, E., C. Verduyn, W. A. Scheffers, J. P. van Dijken, “Enzymatic analysis of the crabtree effect in glucose-limited chemostat cultures of *Saccharomyces cerevisiae*”, *Applied and Environmental Microbiology*, 55 (2), pp. 468-477, 1989.

159. van den Brink, J., A. B. Canelas, W. M. van Gulik, J. T. Pronk, J. J. Heijnen, J. H. de Winde, P. Daran-Lapujade, “Dynamics of glycolytic regulation during adaptation of *Saccharomyces cerevisiae* to fermentative metabolism”, *Applied and Environmental Microbiology*, 74 (18), pp. 5710-5723, 2008.

160. Cheng, L., R. Watt, and P. W. Piper, “Polyubiquitin gene expression contributes to oxidative stress resistance in respiratory yeast (*Saccharomyces cerevisiae*)”, *Molecular and General Genetics*, 243, 3, pp. 358-362, 1994.

161. Xiao, R., J. Lundström-Ljund, A. Holmgren, and H. F. Gilbert, “Catalysis of Thiol/Disulfide Exchange”, *The Journal of Biological Chemistry*, 280, 22, pp. 21099-21106, 2005.

162. Fernandez-Murray, J. P. and C. R. McMaster, “Glycerophosphocholine catabolism as a new route for choline formation for phosphatidylcholine synthesis by the Kennedy pathway”, *The Journal of Biological Chemistry*, 280, 46, pp. 38290-38296, 2005.

163. Newcomb, L. L., J. A. Diderich, M. G. Slattery, and W. Heideman, "Glucose regulation of *Saccharomyces cerevisiae* cell cycle genes", *Eucaryotic Cell*, 2, 1, pp. 143-149, 2003.

164. Mulet, J. M, M. P. Leube, S. J. Kron, G. Rios, G. R. Fink, and R. Serrano, "A novel mechanism of ion homeostasis and salt tolerance in yeast: the Hal4 and Hal5 protein kinases modulate the Trk1-Trk2 potassium transporter", *Molecular and Cellular Biology*, 19, 5, pp. 3328-3337, 1999.

165. Verwaal, R., J. W. G. Paalman, A. Hogenkamp, A. J. Verkleij, C. T. Verris, and J. Boonstra, "*HXT5* expression is determined by growth rates in *Saccharomyces cerevisiae*", *Yeast*, 19, pp. 1029-1038, 2002.

166. Natarajan, K., M. R. Meyer, B. M. Jackson, D. Slade, C. Roberts, A. G. Hinnebusch, and M. J. Marton, "Transcriptional profiling shows that Gcn4p is a master regulator of gene expression during amino acid starvation in yeast", *Molecular and Cellular Biology*, 21 (13), pp. 4347-4368, 2001.

167. Kwast, K. E., P. V. Burke, and R. O. Poyton, "Oxygen sensing and the transcriptional regulation of oxygen-responsive genes in yeast", *The Journal of Experimental Biology*, 201, pp. 1177-1195, 1998.

168. Forsburg, S. L. and L. Guarente, "Identification and characterization of HAP4: a third component of the CCAAT-bound HAP2/HAP3 heteromer", *Genes & Development*, 3(8), pp. 1166-78, 1989.

169. Bourgarel, D., C.-C. Nguyen, and M. Bolotin-Fukuhara, "HAP4, the glucose-repressed regulated subunit of the HAP transcriptional complex involved in the fermentation-respiration shift, has a functional homologue in the respiratory yeast *Kluyveromyces lactis*", *Molecular Microbiology*, 31 (4), pp. 1205-1215, 1999.

170. Hedges, D., M. Proft, and K.-D. Entian, "*CAT8*, a new zinc cluster-encoding gene necessary for derepression of gluconeogenic enzymes in the yeast *Saccharomyces cerevisisae*", *Molecular and Cellular Biology*, 15 (4), pp. 1915-1922, 1995.

171. Pedruzzi, I., N. Burckert, P. Egger, C. de Virgilio, "*Saccharomyces cerevisiae* Ras/cAMP pathway controls post-diauxic shift element-dependent transcription through the zinc finger protein Gis1", *EMBO Journal*, 19(11), pp. 2569-2579, 2000.

172. Zhang, N., J. Wu, and S. G. Oliver, "Gis1 is required for transcriptional reprogramming of carbon metabolism and the stress response during transition into stationary phase in yeast", *Microbiology*, 155, pp. 1690-1698, 2009.

173. Lutfiyya, L. L. and M. Johnston, "Two zinc-finger-containing repressors are responsible for glucose repression of *SUC2* expression", *Molecular and Cellular Biology*, 16(9), pp. 4790-4797, 1996.

174. Chellappa, R., P. Kandasamy, C. S. Oh, Y. Jiang, M. Vemula, and C. E. Martin, "The membrane proteins, Spt23p and Mga2p, play distinct roles in the activation of *Saccharomyces cerevisiae OLE1* gene expression", *The Journal of Biological Chemistry*, 276, pp. 43548-43556, 2001.

175. Young, E. T., K. M. Dombek, C. Tachibana, and T. Ideker, "Multiple pathways are co-regulated by the protein kinase Snf1 and the transcription factors Adr1 and Cat8", The *Journal of Biological Chemistry*, 278 (28), pp. 26146-26158, 2003.

176. Krogan, N. J., M. H. Y. Lam, J. Fillingham, M.-C. Keogh, M. Gebbia, J. Li, N. Datta, G. Cagney, S. Buratowski, A. Emili, and J. F. Greenblatt, "Proteasome involvement in the repair of DNA double-strand breaks", *Molecular Cell*, 16, pp. 1027-1034, 2004.

177. Kuchin, S., V. K. Vyas, and M. Carlson, "Snf1 protein kinase and the repressors Nrg1 and Nrg2 regulate *FLO11*, haploid invasive growth, and diploid pseudohyphal differentiation", *Molecular and Cellular Biology*, 22(12), pp. 3994-4000, 2002.

178. Vyas, V. K., Kuchin, S. and M. Carlson, "Interaction of the repressors Nrg1 and Nrg2 with the Snf1 protein kinase in *Saccharomyces cerevisiae*", *Genetics*, 158, pp. 563–572, 2001.

179. Ramos, F., M. E. Guezzar, M. Grenson, and J-M. Wiame, "Mutations affecting the enzymes involved in the utilization of 4-aminobutyric acid as nitrogen source by the yeast *Saccharomyces cerevisiae*", *European Journal of Biochemistry*, 149, pp. 401-404, 1985.

180. Neves, L., R. Oliveira, and C. Lucas, "Yeast orthologues associated with glycerol transport and metabolism", *FEMS Yeast Research*, 5, 1, pp. 51-62, 2004.

181. Cronwright, G. R., J. M. Rohwer, and B. A. Prior, "Metabolic control analysis of glycerol synthesis in *Saccharomyces cerevisiae*", *Applied and Environmental Microbiology*, 68, 9, pp. 4448-4456, 2002.

182. Ansell, R., K. Granath, S. Hohmann, J. M. Thevelein, and L. Adler, "The two isoenzymes for yeast NAD^+-dependent glycerol 3-phosphate dehydrogenase encoded by *GPD1* and *GPD2* have distinct roles in osmoadaptation and redox regulation", *The EMBO Journal*, 16, 9, pp. 2179-2187, 1997.

183. Sauer U., "High-throughput phenomics: experimental methods for mapping fluxomes", *Current Opinion in Biotechnology*, 15, pp. 58-63, 2004.

184. Cordell, J. H., "Epistasis: what it means, what it doesn't mean, and statistical methods to detect it in humans", *Human Molecular Genetics*, 11, 20, pp. 2463-2468, 2002.

185. Schöner, D., M. Kalisch, C. Leisner, L. Meier, M. Sohrmann, M. Faty, Y. Barral, M. Peter, W. Gruissem, and P. Bühlmann, "Annotating novel genes by integrating synthetic lethals and genomic information", *BMC Systems Biology*, 2,3, 2008.

186. Puniyani A., U. Liberman, and M. W. Feldman, "On the meaning of non-epistatic selection", *Theoretical Population Biology*, 66, pp. 317-321, 2004.

187. Otto S. P., and T. Lenormand, "Resolving the paradox of sex and recombination", *Nature Reviews Genetics*, 3, pp. 252-261, 2002.

188. Martens, J. A., J. Genereaux, A. Saleh, and C. J. Brandl, "Trasncriptional activation by yeast PDR1p is inhibited by its association with NGG1p/ADA3p", *The Journal of Biological Chemistry*, 271, 27, pp. 15884-15890, 1996.

189. Sterner, D. E., and S. L. Berger, "Acetylation of histones and transcription-related factors", *Microbiology and Molecular Biology Reviews*, 64:2, pp. 435-459, 2000.